2010

A General Approach Towards the Synthesis of Amido-Functionalized Biodegradable Polyesters

Joseph Russell
Bucknell University

A GENERAL APPROACH TOWARDS THE SYNTHESIS OF AMIDO-FUNCTIONALIZED BIODEGRADABLE POLYESTERS

by

Joseph D. V. Russell

Presented to the Faculty of
Bucknell University
In Partial Fulfillment of the Requirements for the Degree of

MASTER OF SCIENCE in CHEMICAL ENGINEERING

Approved:

Dr. Brandon M. Vogel
Advisor

Dr. Timothy Raymond
Department Chair

Dr. Eric Tillman
Committee Member

Dr. Katsuyuki Wakabayashi
Committee Member

May 13th 2010
May 2010

I, Joseph Russell, do grant permission for my thesis to be copied.

TABLE OF CONTENTS

LIST OF FIGURES

LIST OF TABLES

LIST OF ABBREVIATIONS

α-HA	α-Hydroxy acid
ACE	2-Acetamido-2-hydroxyacetic acid
ACRY	2-Acrylamido-2-hydroxyacetic acid (2-Acrylamidoglycolic acid)
BZ	2-Benzamido-2-hydroxyacetic acid (α-Hydroxyhippuric acid)
DCC	Dicyclohexylcarbodiimide
DCM	Dichloromethane
DiPC	N, N'-Diisopropylcarbodiimide
DMAP	4-Dimethylaminopyridine
DMF	N, N'-Dimethylformamide
DP	Degree of polymerization
DSC	Differential scanning calorimetry
FTIR	Fourier-transform infrared spectroscopy
GA	Glyoxylic acid monohydrate
GPC	Gel permeation chromatography
M_n	Number average molecular weight
M_w	Weight average molecular weight
NMR	Nuclear magnetic resonance
OACE	Oligo(2-acetamido-2-hydroxyacetic acid)
OACRY	Oligo(2-acrylamido-2-hydroxyacetic acid)
OBZ	Oligo(2-benzamido-2-hydroxyacetic acid

OLA	Oligo(lactic acid)
OPYR	Oligo(2-(2-pyrrolidino)-2-hydroxyacetic acid
PC	Polycondensation
PCL	Poly(ε-caprolactone)
PDI	Polydispersity index
PEG	Poly(ethylene glycol)
PGA	Poly(glycolic acid)
PLA	Poly(lactic acid)
pTSA	*p*-Toluenesulfonic acid
PYR	2-(2-pyrrolidino)-2-hydroxyacetic acid
ScTrf	Scandium (III) triflate (scandium (III) trimethanesulfonate)
T_g	Glass transition temperature
TGA	Thermal gravimetric analysis
THF	Tetrahydrofuran
T_m	Melting temperature

ACKNOWLEDGEMENTS

First and foremost, I would like to thank my advisor Dr. Brandon Vogel for his guidance, expertise and patience throughout my thesis work. Dr. Vogel seemed to have a solution to virtually every problem I experienced in lab and was indispensable throughout every phase of my research. I learned a tremendous amount from Dr. Vogel and I wish him the absolute best in his future work at Bucknell University. Hopefully my work will contribute to the synthesis of the ever elusive functionalized polyester! I would also like to thank my committee members Dr. Eric Tillman and Dr. Katsuyuki Wakabayashi for their insight, as well as Dr. Robert Stockland for his valuable assistance with NMR interpretation and sample analysis. I am greatly indebted to all of you.

I would also like to thank my support network of close friends at Bucknell University, specifically my fellow chemical engineering graduate students and our surrogate parents Dr. Brandon Vogel and Dr. Erin Jablonski. From long, early morning hours in the graduate office to Turkegers and movie nights, you all helped make my graduate experience special. I don't know how I could have done this without you.

Lastly, I would like to thank my loving family for all of their encouragement. It was heartwarming to be the benefactor of your support over the past two years. Thank you for listening to me when I was frustrated and for believing in me even when my faith in myself was wavering. You all mean so much to me and I am unbelievably lucky to have you in my life. Thank you so very, very much.

ABSTRACT

The thesis presented here describes methodologies to produce pendant group functionalized polyesters from amido-functionalized α-hydroxy acids. The synthetic methods used to produce the functionalized α-hydroxy acids are compatible with a wide array of functional groups, making this technique highly versatile. The synthesis of functionalized polyesters was investigated to develop polymers with tailored chemical properties that may improve the capabilities of existing biodegradable polyesters for applications in controlled release pharmaceuticals.

Chemically modified α-hydroxy acids were synthesized by reacting glyoxylic acid with a primary or secondary amide. To demonstrate the utility of this reaction, four structurally dissimilar amide substituents were examined including 2-pyrrolidione, benzamide, acetamide and acrylamide. The reaction is synthetically simple, provides high yields and is uniquely flexible, imposing very few structural constraints on the functionalized monomer. The compatibility of this procedure with the collection of functional groups mentioned circumvents the need for protecting groups and multi-step syntheses.

The amido-functionalized monomers were polymerized by two different techniques: melt polycondensation and solution polymerization. Melt polycondensation was conducted by heating the monomer past its melting temperature under reduced pressure. Oligomeric functionalized polyesters (≈ 800 g/mol) with low PDIs (≈ 1.05) were obtained by melt polycondensation. Melt polycondensation was not compatible

with all of the synthesized monomers. Two of the monomers (containing benzamide and acrylamide functionalities) degraded before the polycondensation reaction occurred. Thermal gravimetric analysis confirmed that a process other than polyesterification was occurring, indicating that some amido-functionalized α-hydroxy acids cannot be synthesized in the melt.

Solution polymerization was conducted to polymerize functionalized α-hydroxy acids that were incompatible with melt polycondensation. Several modified Steglich polyesterifications were tested including *p*-toluenesulfonic acid mediated and scandium (III) triflate catalyzed. Only oligomeric functionalized polyesters were formed by this method. A number of possible side reactions including the formation of an N-acylurea and a cyclic polymer ring were possible. The utility of this procedure appears to be limited due to the complexity of the reaction and its inability to produce high molecular weight polymer.

CHAPTER ONE:

INTRODUCTION

1.1 Introduction to Controlled Release Pharmaceuticals

Drug delivery is an important area of research in the pharmaceutical field. Conventional techniques for drug delivery such as intramuscular injections, oral tablets and intravenous therapies have all been developed to transport drugs though the body's primary defenses, such as the skin or the epithelial linings of the stomach and intestines. [1] Although the techniques mentioned are effective at passing through these barriers, they are incapable of further controlling the release and distribution of the drug. An optimal delivery method must efficiently deliver the drug to the affected site, while also keeping the drug concentration within a therapeutic range. To ensure a therapeutic dose reaches the tissue of interest, it is common to overdose a drug, knowing that much of the drug will never arrive at its intended target. This occurs because the drug is often metabolized or excreted by the body before reaching its destination. Although this practice is common, it is far from efficient. Overdosing drugs increases the cost of the therapy and can amplify the risk of side-effects. [2]

Controlled release drug therapies offer a solution to some of the existing drug delivery problems. Conventionally, a drug is loaded in a polymer matrix that erodes, allowing the drug to elute at a controllable rate. [3] As the polymer degrades, the concentration of the drug within the blood stream can be kept within therapeutic levels because elution is controlled by the rate of polymer degradation. Many current therapies

require several doses over the course of treatment to ensure efficiency. The advent of sustained release medicines could increase patient compliance and improve therapeutic results over bolus injections. [4] As seen in Figure 1, bolus injections are often designed to raise concentrations of the drug into a toxic range to increase the length of time the drug stays within the therapeutic window. Controlled release medications could maintain a concentration within the therapeutic range, thereby eliminating the need for an initially toxic dosage. Overall, the further development of sustained release drugs could improve drug efficiency, reduce toxic level side effects and decrease the necessary dosage. [5]

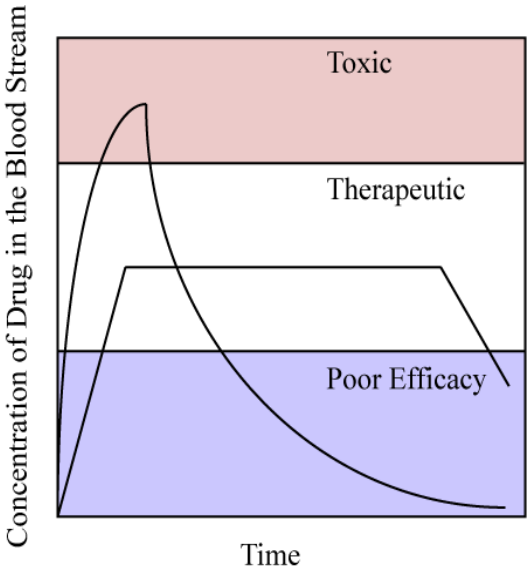

Figure 1: Comparative release profiles of bolus and controlled release pharmaceuticals

For biodegradable polymers to meet the demands of controlled release applications, they must surmount difficulties associated with their toxicity and degradation rates. To engineer materials that are capable of hurdling these challenges, structural alterations to current polymers and the chemistry of such structurally augmented polymers must be explored in greater detail. For instance, the degradation and erosion properties of polymers are dependent on monomeric connectivity, initiators, pendant groups and processing techniques because changes to these factors can influence crystallinity, hydrophilicity, glass transition temperature and the molecular weights of

polymer chains. [6, 7] Depending on the particular application, the physical properties of a polymer might need to be adjusted to meet the required specifications of the drug. The selection of a material for biological use would therefore be dependent on the polymer chemistry associated with a combination of such variables, making further research into chemically modified polymers valuable.

Biodegradable polymers have the potential to be valuable for many medical purposes including drug delivery. The market for the application of biodegradable polymers is strong because pharmaceutical companies have become increasingly focused on controlled release medications, which often utilize biodegradable polymers. Furthermore, augmented mechanical and degradation properties can be achieved by tailoring the chemistry of a polymer, potentially yielding plastics with enhanced physical properties. It is postulated that incorporating tailored biodegradable polymers into next generation controlled release pharmaceuticals would improve treatments for patients by eliminating bolus dosages, while simultaneously increasing the cost effectiveness of the treatment.

The focus of this thesis is to develop experimental methods to generate functionalized biodegradable polyesters. In addition to controlling functionalization, it is important that these procedures are able to produce polymers with sufficient chain lengths and narrow molecular weight distributions. Ultimately, it is desired to compile a library of synthetically generated functionalized polyesters to explore structure-property relationships for improved controlled release devices. Developing a synthetic platform

that is capable of producing monomers with varying functionalities ultimately could shed insight into this complex connection.

The next chapter in this thesis is the literature review section. It outlines the current state of functionalized polyester research and highlights the need for further research in this area. The next chapter also describes the history of biodegradable polyesters and advancements that have made these materials viable for the medical field. Subsequent chapters describe the experimental methods used to produce amido-functionalized α-hydroxy acids and attempts at their polymerization.

1.2 References

(1) Kotwal, A. *Social Science and Medicine* **2005**, *60*, 1133.
(2) Thombre, A. *Drug Discovery Today* **2005**, *10*, 1159.
(3) Uhrich, K.; Shakesheff, K. et al. *Chemical Reviews* **1999**, *99*, 3181.
(4) Hoffman, A. *Advanced Drug Delivery Review* **1998**, *33*, 185.
(5) Collins, J. *Journal of Clinical Oncology* **1984**, *2*, 498.
(6) Middleton, J.; Tipton, A. *Medical Plastics and Biomaterials* **1998**, *5*, 30.
(7) Pan, P.; Inoue, Y. *Progress in Polymer Science* **2009**, *34*, 605.

CHAPTER TWO:

LITERATURE REVIEW

2.1 Introduction and Poly(Lactic Acid) Review Rationale

The literature review section of this thesis serves to highlight important sources in the literature and their contribution to the field of biodegradable polyesters. The primary focus of this literature review will be poly(lactic acid) (PLA) because PLA is a ubiquitous medical grade polyester and possesses a chemical resemblance to the group of synthetic amido-functionalized polyesters presented in this text, making it an exemplary model polymer for analysis. As will be described, PLA is a common, FDA approved biodegradable polyester with a rich history of success in medicine. A wealth of information concerning PLA and its copolymers exists in the literature. While PLA will be the focus of the review, other noteworthy polyesters will be highlighted. The bulk of the literature review will analyze PLA in efforts to shed light on the synthesis of the functionalized polyesters presented subsequently.

2.2 A Brief History of Polyesters

The term polyester refers to a macromolecule that possesses ester linkages within its backbone. The earliest of these polymers were created by Wallace Carothers and his synthetic chemistry team at DuPont Chemical Company in the late 1920's. The impetus for research into polyesters was to make a synthetic material similar to silk. [1] Carothers also created Nylon, the first polyamide, and Neoprene, the first synthetic rubber.

Carothers and his team created the first polyesters by reacting dicarboxylic acids like hexadecamethylene dicarboxylic acid with diols like trimethylene glycol. [2, 3] The polycondensation reaction could also be conducted by substituting diacid chlorides or diesters in place of the dicarboxylic acid. An example of this reaction is shown below in Figure 2. In the figure, the R and R' groups correspond to the polymer formed from the reaction of trimethylene glycol and hexadecamethylene dicarboxylic acid.

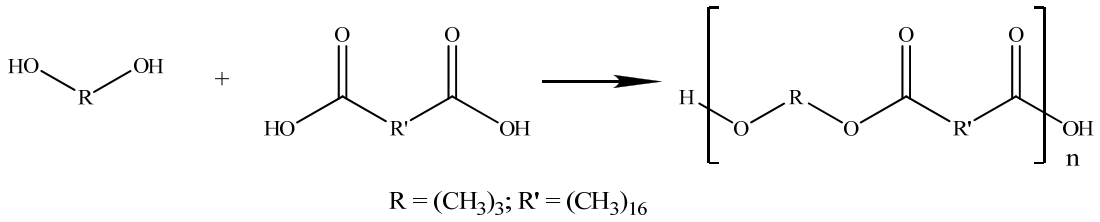

Figure 2: Schematic of the polycondensation reaction between a diol and a dicarboxylic acid

Although the first polyesters were considered successful, they had low melting points and poor hydrolytic stability. [3] Another problem was that the polyesters had low molecular weights (< 4,000 g/mol), a flaw that significantly limited their physical properties and usefulness. [4] The failures of these early polyesters led to the development of other diol and dicarboxylic acid combinations. Such experimentation eventually led to the creation of polyesters like poly(ethylene terepthalate) (PET), which has a high melting temperature and good hydrolytic stability. [3]

2.3 Biodegradation and Erosion

Degradable polyesters intended for medicinal uses are capable of degrading *in vivo*. Biodegradation describes the occurrence of polymer chain scission caused by cleaving agents in the body, specifically water and naturally occurring enzymes. [5-8] During this process, cleaving agents attack hydrolyzable bonds in the polymer chain, breaking the backbone down into oligomers, monomers or other small molecules. [7] Ideally, the products of degradation are compounds already found in the body or analogues of biological molecules that are non-toxic. This class of polymer is useful because the material placed *in vivo*, either surgically or by ingestion, does not require surgical removal.

Polymers can be degraded by a number of different processes including photo-, thermo-, mechanical and chemical degradation. [9] Of these processes, the most biologically relevant are thermal and chemical. Factors affecting the degradation of polymers include composition, pH of the degradation products, polymer crystallinity and polymer hydrophilicity. [10-12] The distinction between degradable and non-degradable polymers is imprecise, but it is based on the length of time necessary for degradation, as biodegradable polymers are defined as those that degrade on an "acceptable time scale" when in contact with biological environments. [9]

The erosive nature of a biodegradable polymer is another important factor governing the degradation properties of a biodegradable plastic. Erosion is defined as the loss of mass from the polymer. [13] To reiterate this distinction, degradation should be considered a chemical process involving chain scission, whereas erosion is a physical

phenomenon consisting of the transport of degradation products away from the polymer bulk. Mass loss caused by erosion typically occurs by diffusion or dissolution of the polymer into the surrounding medium. [14]

Erosion typically occurs by one of two basic mechanisms: bulk or surface erosion. [11] A polymer is said to be surface eroding when it loses mass to its surroundings only from the interface between the polymer and the environment. This occurs because the rate at which water enters into the polymer bulk is much slower compared to the rate that the polymeric surface degrades. [13] Therefore, the amount of surface area is proportional to rate of erosion. Poly(anhydrides) are examples of surface eroding polymers. [15]

Bulk erosion occurs when water can swell into the polymer and cause degradation to both the interior and exterior of the material. When water enters into the polymer, it cleaves chemical bonds by hydrolysis and reduces the chains into smaller components. This process is often accelerated by water influx induced by osmotic pressure. [16] Most polymers, including polyesters, have bulk eroding characteristics.

In both cases, hydrolysis is often the reason for polymer degradation and erosion. The erosion characteristics of a polymer are largely governed by the hydrophilicity of its backbone or end groups and its chemical stability. From a utility standpoint, surface erosion is typically preferred because the material will maintain its structural integrity and mechanical properties during degradation. [16] Homogeneous surface erosion also allows for linear release kinetics of an implanted drug, making it a desirable quality for drug delivery. Surface eroding polymers can protect water sensitive drugs from the

aqueous environment of the body by reducing water permeation into the bulk of the polymer. [17] This ensures that acid or water sensitive drugs impregnated in the polymer matrix will not degrade until they are exposed to the aqueous environment at the polymer surface.

2.4 Poly(Lactic Acid) (PLA)

Poly(lactic acid) (PLA) is a biodegradable, thermoplastic polyester formed from the polymerization of lactic acid and is FDA approved for medical use. Lactic acid, the monomer of PLA, is produced commercially through the fermentation of corn or sugarcane, but can also be derived from petroleum products. [18] The monomer was first isolated from milk in 1780 by Carl Scheele, lending it the alias "milk acid". [19] Lactic acid belongs to a class of compounds known as α-hydroxy acids. The α-hydroxy acids are characterized by a carboxylic acid adjacent to a carbon possessing both a hydroxyl group and an unspecified substituent as shown in Figure 3. For lactic acid, the R group is a methyl group. For glycolic acid, the monomer of poly(glycolic acid) (PGA), the R group is a hydrogen atom.

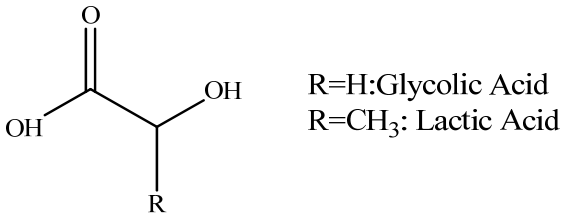

Figure 3: Generic structure of an α-hydroxy acid

Lactic acid has a chiral center located at the carbon directly connected to the R and hydroxyl groups. There are two stereoisomers of lactic acid, D and L lactic acid. The two stereoisomers of lactic acid are presented in Figure 4. The most common and biologically active enantiomer is L lactic acid. [20]

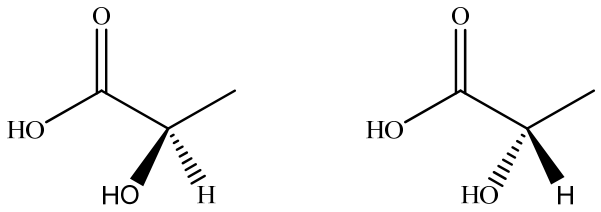

Figure 4: From left to right, the D and L enantiomers of lactic acid

Due to the chirality of lactic acid, PLA can form three distinct structures: PLLA containing only L-lactic acid, PDLA containing only D-lactic acid or a combination of the two enantiomers, PDLLA. The stereochemistry of PLA affects degradation by dictating the crystallinity of the polymer. Amorphous polymer regions are more readily hydrolyzed than crystalline segments, making the degree of crystallinity important to degradation. [21] Crystallinity is reduced when both of the stereoisomers are present (i.e. PDLLA) because efficient packing of the polymer chains cannot occur. [21] Consequently, controlling the stereochemistry of the lactic acid monomer units is very important to controlling the degradation properties of the polymer.

The first reported use of polyesters in the medical field was by surgeons who used PLLA as both sutures and bone fixation materials in the mid 1960's. [22] The polyester was chosen because it possessed a number of suitable qualities including biodegradability, biocompatibility and good mechanical properties. [23] The formation of

PLA from lactic acid is shown in Figure 5. When PLA degrades it decomposes into lactic acid, which is produced during anaerobic respiration in human muscles. Consequently, the byproducts of PLA degradation are non-toxic, making PLA a viable material for bioresorbable sutures. [24]

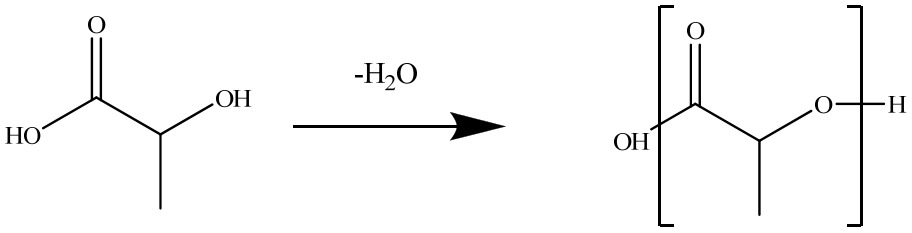

Figure 5: The formation of PLA from lactic acid

Currently, PLA finds use in an assortment of applications outside of medicine and is a common material for recyclable cups and bottles. [25] Environmental studies involving PLA based products have shown that under moist compost conditions, PLA degrades completely to lactic acid by the seventh week of exposure. [26] Similar studies have shown that temperature, pH and humidity all affect the rate of degradation. [27] An added advantage of using PLA is its sustainability. Poly(lactic acid) can be derived from common, sustainable materials that are not directly dependent on petroleum, unlike that of many medical grade polymers, making PLA a greener alternative to petro based materials.

Unaltered PLA typically exhibits high tensile strength and elastic modulus, as displayed in Table 1. [25] The physical properties of these polymers however, are highly dependent on the average molecular weights of the sample. [28] Strong mechanical properties are valuable for biomedical applications that require structural integrity, such

as surgical orthopedic implants. Although the present research is focused on drug delivery, a brief summary of mechanical property information is presented as a reference.

Table 1: Mechanical properties of extrusion/thermo-reforming grade PLA (≈70,000 g/mol) [25]

Tensile Strength at Break (MPa)	53
Tensile Yield Strength (MPa)	60
Tensile Modulus (GPa)	3.5
Tensile Elongation (%)	6.0

Along with the need to understand the mechanical properties of PLA, it is important to understand its thermal properties. A sample of PDLLA with a molecular weight of 27,500 g/mol was found to have a glass transition temperature (T_g) equal to 48 °C, while a PDLLA sample with a molecular weight of roughly 117,000 g/mol was found to have a T_g = 53 °C. [28] When a PLA sample is highly enatiomerically pure (i.e. PLLA), the melting temperature (T_m) is typically 180 °C.

2.5 Polymerization Techniques

2.5.1 Condensation polymerization of PLA

An initial detriment to the production of medical grade polyesters was the relatively low molecular weights of the polymer chains. Originally, PLA was formed through melt polycondensation reactions, which were only able to produce low molecular weight polymers (<4,000 g/mol). [29] Low molecular weights were achieved in part because the polycondensation of lactic acid is an equilibrium reaction that forms water as a byproduct. [25] Excess water is detrimental for two separate reasons. From a kinetic

standpoint, water buildup causes an increase in products, which limits the extent of reaction by forcing the equilibrium towards the reactants according to Le Chatelier's principle. Secondly, PLA chains that form during synthesis can be hydrolyzed by the excess water. Polycondensation reactions of polyesters proceed through a standard condensation polymerization pathway, as shown in Figure 6. Typically, a melt condensation polymerization is conducted by heating monomers under vacuum to remove water residue.

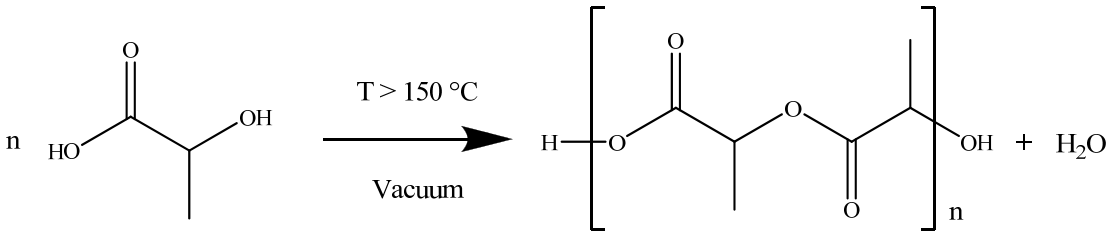

Figure 6: The polycondensation reaction of lactic acid into PLA

A technique used to alter the equilibrium between water and PLA in efforts to drive the polymerization is azeotropic distillation. The distillation is conducted by placing lactic acid in a large volume of miscible solvent. High boiling point solvents like diphenyl ether or *p*-xylene are used to remove water via azeotropic distillation.[30] For example, a reaction vessel was charged with the distillation solvent, lactic acid (as a 90 % lactic acid aqueous solution) and stannous chloride as a catalyst. The reaction was then azeotropically distilled for 20 to 40 h.[30] Molecular weights using this procedure were found to be greater than 100,000 g/mol and the procedure was found to be applicable with PLA-PGA copolymer systems.[31] However, the solvents involved (i.e. p-xylene, etc.) in the distillation are often hazardous and the experimental protocols and energy

demands are often intensive. [23] Such issues make processing challenging and often lead to more expensive PLA.

Solution polycondensation is another technique that has been explored to produce PLA and other polyesters. One such solution polymerization method is the Steglich esterification. The Steglich reaction was developed by W. Steglich in the late 1970's as a method to esterify sensitive carboxylic acids and alcohols. [32] The procedure entailed reacting the carboxylic acid and alcohol with a carbodiimide in the presence of an acyl transfer agent. Commonly, the carbodiimide used is dicyclohexylcarbodiimide and the acyl transfer agent is 4-dimethylaminopyridine.

In a number of reports in the literature, the esterification method has been extended to polyesterifications. Moore and Stupp esterified 4-(5-(4-hydroxy-phenyl)pentyl) benzoic acid to a degree of polymerization of 50 repeat units, indicating that the esterification was effective for bifunctional molecules. [33] Wagener et al. reported that the polyesterification of 3-hydroxy-2-phenylpropionic acid, a β-hydroxy acid, could produce polymer exceeding 7,500 g/mol. [34] High molecular weight PLA greater than 100,000 g/mol was also synthesized by this method. [35] The major drawback of Steglich polyesterification is that both reagents involved in the esterification (i.e. the carbodiimide and 4-dimethylaminopyridine) are highly toxic. However, purifications steps were shown to effectively remove these compounds. [36] A basic Steglich polyesterification is shown for PLA in Figure 7.

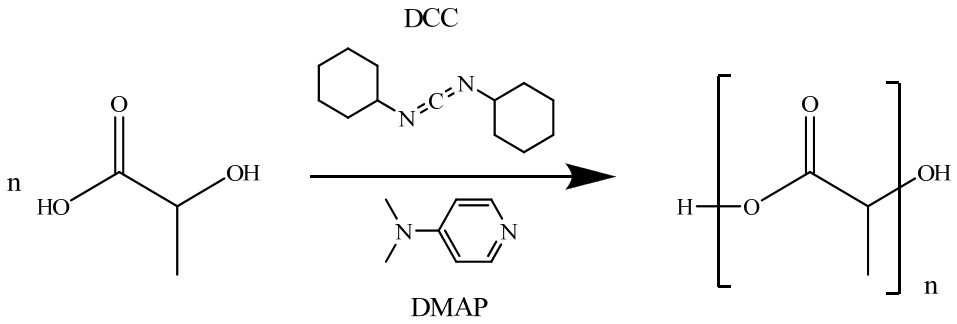

Figure 7: Steglich polyesterification of PLA

2.5.2 Ring opening polymerization of PLA

Ring Opening Polymerization (ROP) is the commercially preferred method of PLA synthesis. [37] In this method, a cyclic dimer composed of two lactic acid molecules is formed. The ROP is preferred because it increases control over the polymerization and can be conducted under milder conditions with decreased reaction times. [38] Due to this control, ROP can generate a wide range of molecular weight PLA samples and is capable of producing higher molecular weight PLA than traditional condensation polymerization. [39] The procedure is known as a ring opening polymerization because lactide, the cyclic dimer of lactic acid, is opened during polymerization.

In ROP, lactide is typically formed either by the dehydration of two lactic acid molecules or by the depolymerization of lactic acid oligomers (OLA), often caused by backbiting induced by a catalyst. [25, 40] The depolymerization of OLA into lactide is the preferred technique to obtain the dimers. [41] Due to the chirality of lactic acid, three stereoisomers of lactide exist: LL-lactide, DD-lactide and DL-lactide, also known as meso-lactide. [41] The three stereoisomers of lactide are presented below in Figure 8.

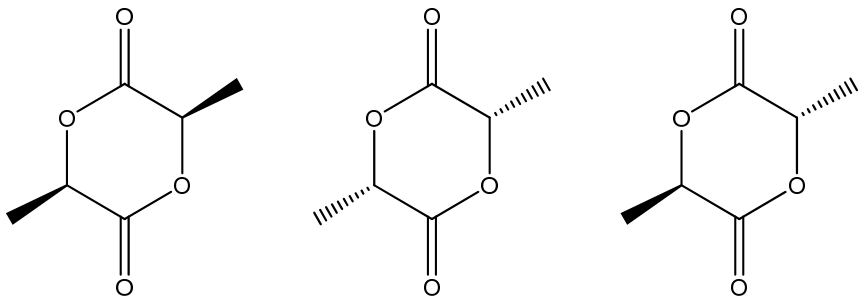

Figure 8: The three stereoisomers of lactide from left to right: DD-lactide, LL-lactide and DL(meso)-lactide

A characteristic method of producing lactide involves placing OLA (usually < 2,000 g/mol) under reduced pressure (250 Pa or less), while heating between 150-200 °C. The lactide is then sublimated out of the reaction vessel and condensed. [37, 41-43] Tin compounds like stannous 2-ethylhexanoate are most commonly used to catalyze the depolymerization reaction. Noda et al. found that 1 wt% stannous 2-ethylhexanoate was capable of converting L-OLA into lactide with a yield of nearly 90%. Of the lactide formed, 98% of the lactide was LL-lactide with the remaining being meso-lactide. In the same study Zn and Zr catalysts were tested, but were less effective. [43]

Once the lactide ring is formed, the ROP is usually conducted between 100 °C and 200 °C (depending on the catalysts and solvent if present) and initiated by metal catalysts like Sn and Al or metallic oxides of these metals. [37, 44-46] A typical ROP procedure is shown in Figure 9. Compared to polycondensation, ROP has proven to yield higher average molecular weights, often greater than 70,000 g/mol, with lower polydispersity. [47] The ability to yield high molecular weight polyesters lends greater control over mechanical properties because mechanical characteristics are highly dependent on molecular stereochemistry and average chain molecular weight. [48] The

stereochemistry of lactides during ring opening polymerizations can also be controlled by using chiral aluminum and yttrium alkoxide catalysts. [49]

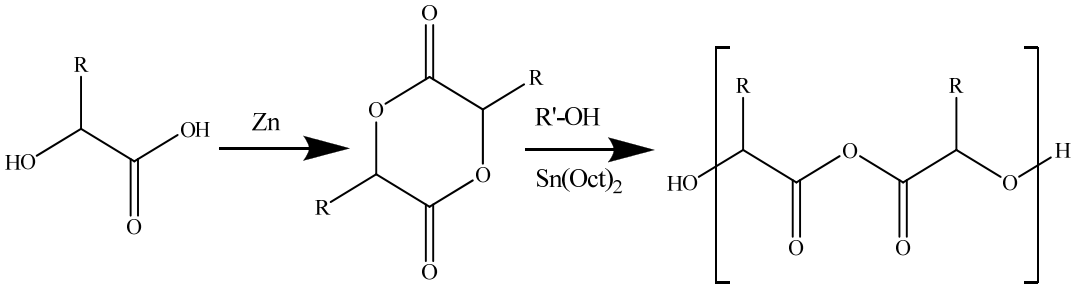

Figure 9: A diagram of a ring opening polymerization involving cyclic diesters

The polymerization of lactide into PLA is dictated by the susceptibility of the ring to be opened. Thus, the tendency of lactide to polymerize is dependent on ring strain and the existence of a suitable ring opening mechanism. [50] Ring strain is a well known phenomenon and occurs when bond angles inside of the ring are forced into non-ideal conformations to complete the cycle. Six membered rings like lactide, however, have little bond distortion due to their geometry, making them more thermodynamically favorable. [50] Consequently, initiators are needed to start the reaction and to generate a favorable mechanism for polymerization.

The ROP of lactide can be conducted in solution, suspension or in bulk, with bulk being the most common. The mechanism of the ROP is dictated by the initiator and catalyst used in the polymerization. [51] Coordination-insertion, ionic and enzymatic mechanisms are the most widely reported, with coordination-insertion being the most common of the three. [50, 52] Not surprisingly, the most common initiators (i.e. Sn and Al catalysts) are coordination-insertion mechanism initiators. [44, 45]

The coordination-insertion mechanism was given its name because the monomer, in this case lactide, is inserted into the metallic or metal-alkoxide bonds of the catalyst, which causes bond distortion. [50] The distortion causes increased stress on the ring, which in turn makes the ring more reactive and more apt to polymerize. A schematic of a coordination insertion ROP is shown in Figure 10 and is a variation on two schematics found in the literature. [37, 53] In the figure, R` and R`` represent organics attached to M, the metallic center.

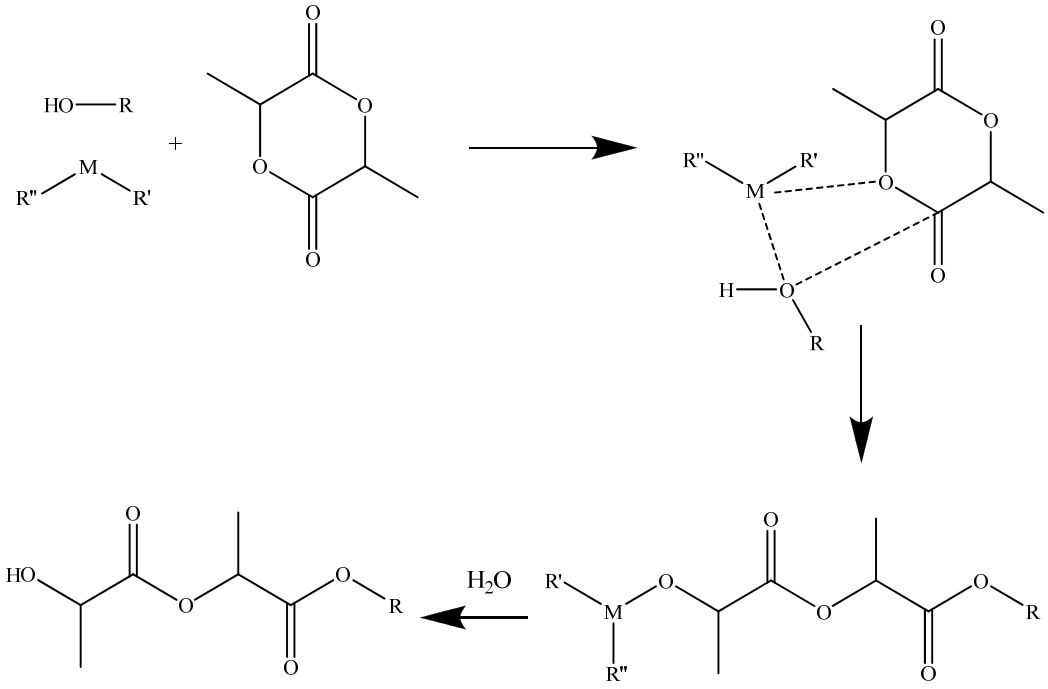

Figure 10: The coordination insertion ROP of lactide where R` and R`` represent organics attached to M, the metallic center

The coordination-insertion ROP of lactide proceeds by a three step mechanism. [53] First, the lactide is coordinated into the metal center of the organometallic catalyst, making one of the carbonyl groups of the lactide more reactive. Then, the ring is opened

by the nucleophilic addition of an alcohol (or water) that was added to act as an initiator causing the cleavage of the acyl-oxygen bond. Lastly, water present in the reaction separates the metallic catalyst. To reduce heavy metal containing initiators, new biologically based initiators have been developed. Organic bases such as creatinine have been used to facilitate a coordination-insertion ROP with molecular weights exceeding 15,000 g/mol and a polydispersity index equal to 1.28. [54]

There are two types of ionic ROPs: anionic and cationic. [52] Both polymerization techniques are of interest because of the mild conditions that are required for polymerization and because the initiators used are typically less toxic than coordination-insertion initiators. [55] For anionic polymerizations, lactide was placed in a solvent under an argon atmosphere in the presence of an initiator such as lithium diisopropylamide or dibutyl magnesium to start the polymerization. [56] Anionic polymerizations can occur at temperatures less than 70 °C in an appropriate solvent (THF was often utilized) and have been shown to produce high molecular weight samples greater than 20,000 g/mol. [55, 56] Anionic polymerization is thought to occur by nucleophilic attack of the lactide carbonyl or by deprotonation and cleavage of the ester linkage. As a consequence of this mechanism, a planar anion forms, making the formation of PDLLA unavoidable. [52, 56]

The cationic ROP of lactide is initiated by protonating or alkylating one of the carbonyl groups of the lactide, allowing for a nucleophilic attack by another monomer at the electrophilic carbon. [52, 57] Cationic ROP is less common than anionic ROP because very strong acids and carbocation donors are required to initiate polymerization. [52]

Cationic polymerization typically involves reacting lactide with the chosen catalyst at temperatures between 100 to 180 °C. [58] Due to the nucleophilic attack on the planar carbonyl carbon, stereochemistry is difficult to control and is impossible at temperatures greater than 50 °C. [58] Below 50 °C however, the reaction is slower and poor molecular weights are obtained, forcing the issue of stereochemical control and the need for higher molecular weight samples. Recent advances in this field have focused on improving the initiators used. Gold-N-heterocyclic carbenes have generated PLA samples with molecular weights greater than 10,000 g/mol with PDIs around 1.20. [59]

Lastly, the ROP of lactide can occur enzymatically. There are a number of benefits to using enzymes rather than metal compounds as catalysts, mainly stemming from biocompatibility and renewability. [60] As was mentioned before, many commonly employed metallic catalysts are toxic, raising concerns about their use for biomedical applications. Another issue is that many of the organometallic catalysts and initiators are synthesized from petroleum products, making them less sustainable. In contrast, enzymes have a number of possible benefits that may make them viable alternatives to current metallic initiators.

Enzymatic ROPs are typically conducted under mild conditions and produced polymers with high enantioselectivity. The enzymes can be derived from sustainable resources and are often soluble in organic solvents. [60] Lipases have been cited because they are effective at cleaving ester bonds, are often biocompatible and can polymerize unprotected hydroxy acids to yield linear polymers. [61] A number of enzymes were found to generate high molecular weight PLA from LL, DD and meso-lactide. For example,

LL-lactide was reacted at 100 °C and converted into PLLA with a molecular weight of 48,000 g/mol by strains of *Pseudomonas*. [60] Good stereoselectivity was also achieved as 82% of the sample was PLLA. However, to achieve high molecular weights, long reaction times were required. The 48,000 g/mol PLLA sample mentioned previously was obtained after reacting for 168 h (7 d). [60] Other PLA samples produced from the different enantiomers of lactide or by using different lipases appeared to have similar properties and similar reaction times.

2.5.3 Post polymerization

After the polymerization of PLA or OLA, a number of techniques can be used to improve the molecular weight of a polymer sample or alter its morphology. Three common methods cited in the literature are melt modification, radiation induced cross-linking and solid state polycondensation (a variation of melt modification). [23] Melt modification is primarily used to improve the processing characteristics of PLA, but is also used to alter physical properties. In some cases, peroxides such as tert-butyl peroxybenzoate were added at a ratio of 0.5 wt% to PLA to reduce melt degradation. [62] Peroxides are added because they are capable of deactivating residual catalysts (like Sn compounds) that could degrade the polymer. [63] However, peroxides were found to alter the morphology of the PLA by reducing the crystallinity of the sample, which in turn increases the rate of hydrolysis and biodegradation. [64] The decrease in crystallinity is believed to be caused by branching or cross-linking induced by the peroxide, which reduces the rate of crystallization. [65] In some cases, the degree of cross-linking was high

enough to produce swelling PLA gels when peroxides such as dicumyl peroxide were employed. [66]

Another melt modification technique uses diisocyanates as chain extenders. Until the last 20 years, it was believed that high molecular weight PLA could not be achieved in the melt, stemming from the water equilibrium issues listed previously and because of a build-up in melt viscosity during polymerization. [67] These factors not only reduced the chain molecular weights, but also produced polymers with limited physical properties. [68] One method to eliminate this issue was to add a diisocyanate compound like methylenediphenyl diisocyanate (MDI) or toluene-2,4-diisocyanate (TDI) as a chain extender. [69] Low molecular weight pre-polymer formed through melt polycondensation was increased in molecular weight by connecting PLA chains using the diisocyanate as a bridge, effectively creating a polyester-urethane. An example of PLA chain extension with a diisocyanate is depicted in Figure 11.

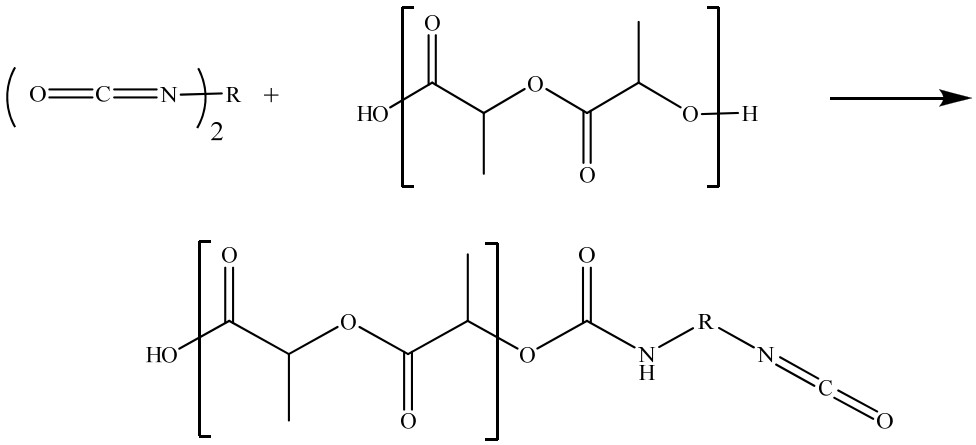

Figure 11: A generic PLA chain extending reaction with a diisocyanate

The diisocyanate molecule increased the PLA molecular weight by reacting with either the terminal hydroxyl or carboxyl group present on the low molecular weight PLA chain. Due to the bifunctionality of the diisocyanate, another terminal hydroxyl or carboxyl group from a different PLA chain could react with the isocyanate pendant group. In doing so, the two PLA chains were connected via the diisocyanate molecule, doubling the molecular weight of the PLA chain.

Molecular weights of nearly 400,000 g/mol were reported using diisocyanates to modify oligomeric PLA produced by melt polycondensation. [70] Although successful, this method often involved expensive and toxic reagents. Processing complications caused by the reactants toxicity often made for a more expensive polymer. The removal of toxic linking agents is another major issue if the increased molecular weight PLA is to be used as a medical polymer.

Radiation induced cross-linking is primarily used to increase the molecular weight of the PLA sample or to increase the T_g. This procedure involves adding a poly-functional molecule like ethylene glycol or triallyl isocyanurate to the low molecular weight PLA and then applying radiation. [71] Although poly-functional molecules are not required for cross-linking, they are added because radiation serves to cleave PLA chains, which can react with the poly-functional molecule and aid in cross-linking. [72] Using this technique, a PLA sample with a molecular weight of 4,000 g/mol was increased to approximately 50,000 g/mol after the addition of $SnCl_2 \cdot H_2O$, *p*-toluenesulfonic acid and subsequent microwave irradiation under specific radiation and pressure sequences. [73] Similar to melt-modifications, an increase in cross-linking decreased the crystallinity of

the polymer and correspondingly, increased the rate of hydrolysis. Despite the increased rate of hydrolysis, cross-linked PLA possessed a greater resistance to enzymatic degradation. [71]

Solid state polycondensation was also discussed in the literature. In solid state polycondensation, a PLA sample of lower molecular weight was heated near the T_m (≈180 °C) of the polymer. According to Moon et al., reaction temperature in this range increased the mobility of the PLA chains in the amorphous regions, the reactivity of the PLA terminal hydroxyl groups and helped to avoid side reactions by reacting at more moderate temperatures. [67] In the procedure developed by Moon, pre-polymer OLLA was formed with a molecular weight around 600 g/mol. [67] To the OLLA, *p*-toluenesulfonic acid and a metal catalyst were added as co-catalysts. The mixture was then heated to 180 °C at 10 torr for 5 h, resulting in a polymer with a molecular weight of 100,000 g/mol. [74] After cooling and drying, the polymerization was reinitiated at 150 °C and 0.5 torr for 10 h. The resulting PLA was 85% crystalline, had a M_n = 320,000 g/mol, a T_m = 178 °C and a PDI of 3.4. [74]

2.6 Copolymerization of PLA

Despite the valuable properties of polymerized α-hydroxy acids like PLA, their unaltered physical properties are not always able to meet the design criteria for a particular application. An important factor of any polymer being considered for a medical application is the degradation rate of the polymer. Degradation rates for PLA are generally slow, limiting its applicability for some medical purposes. [48] Poly(lactic acid)

degrades slowly because of its low hydrophilicity, high percent crystallinity (as PLLA is often used) and high glass transition temperature (60 °C) as compared to body temperature (37 °C). [75] These properties can combine to interfere with the usefulness of PLA for a variety of medical applications including sutures and drug delivery systems. Depending on the sample (i.e. crystallinity and molecular weight), 40 % of the original polymer mass of PLLA implanted in the body will remain after 170 d of *in vivo* contact. [24] The surface area to volume ratio of the implant was also found to be important because PLA is a bulk eroding material. [24]

To adjust degradation rates, previous research often focused on generating copolymers of PLA. The most common PLA copolymer is formed by incorporating poly(glycolic acid) (PGA) into the polymer backbone. [76-79] As was mentioned earlier in the review, glycolic acid is an α-hydroxy acid that is structurally very similar to lactic acid. Glycolic acid does not have a chiral center however, because the R group is a hydrogen atom. When lactic acid and glycolic acid are polymerized together, they can form copolymers consisting of repeating PLA and PGA units, shown in Figure 12.

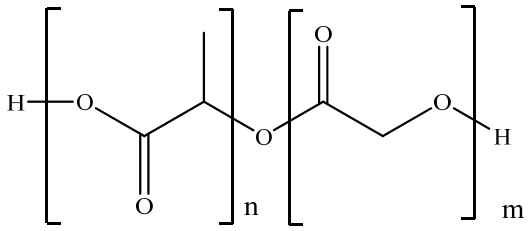

Figure 12: Schematic of PLGA copolymer

Copolymers composed of PLA-PGA (PLGA) can be formed by either polycondensation or ROP. [78] The polycondensation of PLGA copolymer involves

polymerizing lactic acid and glycolic acid, while the ROP of the copolymer uses lactide and glycolide, the cyclic dimer of glycolic acid. The co-polyester formed through polycondensation yielded only oligomeric PLGA with molecular weights approximately 2,000 g/mol. [78, 80] In comparison, copolymer formed through ROP can achieve molecular weights of 45,000 g/mol or higher. [81]

The polymer PGA was shown to be a useful biomaterial even when not polymerized with PLA. It was originally employed in the 1960's as the first synthetic, completely absorbable suture, but was limited because of its slow degradation rate (due to high crystallinity) and its near insolubility in most processing solvents. [82] Thus, PGA was more valuable when it was copolymerized. Modern polycondensation reactions using catalysts are able to produce PGA chains with molecular weights around 90,000 g/mol, which is comparable to PGA formed through the ROP of glycolide. [83]

The pairing of PLA and PGA for copolymerization is valuable because of the unique thermal and mechanical properties each respective polymer possesses. The T_m for PGA is 228 °C, which is higher than that of PLA (185 °C). In contrast, the T_g for PGA is 37 °C, which is lower than that of PLA (60 °C). [84] The copolymer is often amorphous with a decreased T_g, but an enhanced toughness relative to pure PLA. [84] Increasing the amount of PGA in the backbone also increases the hydrophilicity of the polyester.

To further demonstrate how generating copolymers can alter physical properties, degradation time is plotted as a function of the mass ratio of PLA/PGA in Figure 13. The fabrication of co-polyesters can alter degradation rates and hydrophilicity, but can also detrimentally affect mechanical properties by altering crystallinity, T_g and other factors

that determine the physical properties of a polymer. [11] The effects of altered crystallinity as a function of co-polymer composition are displayed in Figure 14. The polymer properties in both graphs reach their lower extremes when the copolymers are composed of a 50-50 ratio of PLA and PGA. It should also be noted that the wt% PGA added to PLA does not linearly affect either degradation or crystallinity.

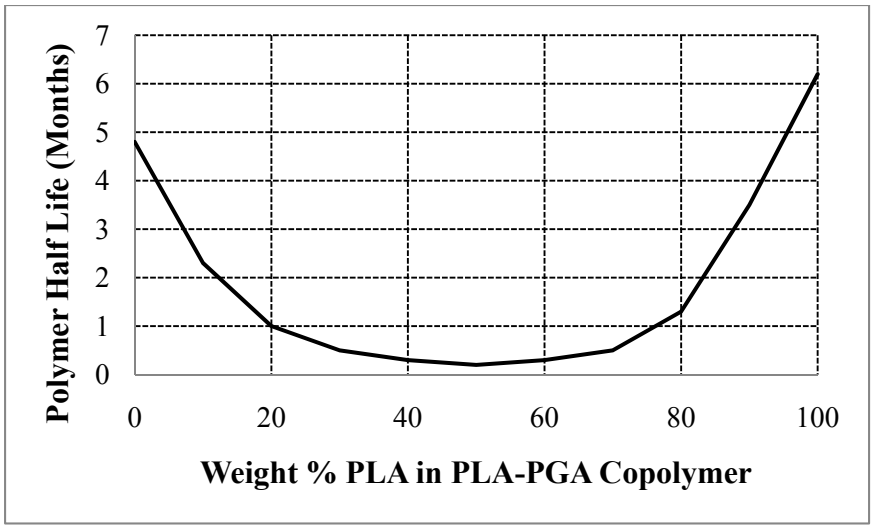

Figure 13: Weight ratio of PLA in PLGA versus degradation rate (recreation). [11]

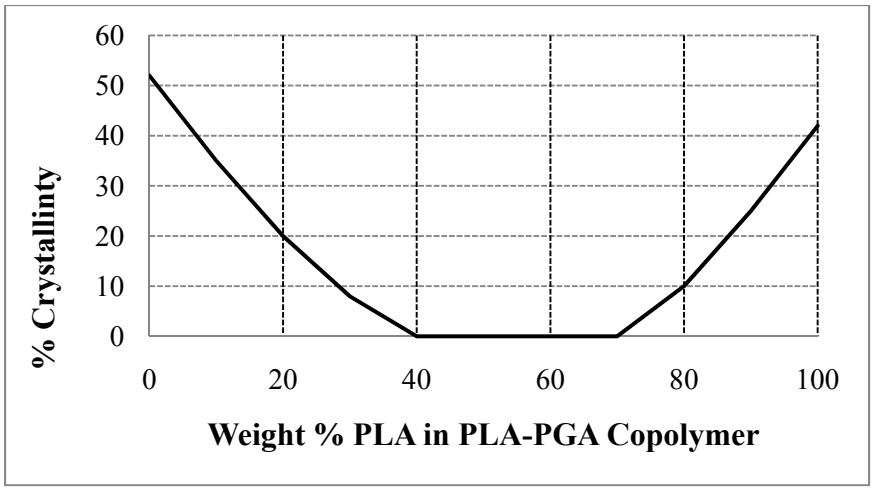

Figure 14: Percent crystallinity of co-polymer generated as a function of glycolic/lactic acid composition (recreation). [11]

Although PLGA is arguably the most common PLA copolymer, a number of PLA copolymers have been fabricated to manipulate the properties of pure PLA. One such PLA copolymer incorporates poly(ethylene glycol) (PEG) into the polymer backbone. [85] Commonly, PEG is used in the formation of hydrogels, which are cross-linked polymers swollen with water. [86] Degradation rates of PLGA-PEG and PLA-PEG were faster than pure PLA and the degradation rate was affected by the amount of PEG relative to that of PLA or PLGA. [87] The structure of a PLA-PEG copolymer is shown in Figure 15. By combining PLA, PGA and PEG, degradation rates were tuned to approximately 65 % after 48 d. [85] Contrasted with the degradation rates listed previously (i.e. half life of 170 d), copolymerization was capable of significantly modifying the physical properties of PLA.

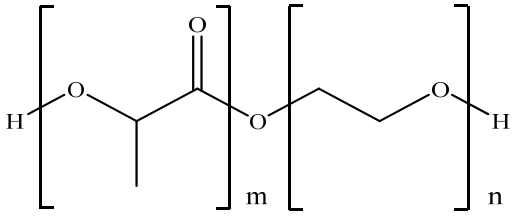

Figure 15: Structure of PLA-PEG copolymer

Polymers composed of PLA and PEG have a number of interesting properties beyond altered degradation rates that make them interesting biomaterials. A few PLA-PEG copolymers were found to have altered physical states (i.e. gel, solid, etc.) when exposed to stimuli. Thermo-reversible gels were formed when di- and tri-block PEG was combined with PLA. [88] The creation of the swelling hydrogel was dependent on the concentration of the polymer in water and was caused by differences in monomeric

hydrophilicity. At high PLA-PEG concentrations in water a hydrogel was produced, with the degree of swelling and physical state being temperature dependent. [88, 89] The temperature dependence was unique in that some PLA-PEG copolymers could be gels or liquids at lower temperatures, but could form solids at higher temperatures. [88] This characteristic is potentially valuable for an injectable polymer system in that the polymer would flow at room temperature, but would solidify after entering the body. [90] Similar PLA-PEG copolymers were shown to control cell growth during tissue engineering applications due to their ability to immobilize proteins. [91]

The last PLA copolymer described is PLA copolymerized with ε-caprolactone. When ε-caprolactone is polymerized, it forms poly(ε-caprolactone) (PCL). The structure of both ε-caprolactone and PCL are shown in Figure 16.

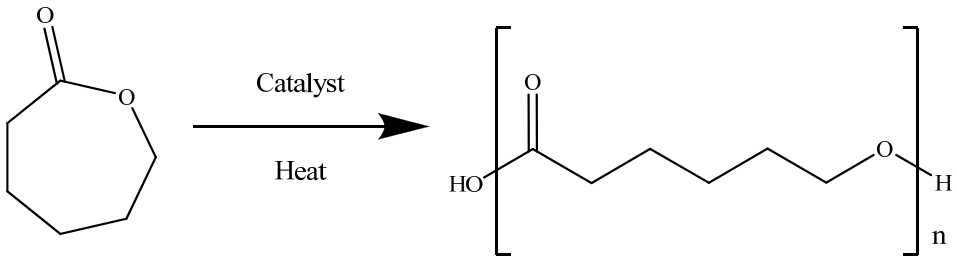

Figure 16: The structure of ε-caprolactone and PCL

Originally, PCL was investigated because it was found to be cleaved enzymatically rather than hydrolytically, reducing the degradation rate. [86, 92] The use of a PLA-PCL copolymer met early setbacks because only random copolymers could be synthesized. The copolymers possessed degradation rates faster than either of the pure compounds, which limited their application. [93] The problem was remedied by producing PLA-PCL block-copolymers, which possessed moderate degradation rates in between the

pure polymers, as well as more predictable permeation rates for implanted materials. [94] The structure of a generic PLA-PCL copolymer is shown below in Figure 17. In a study conducted by Ye et al., a copolymer composed of 32 wt% ε-caprolactone and 68 wt% lactic acid, was found to have degraded by only 5 wt% after 25 d *in vitro* at 35 °C. [93] Using organometallic catalysts, copolymerizations conducted near 150 °C have produced molecular weights of 30,000 g/mol with percent crystallinity varying between 30 % and 70 % depending on the ratios of PLLA and PCL used. [95, 96]

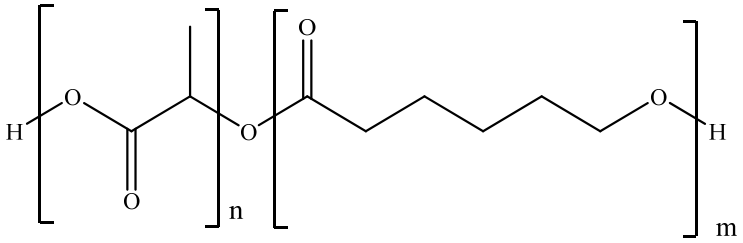

Figure 17: Structure of a copolymer consisting of PLA and PCL

While some properties of polyesters like glass transition temperature or tensile strength can be adjusted by creating copolymers, the effectiveness of copolymers is limited. Copolymerization requires that a suitable polymer additive exists and can be polymerized with the pure polymer to produce a material with the desired characteristics. Thermal degradation [97] and unstable polymerization conditions [48] can also occur during the synthesis of the copolymer. Thus, although copolymerization can create valuable materials, other chemical modifications may be necessary to produce biodegradable polyesters with the desired physical properties.

2.7 Functionalization of PLA

In the previous section, copolymerization was described as the polymerization of two or more different polymers to form a new polymer. Another technique to modify polymer properties is functionalization. The difference between functionalization and copolymerization, although vague, is that functionalization alters polymer properties by adding functional groups (also known as pendant or substituent groups) to the polymer chain, whereas copolymerization involves polymerizing two or more unfunctionalized monomers together. [98] The pendant groups most often extend from the polymer backbone, making this technique distinguishable from copolymerization. The remainder of this section highlights how functionalization can alter the physical properties of PLA and produce unique polymers with customizable properties.

There are two primary methods to facilitate the functionalization of polyesters. The first involves functionalizing the monomer, while the second involves chemically altering an already existing polymer chain. [98] Chemically modifying the monomer has proven to be successful and is preferred because the procedure increases control over the functionalization and causes fewer side reactions such as chain scission. [53] The synthesis of functionalized lactide monomers commonly occurs by replacing the methyl R group of the lactide with other functional groups. The functionalized lactides are then opened through ring opening polymerization and the corresponding polyesters are produced. The second method occurs after polymerization when the functional group is grafted to the already existing polymer chain. [99]

2.7.1 Monomer functionalization

For PLA, functionalized monomers usually refer to functionalized lactones (lactone indicates a generic R group rather than lactide, which implies a methyl group) or lactones produced from functionalized lactic acid molecules. [53] Pendant groups like benzyloxymethyl, [98, 100] hydroxymethyl [98] and 1-butene [101] were all capable of being added to the lactone monomer. The structures of a few asymmetric functionalized dimers are provided below in Figure 18. The R groups represent a methyl or hydrogen depending on whether functionalized glycolide or lactide was desired. Substituent groups from left to right are hydroxymethyl, 1-butene and benzyloxymethyl.

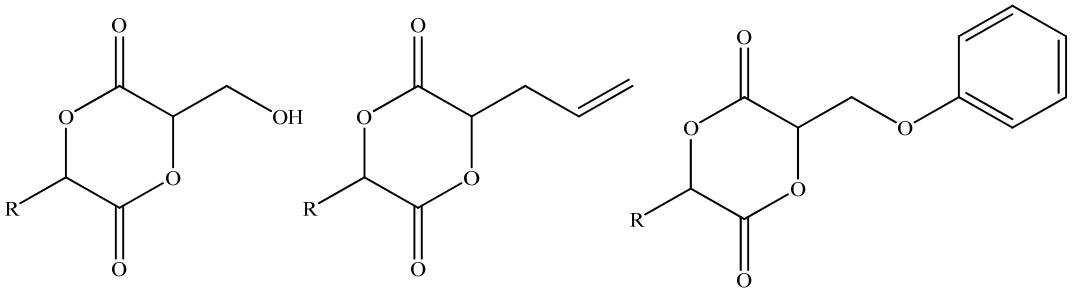

Figure 18: Structures of functionalized lactones

The functionalized lactones detailed above were created by Lee-mhuis et al. [98, 100, 101] The dimers functionalized with hydroxymethyl and benzyloxy-methyl were both produced from an L-serine derivative, O-benzyl-L-serine. A number of synthetic steps were required to convert the amino acid derivative into the functionalized lactone. For the benzyloxymethyl substituent, the initial reaction involved converting O-benzyl-L-serine into an α-hydroxy acid functionalized with benzyloxy-methyl using $NaNO_2$ and sulfuric acid in acetonitrile. Two of the functionalized α-hydroxy acid

molecules were then combined through a reaction with 2-bromopropionyl bromide, triethylamine and 4-dimethylaminopyridine (DMAP) in ice-cooled dichloromethane. Lastly, the cyclic dimer was formed by dissolving the previous product in N,N'-dimethylformamide (DMF), which was added dropwise into a Na_2CO_3 / DMF solution. The synthesis of the functionalized lactone is shown in Figure 19. Extensive extraction and purification was required to isolate the lactide and yields were compromised due to losses between steps.

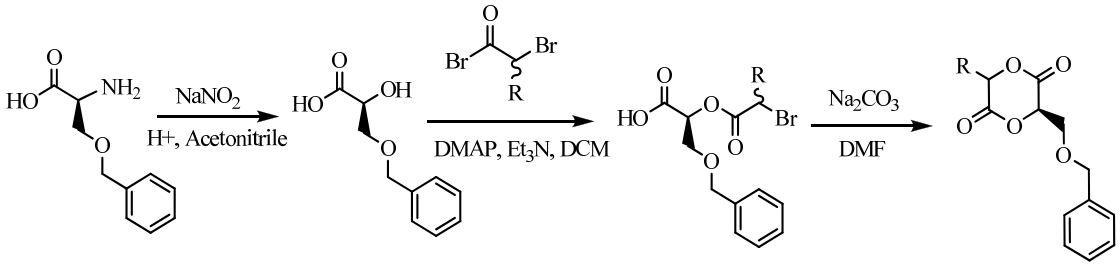

Figure 19: Synthesis of functionalized lactone from a L-serine derivative

The cyclic dimer functionalized with 1-butene was created with glyoxylic acid. [101] In this procedure, glyoxylic acid was reacted with Zn powder, $BiCl_3$ and allyl bromide in ice cold THF. Allyl bromide was added to form the α-hydroxy acid bearing the 1-butene group. The steps necessary to convert the allyl α-hydroxy acid to the ring structure were very similar to that of the previous procedure. First, a dimer was formed using bromoacetyl bromide and then the cyclic dimer was formed by reaction with a sodium carbonate solution. The synthesis of an asymmetric alkene functionalized lactone is shown in Figure 20.

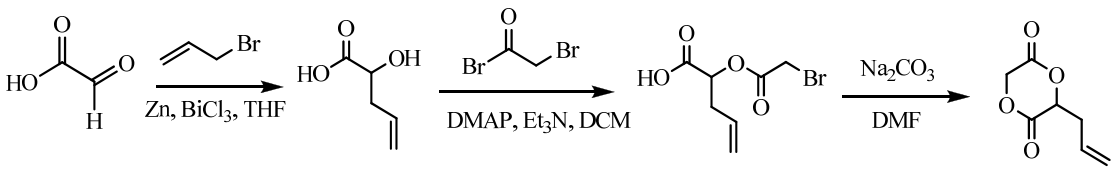

Figure 20: Synthesis of an asymmetric 1-butene lactone

Thermal properties have recently been altered by functionalization. Prior to functionalized lactones, thermal properties were adjusted by cross-linking, but the enhancement to the thermal transition was often modest. [66, 102] By contrast, when a lactone was functionalized with bulky substituents like cyclohexyl groups in place of the lactic acid methyl group, the T_g of the polyester could be increased. [103] A diagram of PLA functionalized with cyclohexyl groups is diagramed in Figure 21.

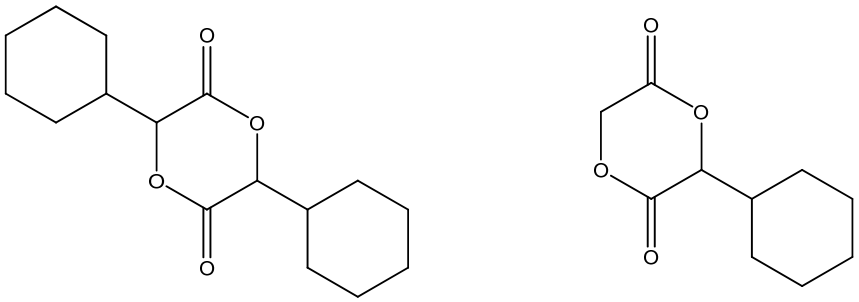

Figure 21: An example of a glycolide molecule functionalized to varying degrees with cyclohexyl groups

Jing et al. prepared the cyclohexyl substituted lactones by first dehydrogenating mandelic acid to form a cyclohexyl α-hydroxy acid. [103] The cycle was then formed through one of two synthetic pathways depending on whether a symmetric or asymmetric dimer was desired. The first involved reacting the α-hydroxy acid with *p*-toluenesulfonic acid in toluene for 6 d, while performing azeotropic distillation. The second method, for

asymmetric dimer synthesis, involved reacting the α-hydroxy acid with 2-bromoproponiyl bromide and triethylamine, forming a dimer by the synthetic methods reported by Leemhuis et al. [100, 101] The ring was closed by reaction with $NaHCO_3$ in cold acetone.

The cyclohexyl functionalized lactone was polymerized by ROP and produced a polymer with a M_n = 9,000 g/mol. [103] The polyester was found to have a T_g = 98 °C, which is 43 °C higher than that of PLA obtained from unfunctionalized lactide. [103] The T_g was altered because the large, bulky side groups increased the rigidity of the polymer backbone, which is known to increase the glass transition temperature. [104] Similarly, other research teams have generated symmetric, functionalized lactones by adding alkyl groups like ethyl, isobutyl or hexyl chains to the lactide in place of the methyl group. [104] These substituents produced polylactides with T_g of 12 °C, 22 °C and -37 °C, respectively. The structures of these molecules are presented below in Figure 22. The aliphatic functionalities from left to right are ethyl, isobutyl and hexyl substituents. It was observed that as the length of the alkyl group increased, the T_g decreased, but branching caused an increased T_g.

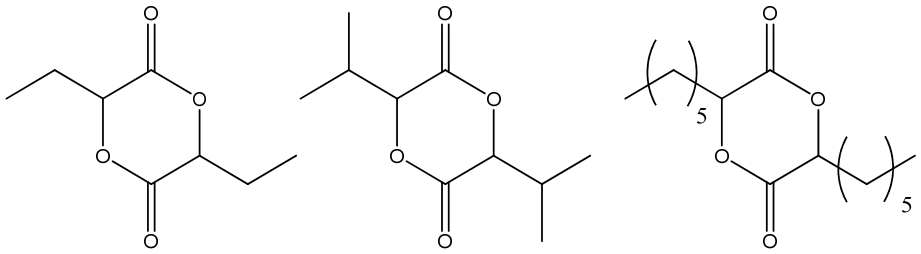

Figure 22: Allyl substituted lactides

Functionalities were also added to the monomer to alter the degradation properties of PLA. In the previous example where a lactone was functionalized with alkyl groups, [104] the degradation rate of the resulting polymer was decreased due to an increase in hydrophobicity caused by the addition of the aliphatic alkyl groups. The increase in hydrophobicity helped slow the penetration of water into the polymer and decreased the degradation rate. Other teams have synthesized lactide with phenyl functionalities as the substituent groups to alter degradation properties. [105] The aromatic modified lactone was produced by reacting phenyllactic acid with *p*-toluenesulfonic acid in xylene for 7 d. The lactide was then polymerized by ROP and degradation tests were conducted on the resulting polymer. After 30 d in a 55 °C buffer solution, a sample of phenyl-PLA had only lost 10 % of its mass, but lost 90 % of its mass after 50 d. [105]

The advantages of functionalizing a monomer prior to polymerization are that the degree of monomer functionalization can be controlled, chain cleavage can be avoided and polymer architecture may be modified. [98, 106] In addition to the functionalities outlined previously, other substituents like acetylene, [107] D-gluconic acid [108] and cyclopentene [109] have been added to the lactone ring, but were prepared by different methods. Establishing a simple and versatile synthetic procedure for the preparation of functionalized monomers is often difficult. In many of the cited sources, multi-step chemical techniques and protecting groups were necessary to produce the desired monomer. These limitations often reduce the array of functionalized polyesters that may be created because it is difficult to determine a synthetic pathway for a desired chemical

functionality. [53, 98, 100] Furthermore, these methods are not conducive to larger scale operations such as drug delivery studies.

2.7.2 Polymer functionalization

The second method of functionalization is the chemical modification of an existing polymer chain. This technique involves altering a previously synthesized polymer, rather than altering the monomer before polymerization. Recently, a PLLA chain was chemically altered to produce a sample that demonstrated surface eroding properties. The polymer was produced by reacting oligomeric PLLA (OLLA) with long, aliphatic end terminated diols like 1,8-octadiol. [16] Through a condensation reaction, the OLLA reacted with the diol, which incorporated the aliphatic diol segment into the backbone of the OLLA. To increase the molecular weight of the chains, aliphatic diacid chlorides like suberoyl chloride were used, resulting in high molecular weights of 120,000 g/mol. [16] The structure of the resulting polymer is shown below in Figure 23. The CH_2 in parentheses with n is the diol segment. The CH_2 in parentheses with the n' is the diacid chloride segment.

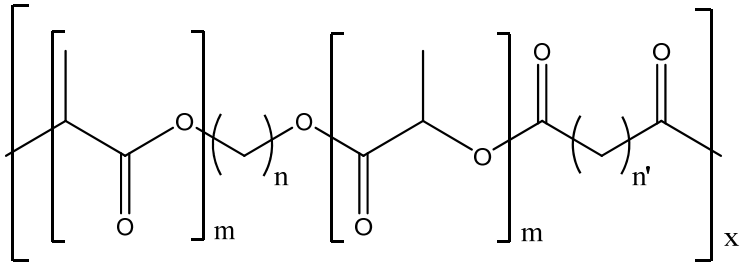

Figure 23: Surface eroding PLA

This reaction has been classified as post polymerization modified because OLLA chains were functionalized, while the monomers were not. The achievement of surface eroding PLA is exciting because surface eroding polymers have a number of advantages over bulk eroding plastics, but the only known unaltered surface eroding polymers are poly(anhydrides) and poly(orthoesters). [9, 110]

Strong bases such as lithium N,N'-diisopropyl amide (LDA) have been used to functionalize existing polymer chains by deprotonating the carbon adjacent to the terminal carboxylic acid group. [111] In doing so, a carbocation was formed that could react with an electrophile. Saulnier et al. added the electrophile bromoacetic acid benzyl ester after reacting PLA with LDA to form functionalized PLA. [111] A diagram of the reaction is presented below in Figure 24 where the R group is either a methyl or a hydrogen. In a similar procedure developed by the same team, PCL was functionalized using LDA. [112] Pendant groups added to PLC included unsaturated alkane groups, halides, alkenes and other hydrophilic groups. [113, 114]

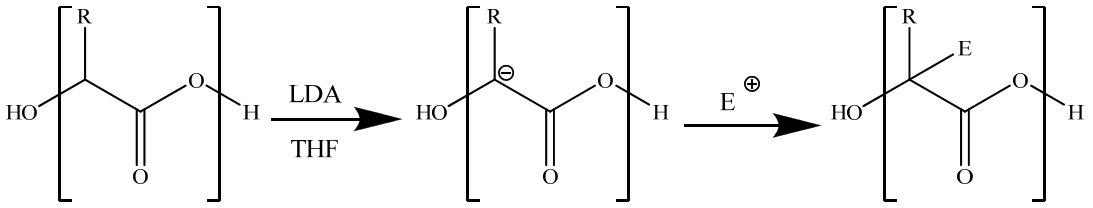

Figure 24: A schematic of a polymer functionalization induced by a strong base

The pros and cons of the second method were thought to be the opposite of those concerning functionalized monomer synthesis. The synthetic steps necessary to create the desired polyester were somewhat easier, but the ease of adjustment was coupled with

a decreased ability to control the level of functionality and an increased risk of chain scission. [98] Also, harsh chemicals are often used, which made purification of the resulting polymer vital if the material was to be used for medical applications.

2.8 Summary and Project Objectives

Biodegradable polyesters hold great promise as biomaterials. Polyesters like PLA are becoming increasingly popular as solutions to current material problems in medicine because of their biocompatibility and favorable physical properties. Despite the success of biodegradable polyesters, the properties of the pure polymers are not always suitable for a particular application. Conventionally, synthetic approaches to modified polymers have focused on copolymers of PLA and other polymers in efforts to surmount the material restrictions of unaltered PLA. While copolymers have met a certain degree of success, this technique is inherently limited because a suitable copolymer may not exist.

Polymer functionalization is one area of research that has focused on tailoring polyester properties by adding pendant functional groups. Using this technique, new materials can be made that are not limited by the structures of current biocompatible polymers. Functionalization appears to be a viable solution to many current polymer problems, but in practice, very few practical examples of polyester functionalization exist in the literature. Although a large volume of research has been conducted on functionalized polyesters, the experimental methods necessary are complicated and are generally limited in their ability to create a diverse range functionalities. Furthermore,

the necessary synthetic methods often require multiple steps, protecting groups and complicated chemical procedures. [25, 115]

Due to these difficulties, the goal of this thesis is to develop experimental methods capable of producing functionalized α-hydroxy acids and ultimately, tailored biodegradable polyesters with adjustable properties. There are two significant hurdles to overcome when trying to produce functionalized polyesters. First, the desired functionalized monomer must be produced and secondly, an efficient polymerization method must be developed that yields controllable molecular weights. The remainder of this thesis investigates techniques towards synthesizing novel, amido-functionalized biodegradable polyesters.

2.9 References

(1) Scheirs, J.; Long, T. *Modern Polyesters: Chemistry and Technology of Polyesters and Copolyesters;* Wiley: 2003; pp 3.
(2) Paul, D. *Encyclopedia of Polymer Science and Engineering;* 1985; Vol. 12, pp 118.
(3) Pang, K.; Tonelli, A. et al. *Progress in Polymer Science* **2006**, *31*, 1009.
(4) Carothers, W. *Journal of the American Chemical Society* **1929**, *51*, 2548.
(5) Lee, J. W.; Bright, F. et al. *Pharmaceutical Research.* **2003**, *20*, 149.
(6) Katti, D. S.; Langer, R. et al. *Advanced Drug Delivery Reviews* **2002**, *54*, 933.
(7) Vert, M.; Garreau, H. et al. *Journal of Controlled Release* **1991**, *16*, 15.
(8) Vert, M.; Mauduit, J. et al. *Biomaterials* **1994**, *15*, 1209.
(9) Gopferich, A. *Biomaterials* **1996**, *17*, 103.
(10) Pan, P.; Inoue, Y. *Progress in Polymer Science* **2009**, *34*, 605.
(11) Middleton, J.; Tipton, A. *Medical Plastics and Biomaterials* **1998**, *5*, 30.
(12) Vert, M.; Garreau, H. et al. *Clinical Materials* **1992**, *10*, 3.
(13) Burkersroda, F. v.; Göpferich, A. et al. *Biomaterials* **2002**, *23*, 4221.
(14) Tamada, J.; Langer, R. *Proceedings of the National Academy of Science (USA)* **1993**, *90*, 552.
(15) Vogel, B. M.; Mallapragada, S. K. *Biomaterials* **2005**, *26*, 721.
(16) Xu, X.; Prasad, S. et al. *Biomaterials* **2006**, *27*, 3021.
(17) Uhrich, K.; Shakesheff, K. et al. *Chemical Reviews* **1999**, *99*, 3181.
(18) Narayanan, N.; Srivastava, A. et al. *Journal of Biotechnology* **2004**, *7*, 167.
(19) Vu, D.; Miller, D. et al. *Fluid Phase Equilibrium* **2005**, *236*, 125.
(20) de Santis, P.; Kovacs, A. J. *Biopolymers* **1968**, *6*, 299.
(21) Mochizuki, M.; Hirami, M. *Polymers for Advanced Technologies* **1997**, *8*, 203.
(22) Kulkarni, R.; Leonard, F. et al. *Journal of Biomedical Materials Research* **1971**, *5*, 169.
(23) Maharana, T.; Negi, Y. et al. *Progress in Polymer Science* **2009**, *34*, 99.
(24) Gupta, B.; Hilborn, J. et al. *Progress in Polymer Science* **2007**, *32*, 455.
(25) Drumright, R.; Henton, D. et al. *Advanced Materials* **2000**, *12*, 1841.
(26) Greene, J. *Journal of Polymers and the Environment* **2007**, *15*, 269.
(27) Kale, G.; Singh, S. et al. *Packaging Technology and Science* **2007**, *20*, 49.
(28) Gu, S.; Ren, J. et al. *Polymer International* **2008**, *57*.
(29) Ajioka, M.; Yamaguchi, A. et al. *Journal of Polymers and the Environment* **1995**, *3*.
(30) Dutkiewicz, S.; Tomaszewski, W. et al. *Fibers and Textiles in Eastern Europe* **2003**, *11*, 66.
(31) Ajioka, M.; Kashima, T. et al. *Polymer Degradation and Stability* **1998**, *59*, 137.
(32) Neises, B.; Steglich, W. *Angewandte Chemie International Edition* **1978**, *17*, 522.
(33) Moore, J.; Stupp, S. *Macromolecules* **1990**, *23*, 65.
(34) Wagener, K.; O'Gara, J. et al. *Journal of Macromolecular Science* **1994**, *A31*, 775.
(35) Bucholtz, B. US Patent 5302694, 1994.
(36) Zhao, H.; Greenwald, R. et al. *Journal of Organic Chemistry.* **1998**, *63*, 7559.
(37) Albertsson, A.; Varma, I. *Biomacromolecules* **2003**, *4*, 1466.
(38) Edlund, U.; Albertsson, A. *Advanced Drug Delivery Reviews* **2003**, *55*, 585.

(39) Hyon, S.; Ikada, Y. et al. *Biomaterials* **1997**, *18*, 1503.
(40) Gilding, D.; Reed, A. *Polymer* **1979**, *20*, 1459.
(41) Tsuji, H.; Fujie, K. et al. *Polymer Degradation and Stability* **2003**, *81*, 501.
(42) Muller, M. US Patent 5053522, 1991.
(43) Noda, M.; Okuyama, H. *Chemical Pharmaceutical Bulletin* **1999**, *4*, 467.
(44) Mecerreyes, D.; Jerome, R. *Macromolecular Chemistry and Physics* **1999**, *200*, 2581.
(45) Kricheldorf, H.; Kreiser-Saunders, I. *Macromolecular Symposia* **1996**, *103*, 85.
(46) Brode, G.; Koleske, J. *Journal of Macromolecular Science* **1972**, *A6*, 1109.
(47) Södergård, A.; Stolt, M. *Progress in Polymer Science* **2002**, *27*, 1123.
(48) Takacs, E.; Vlachopoulos, J. *Plastics Engineering* **2008**, *9*, 28.
(49) Ovitt, T.; Coates, G. *Journal of the American Chemical Society* **2002**, *7*, 1316.
(50) Spassky, N. *Ring Opening Polymerization;* Rapra Technology Ltd.: 1995; Vol. 8, pp 5.
(51) Nieuwenhuis, J. *Clinical Materials* **1992**, *10*, 59.
(52) Kricheldorf, H. *Chemosphere* **2001**, *43*, 49.
(53) Dechy-Cabaret, O.; Bourissou , D. et al. *Chemical Reviews* **2004**, *104*, 6147.
(54) Wang, C.; Zhao, X. et al. *Biomaterials* **2004**, *25*, 5797.
(55) Kricheldorf, H.; Lee, S. *Polymer* **1995**, *36*, 2995.
(56) Bhaw-Luximon, A.; Belleney, J. et al. *Polymer* **2001**, *42*, 9651.
(57) Gupta, M.; Deshmuhk, V. *Colloid and Polymer Science* **1982**, *260*, 308.
(58) Kricheldorf, H.; Dunsing, R. *Die Makromolekulare Chemie* **1986**, *187*, 1611.
(59) Ray, L.; Ghosh, P. et al. *Journal of Organometallic Chemistry* **2007**, *692*, 4259.
(60) Albertsson, A.; Srivastava, R. *Advanced Drug Delivery Reviews* **2008**, *60*, 1077.
(61) Schmid, R.; Verger, R. *Angewandte Chemie International Edition* **1998**, *37*, 1608.
(62) Södergård, A.; Näsman, J. *Polymer Degradation and Stability* **1994**, *46*, 25.
(63) Södergård, A.; Näsman, J. *Industrial and Engineering Chemistry Review* **1996**, *35*, 732.
(64) Södergård, A.; Näsman, J. et al. *Polymer Degradation and Stability* **1996**, *51*, 351.
(65) Södergård, A.; Näsman, J. et al. *Industrial and Engineering Chemistry Review* **1995**, *34*, 1203.
(66) Nijenhuis, A.; Pennings, A. et al. *Polymer* **1996**, *37*, 2783.
(67) Moon, S.; Kimura, Y. et al. *Journal of Polymer Chemistry* **2000**, *39*, 1673.
(68) Miyoshi, R.; Sakai, T. et al. *International Polymer Processing* **1996**, *11*, 320.
(69) Zhong, W.; Yang, Y. et al. *Journal of Applied Polymer Science* **1999**, *74*, 2546.
(70) Hiltunen, K.; Harkone, M. et al. *Journal of Applied Polymer Science.* **1997**, *63*, 1091.
(71) Nagasawa, N.; Tamada, M. et al. *Nuclear Instruments and Methods in Physics Research Section B* **2005**, *236*, 611.
(72) Yoshii, F.; Kume, T. et al. *Nuclear Instruments and Methods in Physics Research Section B* **2003**, *208*, 370.
(73) Peng, W.; Liuyi, T. et al. CN Patent 1594394 A, 2005.
(74) Moon, S.; Kimura, Y. *Polymer* **2001**, *42*, 5059.
(75) Middleton, J.; Tipton, A. *Biomaterials* **2000**, *21*, 2335.
(76) Reed, A.; Gilding, D. *Polymer* **1981**, *22*, 494.

(77) Cohn, D.; Marom, G. et al. *Polymer* **1987**, *28*, 2018.
(78) Ferruti, P.; Deghenghi, R. et al. *Biomaterials* **1995**, *16*, 1423.
(79) Athanasiou, K.; Agrawal, M. et al. *Biomaterials* **1996**, *17*, 93.
(80) Yoshida, M.; Matsuda, K. et al. *International Journal of Pharmaceuticals* **1995**, *115*, 61.
(81) Mooney, D. L.,Robert et al. *Biomaterials* **1996**, *17*, 1417.
(82) Shawe, S.; Farrar, D. et al. *Journal of Material Science* **2006**, *41*, 4832.
(83) Takahashi, K.; Kimura, Y. et al. *Polymer* **2000**, *41*, 8725.
(84) Subarna, S. Dissertation: *Synthesis of Biodegradable Poly Lactic Acid Polymers*, University of Poona, 2003.
(85) Kim, K.; Hadjiargyrou, M. et al. *Biomaterials* **2003**, *24*, 4977.
(86) Ratner, B.; Peppas, N. Eds.; In *Biomaterials Science: An Introduction to Materials in Medicine;* Elsevier Academic Press: 2004; pp 100.
(87) Penco, M.; Deghenghi, R. et al. *Biomaterials* **1996**, *17*, 1583.
(88) Jeong, B.; Kim, S. et al. *Journal of Polymer Science* **2000**, *37*, 751.
(89) Jeong, B.; Wan, S. et al. *Colloids and Surfaces B: Biointerfaces* **1999**, *16*, 185.
(90) Jeong, B.; Kim, S. et al. *Journal of Controlled Release* **1999**, *62*, 109.
(91) Tessmar, J.; Göpferich, A. et al. *Biomaterials* **2003**, *24*, 4475.
(92) Penco, M.; Di Landro, L. et al. *European Polymer Journal* **2000**, *36*, 901.
(93) Ye, W. P.; Xu, Y. et al. *Reactive and Functional Polymers* **1997**, *32*, 161.
(94) Ye, W.; Chien, Y. *Journal of Controlled Release* **1996**, *41*, 259.
(95) Lostocco, M.; Huang, S. et al. *Polymer Degradation and Stability* **1998**, *59*, 303.
(96) Kister, G.; Vert, M. et al. *Polymer* **2000**, *41*, 925.
(97) Signori, F.; Bronco, S. et al. *Polymer Degradation and Stability* **2009**, *94*, 74.
(98) Leemhuis, M.; Hennink, W. et al. *Macromolecules* **2006**, *39*, 3500.
(99) Nadeau, V.; Hildgen, P. et al. *Polymer* **2005**, *46*, 11263.
(100) Leemhuis, M.; Hennink, W. et al. *European Journal of Organic Chemistry* **2003**, *2003*, 3344.
(101) Leemhuis, M.; Hennink, W. et al. *European Polymer Journal* **2008**, *44*, 308.
(102) Grijpma, D.; Pennings, A. et al. *Polymer Bulletin* **1991**, *25*, 327.
(103) Jing, F.; Baker, G. et al. *Macromolecules* **2007**, *20*, 9304.
(104) Yin, M.; Baker, G. *Macromolecules* **1999**, *32*, 7711.
(105) Simmons, T.; Baker, G. *Biomacromolecules* **2001**, *2*, 658.
(106) Finne, A.; Albertsson, A. C. *Journal of Polymer Science* **2003**, *42*, 444.
(107) Parrish, B.; Emrick, T. et al. *Journal of the American Chemical Society* **2005**, *127*, 7404.
(108) Marcincinova-Benabdillah, K.; Vert, M. et al. *Biomacromolecules* **2001**, *2*, 1279.
(109) Parrish, B.; Emrick, T. *Macromolecules* **2004**, *37*, 5863.
(110) Göpferich, A.; Tessmar, J. *Advanced Drug Delivery Reviews* **2002**, *54*, 911.
(111) Saulnier, B.; Vert, M. et al. *Macromolecular Bioscience* **2004**, *4*, 232.
(112) Ponsart, S.; Vert, M. et al. *Biomacromolecules* **2000**, *1*, 275.
(113) Detrembleur, C.; Jermome, R. et al. *Macromolecules* **2000**, *33*, 14.
(114) Lou, X.; Jerome, R. et al. *Macromolecular Rapid Communications* **2003**, *24*, 161.
(115) Collins, J. M. *Journal of Clinical Oncology* **1984**, *2*, 498.

CHAPTER THREE:

MATERIALS AND METHODS

3.1 Materials

All of the chemicals unless otherwise mentioned were purchased from Sigma-Aldrich (St. Louis, MO). Ethanol was purchased from Pharmco-Aaper (Brookfield, CT). Magnesium sulfate was purchased from Fischer Scientific (Rochester, NY). Scandium (III) triflate was purchased from Oakwood Products, Inc. (West Columbia, SC). The deuterated solvents, *d*-chloroform and *d6*-dimethyl sulfoxide, were purchased from Cambridge Isotope Laboratories, Inc. (Andover, MA). Dried solvents (tetrahydrofuran, benzene, hexanes and dichloromethane) were obtained from the Department of Chemistry at Bucknell University and no further drying was conducted by the author. The solvents were dried by passage through a column of activated alumina. Lastly, all solvents and chemicals were used as obtained unless otherwise indicated.

3.2 Instrumentation

Thermal analyses of products were conducted with Thermal Gravimetric Analysis (TGA) and Differential Scanning Calorimetry (DSC). A TA Instruments (Newcastle, DE) SDTQ600 TGA and a TA Instruments Q1000 DSC were used. Results from both instruments were analyzed with TA Universal Analysis software. For TGA, 10-20 mg of a sample was heated at a rate of 10 °C per min under a nitrogen atmosphere in a platinum crucible. For DSC, 5-10 mg of a sample was heated at a rate of 10 °C per min under a

nitrogen atmosphere in a hermetic aluminum pan and referenced to an empty pan. Results from DSC trials are reported upon heating. Two cycles were conducted to erase possible thermal history and all reported thermal information was calculated from the second pass.

Molecular weights were determined by Gel Permeation Chromatography (GPC). To perform GPC, a Hewlett-Packard (Palo Alto, CA) 1090 High Performance Liquid Chromatograph equipped with two 300 mm (I.D. 7.5 mm) PLgel 10μm MIXED-B organic GPC columns was employed. Tetrahydrofuran was used as the eluent and samples were tested at a rate of 1 mL per min. All trials were conducted at room temperature. Eluent passed through a Grace (Deerfield, IL) Linear UVIX-205 Ultraviolet Absorbance Detector, a Wyatt (Dernbach, Germany) miniDAWN Treos Multi-Angle Light Scattering Detector and a Hewlett-Packard 1037A Refractive Index Detector. Varian Inc. (Palo Alto, CA) polystyrene Low EasiVials standards (12 polystyrene samples ranging from 38,600 g/mol to 100 g/mol (M_n)) and narrow-distribution polystyrene samples from Scientific Polymer Products (197,000 g/mol, 8,900 g/mol and 4,800 g/mol (M_n)) were used to calibrate the retention time of the columns. Samples were prepared at approximately 3 mg/mL concentration in THF and filtered through a Whatman (Springfield Mill, UK) 0.02 micron membrane filter. A 0.5 μL injection loop was used for inserting samples into the chromatography columns.

Chemical structures were verified with Infrared Spectroscopy (IR) and Nuclear Magnetic Resonance (NMR). Fourier Transform Infrared Spectroscopy (FTIR) was performed using a Thermo Scientific (Waltman, MA) Nicolet 380 FTIR. The sample

was analyzed with 128 scans after background collection. ^{1}H NMR spectra were obtained using a Varian Inc. VXR 400 MHz spectrometer. All compounds were characterized in either deuterated chloroform ($CDCl_3$) (99.8%-*d*) or deuterated dimethyl sulfoxide (DMSO) (99.9%-*d*). Chemical shifts were calibrated to the residual solvent peaks: $CDCl_3$ (δ = 7.26 ppm) or DMSO (δ = 2.50 ppm).

3.3 Experimental Methods

The experimental methods section of this thesis is broken into three sections: monomer synthesis, melt polycondensation and solution polymerization. The monomer synthesis section details the procedures to produce all four monomers. The melt polycondensation section details the formation of melt synthesized polymers and the effects of catalysts on this system. Lastly, the synthetic methods to produce polymers generated through solution polymerization are outlined.

3.3.1 General synthesis of amido-functionalized α-hydroxy acids

Amido-functionalized α-hydroxy acids were prepared by reacting glyoxylic acid monohydrate with a primary or secondary amide. The reaction occurred by introducing both glyoxylic acid and the amide into a solvent, which was stirred continuously for the duration of the reaction. Care was taken to avoid exposing certain monomers to full vacuum as a severe reduction in pressure induced the early stages of polymerization. These monomers were dried under less rigorously reduced pressure, supplied by a house vacuum line. If the possibility for spontaneous polymerization under full vacuum

existed, drying was conducted in house vacuum. The use of house vacuum versus full vacuum is indicated for a specific monomer.

3.3.1.1a Solution synthesis of 2-(2-pyrrolidino)-2-hydroxyacetic acid (PYR)

To a 125 mL Erlenmeyer flask, glyoxylic acid monohydrate (GA) (50 mmol, 4.60 g) and a magnetic stir bar were added. Diethyl ether (75 mL) was added and stirred. To the suspension, 2-pyrrolidone (47.5 mmol, 4.04 g, 3.60 mL) was added and the flask was sealed with a rubber septum. The reaction was carried out overnight at room temperature with constant stirring. Upon completion, a white solid precipitated from the reaction medium. The crude product was vacuum filtered and rinsed with diethyl ether (3 x 30 mL). The solid was dried under reduced vacuum (≈ 50.8 kPa) for 12 h. After drying, the monomer was dissolved in hot ethyl acetate (≈ 65 °C) at a ratio of 1 mL per 100 mg of product. The solution was cooled to room temperature and then placed in a -10 °C freezer overnight. The resulting solid precipitate was vacuum filtered, rinsed with diethyl ether (3 x 30 mL) and then dried under vacuum (≈ 50.8 kPa) overnight at room temperature.

3.3.1.1b Melt synthesis of 2-(2-pyrrolidino)-2-hydroxyacetic acid (PYR)

To a 125 mL Erlenmeyer flask, GA (50 mmol, 4.60 g) and a magnetic stir bar were added. The flask was sealed with a rubber septum and heated to 60 °C under a nitrogen purge for 1 h. To the molten GA, 2-pyrrolidone (47.5 mmol, 4.04 g, 3.60 mL) was syringed into the flask. The reaction was carried out overnight at room temperature

with constant stirring. Upon completion, a clear viscous solid was obtained. The crude monomer was dissolved in hot ethyl acetate (≈ 65 °C) at a ratio of 1 mL per 100 mg of crude product. The solution was cooled to room temperature and then placed in a -10 °C freezer overnight. The resulting solid precipitate was vacuum filtered, rinsed with diethyl ether (3 x 30 mL) and then dried under reduced vacuum (≈ 50.8 kPa) overnight at room temperature.

3.3.1.2 Synthesis of 2-benzamdio-2-hydroxyacetic acid (BZ)

To a 125 mL Erlenmeyer flask was added GA (50 mmol, 4.60 g) and a magnetic stir bar. Diethyl ether (75 mL) was added and stirring was initiated. To the suspension, benzamide (47.5 mmol, 5.75 g) was added and the flask was closed with a rubber septum. The reaction was carried out overnight at room temperature under constant stirring. Upon completion, a white solid was obtained. The solid was vacuum filtered and rinsed with diethyl ether (3 x 30 mL). The solid was dried under full vacuum (≈ 102 kPa) for 12 h. After drying, the monomer was dissolved in hot ethanol (≈ 65 °C) at a ratio of 1 mL per 100 mg of product. The solution was cooled to room temperature and then placed in a -10 °C freezer overnight. The resulting precipitate was vacuum filtered, rinsed with diethyl ether (3 x 30 mL) and dried under full vacuum (≈ 102 kPa) at room temperature.

3.3.1.3 Synthesis of 2-acrylamido-2-hydroxyacetic acid (ACRY)

To a 125 mL Erlenmeyer flask wrapped with aluminum foil was added GA (50 mmol, 4.60 g) and a magnetic stir bar. Ethyl acetate (75 mL) was added and stirring was initiated. To the slurry, acrylamide (47.5 mmol, 3.37 g) was added and the flask was closed with a rubber septum. The reaction was carried out overnight at 50 °C under constant stirring. Upon completion, a white solid precipitated from the reaction medium. The solid was vacuum filtered and rinsed with diethyl ether (3 x 30 mL). The solid was dried under full vacuum (≈ 102 kPa) for 12 h. After drying, the monomer was dissolved in boiling water at a ratio of 1 mL per 100 mg of product. The solution was cooled to room temperature and then placed in a 10 °C refrigerator overnight. The resulting precipitate was vacuum filtered, rinsed with cold water (3 x 30 mL) and dried under full vacuum (≈ 102 kPa) at room temperature overnight.

3.3.1.4 Synthesis of 2-acetamido-2-hydroxyacetic acid (ACE)

To a 125 mL Erlenmeyer flask was added GA (50 mmol, 4.60 g) and a magnetic stir bar. Diethyl ether (75 mL) was added and stirring was initiated. To the slurry, acetamide (47.5 mmol, 2.81 g) was added and the flask was closed with a rubber septum. The reaction was carried out overnight at room temperature under constant stirring. Upon completion, a clear viscous gel was formed. The diethyl ether was removed by rotary evaporation and the product was dried under house vacuum (≈ 50.8 kPa) for 24 h at room temperature. After drying, a clear to white gel was obtained and the product was not purified further.

3.3.2 General melt polycondensation of amido-functionalized α-hydroxy acids

Melt polycondensation of the following α-hydroxy acids was performed by heating a sample above its melting temperature and exposing the sample to vacuum. The polymerizations were done in a Kugelrohr vacuum distillation apparatus. Catalytic melt polycondensation reactions were conducted by adding a specified quantity of catalyst to the α-hydroxy acid or to the oligomers produced from uncatalyzed melt polycondensation reactions.

3.3.2.1 Melt polycondensation of oligo(2-(2-pyrrolidino)-2-hydroxyacetic acid) (OPYR)

To a 100 mL round bottom flask was added recrystallized PYR (0.63 mmol, 100 mg) prepared as described previously in section 3.3.1.1. The flask was connected to a Kugelrohr vacuum distillation apparatus, heated to 100 °C and full vacuum (≈ 102 kPa) was applied. Both the flask and the exterior glassware were flame dried during system start-up. The rotation mechanism of the apparatus was not used. The reaction was allowed to proceed for 24 h. Upon completion of the reaction, a clear to faint yellow solid was produced. The product was purified by dissolution in 1 mL of chloroform and precipitation into 10 mL of diethyl ether. The resulting white, viscous product was separated by vacuum filtration through a previously cooled, medium porosity sintered glass frit. The product was rinsed with cold diethyl ether (3 x 15 mL) and dried under full vacuum (≈ 102 kPa) at room temperature.

3.3.2.2 Melt polycondensation of oligo(2-acetamido-2-hydroxyacetic acid) (OACE)

To a 100 mL round bottom flask was added ACE (0.75 mmol, 100 mg), prepared as described in section 3.3.1.4. The flask was connected to a Kugelrohr vacuum distillation apparatus, heated to 70 °C and full vacuum (≈ 102 kPa) was applied. Both the flask and the exterior glassware were flame dried during system start-up. The rotation mechanism of the apparatus was not utilized. The reaction was allowed to proceed for 24 h. Upon completion of the reaction, a clear to faint yellow solid was produced. The polymer was not purified further as no suitable precipitation procedure was determined.

3.3.2.3 Catalytic melt polycondensation of oligo(2-(2-pyrrolidino)-2-hydroxyacetic acid) (OPYR) from PYR monomer with Zn dust

To a 100 mL round bottom flask was added recrystallized PYR (0.63 mmol, 100 mg) prepared as described in section 3.3.1.1. Five weight percent Zn dust (0.076 mmol, 5 mg) was added and the flask was connected to a Kugelrohr vacuum distillation apparatus. The flask was heated to 100 °C and full vacuum (≈ 102 kPa) was applied. Both the flask and the exterior glassware were flame dried during system start-up, while under full vacuum. The rotation mechanism of the apparatus was not utilized. The reaction was allowed to proceed for 24 h. Upon completion of the reaction, a clear, light yellow solid was produced. The polymer was purified by dissolution in 1 mL of chloroform and vacuum filtered through a medium porosity, sintered glass frit to remove insoluble materials. The frit was rinsed with 5 mL of chloroform and the solvent was

removed by rotary evaporation. The product was dried under full vacuum (≈ 102 kPa) for 12 h at room temperature, yielding a viscous solid.

3.3.2.4 Catalytic melt polycondensation of OPYR with Zn dust

To a 100 mL round bottom flask was added OPYR (0.14 mmol, 100 mg) prepared as described in section 3.3.2.1. One weight percent Zn dust (0.015 mmol, 1 mg) and one weight percent *p*-toluenesulfonic acid monohydrate (0.005 mmol, 1 mg) were added and the flask was connected to a Kugelrohr vacuum distillation apparatus. The flask was heated to 125 °C and full vacuum (≈ 102 kPa) was applied. Both the flask and the exterior glassware were flame dried during system start-up, while under full vacuum. The rotation mechanism of the apparatus was not utilized. The reaction was allowed to proceed for 24 h. Upon completion of the reaction, a tan solid was produced. The polymer was purified by dissolution in 1 mL of chloroform and vacuum filtered through a medium porosity, sintered glass frit to remove insoluble materials. The frit was rinsed with 5 mL of chloroform and the solvent was removed by rotary evaporation. The product was dried under full vacuum (≈ 102 kPa) for 12 h, yielding a viscous solid.

3.3.3 General solution polyesterification of amido-functionalized α-hydroxy acids

Solution polyesterification was conducted for monomers that degraded during melt polycondensation polymerization. The polyesterification method described involves reacting the α-hydroxy acid and a carbodiimide in a dry solvent to yield polymer.

Reactions were carried out at low reaction temperatures for a specified amount of time and the reaction was then allowed to warm to room temperature until completion.

3.3.3.1 Solution Polyesterification of oligo(2-benzamdio-2-hydroxyacetic acid) (OBZ)

To a 50 mL Erlenmeyer flask was added recrystallized BZ (0.31 mmol, 50 mg), prepared as described in section 3.3.1.2, scandium (III) triflate (ScTrf) (0.16 mmol, 77 mg), 4-dimethylaminopyridine (DMAP) (0.78 mmol, 95 mg) and a magnetic stir bar. The flask was sealed with a rubber septum and flame dried under a nitrogen purge. Care was taken not to contact the reagents with the flame. Dry dichloromethane (1 mL) was syringed into the vessel and stirring was conducted for 15 min, resulting in a suspension. The mixture was then cooled to -10 °C for 1 h. After cooling, the vessel was placed in a salt-ice water bath and stirred. N,N'-Diisopropylcarbodiimide (DiPC) (0.81 mmol, 102 mg, 0.13 mL) was added by syringe and the reaction was allowed to react in the ice bath for 30 min. The vessel was then removed from the ice bath and allowed to react at room temperature for an additional 2 h. The reaction mixture was then filtered through a medium porosity, sintered glass frit to remove any insoluble material and the filter cake was rinsed with dry dichloromethane (3 x 5 mL) to remove any trapped product. The resulting organic layer was washed successively with 0.1 M HCl (2 x 15 mL), 0.1 M $NaHCO_3$ (1 x 15 mL) and deionized H_2O (1 x 15 mL). The organic layer was then dried with $MgSO_4$ and the solvent was removed by rotary evaporation. Upon drying for 12 h under full vacuum (≈ 102 kPa), a white solid was obtained.

CHAPTER FOUR:

MONOMER SYNTHESIS

4.1 Introduction to Results and Discussion

The following three chapters contain the results and discussion sections of this thesis and detail the synthesis of amido-functionalized α-hydroxy acids and their subsequent polymerization. The synthesis of four functionalized α-hydroxy acid monomers is described in Chapter Four. In the next chapter, Chapter Five, results from experimentation with melt polycondensation of compatible monomers is outlined. Lastly, results from solution polymerization experiments conducted on monomers incapable of undergoing melt-polycondensation are described in Chapter Six. All of these chapters describe attempts at synthesizing amido-functionalized, biodegradable polyesters with tailored physio-chemical properties for improved drug delivery.

4.2 Introduction to Amido-Functionalized α-Hydroxy Acid Synthesis

The general synthetic procedures to produce the amido-functionalized α-hydroxy acids (α-HAs) presented in this text were developed largely by Dov Ben-Ishai et al., beginning in the mid 1970's. [1-5] The α-HAs were originally created as starting materials for multi-step synthesis, such as the creation of synthetic α-amino acids or other biologically active compounds. The value of this reaction is that glyoxylic acid and a primary or secondary amide bearing any functionality are combined to form the corresponding α-HA. The reaction was chosen largely because of its versatility. A wide

range of glyoxylic acid adducts can be created and consequently, a wealth of functionalized monomers can be produced.

The simplicity of this reaction is in contrast to most reported methods of functionalized monomer synthesis, as these procedures often require complex synthetic methods to yield the desired monomer (see section 2.7 for a detailed summary). [6-8] The primary structural constraint imposed by this method is the functionality of the resulting monomer will contain an amido group. This feature is a consequence of the amide or carbamate (also known as a urethane) used in the synthesis of the α-HA. The structure of these functionalities is depicted below in Figure 25. The R group can be either a hydrogen atom or another functional group (halo, aryl, alkyl, etc.) and the R' group can be any number of functional groups (halo, aryl, alkyl, etc.).

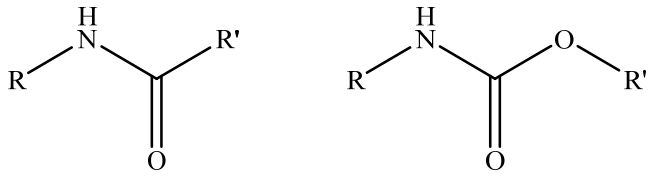

Figure 25: From left to right, amide and carbamate functionalities

Although a few α-HAs have been produced using this synthesis, [2, 5, 9] to the best of the author's knowledge there is little information in the literature concerning the optimization of the reactions or the development of improved synthetic procedures. Due to these inadequacies, it was desired to analyze the reactions of glyoxylic acid and different amides in greater depth to better understand the reaction and its application for the synthesis of new amido-functionalized α-HAs. The reaction between glyoxylic acid and 2-pyrrolidone served as a model reaction and is presented in the following

subsection. The ensuing text in this chapter serves to describe the results from experiments performed into the synthesis of four amido-functionalized α-HAs.

4.3 Synthesis of 2-(2-Pyrrolidino)-2-Hydroxyacetic Acid (PYR)

4.3.1 The general synthesis of PYR

The monomer 2-(2-pyrrolidino)-2-hydroxyacetic acid (PYR) was produced by the reaction of glyoxylic acid monohydrate (GA) and 2-pyrrolidone. The abbreviation PYR was given to this α-HA in reference to the substituent group added to GA, 2-pyrrolidone. Following a procedure detailed by Boaz, [10] GA and 2-pyrrolidone were reacted at a mol ratio of 1.2:1 (GA:2-pyrrolidone) in diethyl ether at room temperature. The reaction is shown in Figure 26.

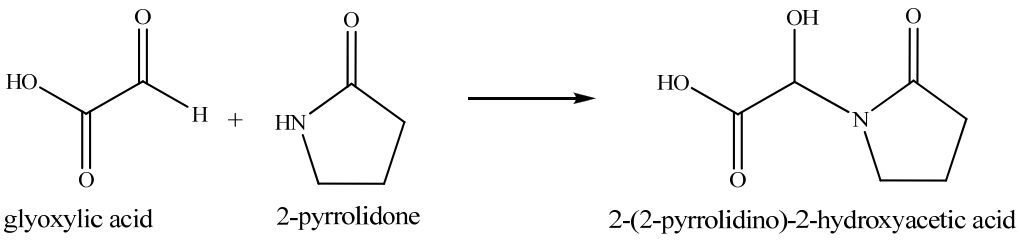

Figure 26: Synthesis of 2-(2-pyrrolidino)-2-hydroxyacetic acid (PYR)

The α-HA formed during the combination of glyoxylic acid and 2-pyrrolidone has a chiral center at the α-carbon. It should be noted that no stereochemical control was imposed during the reaction. Consequently, no restriction was exerted on the nucleophilic attack of the 2-pyrrolidone and both the D and L enantiomers of PYR would be expected. The two enantiomers of PYR are presented in Figure 27. It was assumed that

a racemic mixture of D and L enantiomers existed for all of the monomers synthesized, but the enantiomers are not portrayed in future sections.

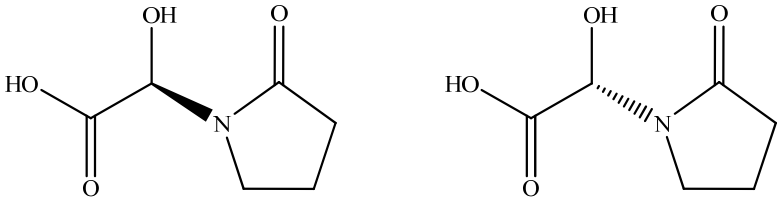

Figure 27: Enantiomers of PYR monomer

Upon addition of 2-pyrrolidone to the slurry of GA in diethyl ether (GA is insoluble in ether), the liquid turned from clear to cloudy white. After approximately 15 min, the solution returned to its original optical clarity, but a thick, colorless gel was observed on the bottom of the reaction flask. Upon reacting overnight, a white solid product formed by precipitation from the solution. The solid was isolated by vacuum filtration and rinsed with ether.

To determine an accurate yield, the product was placed under vacuum to remove residual ether. However, placing the product under full vacuum (≈ 102 kPa) was found to alter the substance. After exposure to full vacuum, the once solid powder solidified, as a viscous, opaque semi-solid was formed. This process was the early stages of polymerization. To prevent the polymerization from forming, but still dry the PYR, the monomer was placed under house vacuum (≈ 50.8 kPa), effectively suppressing the polymerization. After drying, excellent yields were obtained consistently ranging from 90-99 %.

Purification of PYR was initially attempted using Sohxlet extraction with diethyl ether. Sohxlet extraction is a method of continuously extracting the product with a solvent. Although this method of purification should be effective at removing 2-pyrrolidone impurities, it was not believed to be effective for removing GA because GA is insoluble in diethyl ether. Consequently, recrystallization was examined. Determining a recrystallization solvent was a challenging task as PYR was soluble in a number of solvents at room temperature. Alcohols, acetonitrile and acetone were all found to be ineffective. However, PYR was effectively recrystallized from hot ethyl acetate. Good yields were obtained using ethyl acetate, typically exceeding 80 %.

To confirm the synthesis of PYR, FTIR and NMR spectroscopic techniques were used. First, NMR was conducted using *d6*-DMSO as the solvent. The ^{1}H NMR spectrum for PYR is shown in Figure 28. The peak at $\delta = 2.50$ ppm is the residual solvent peak and the broad peak at $\delta = 3.33$ ppm is residual water. A somewhat unexpected result was observed as the peak corresponding to the five position of the pyrollidone ring (d) was a doublet of multiplets, rather than a single triplet. This was caused by diastereotopic hydrogens at that location. Diastereotopic hydrogens occur when replacing a hydrogen atom would create a new chiral center at the carbon atom connected to the diastereoptopic hydrogen, when another adjacent chiral center is present. If the hydrogen at the five position were replaced with another species, a chiral center would form. Consequently, the hydrogens at the five position were found to be diastereotopic, which would affect the splitting observed by NMR.

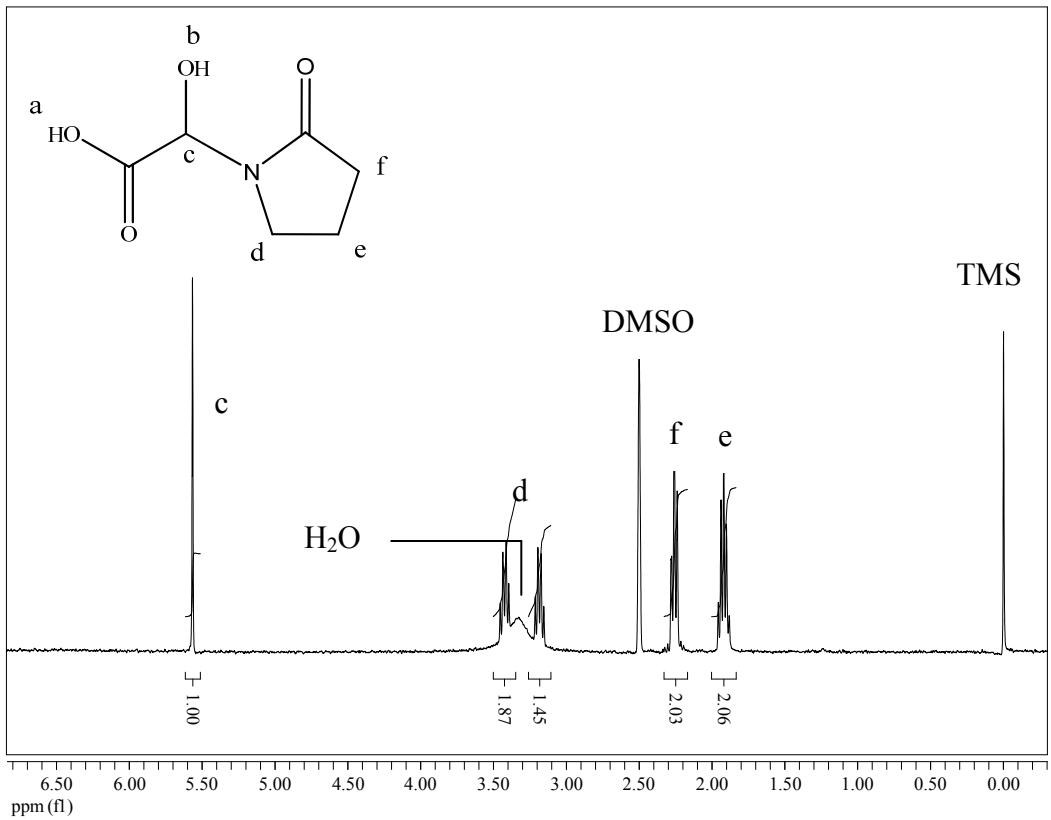

Figure 28: ^{1}H NMR spectrum for PYR monomer

To confirm the results from NMR, FTIR was conducted and the spectrum is shown below in Figure 29. The two broad peaks at 3,400 cm^{-1} and 3,150 cm^{-1} were likely the O-H shifts characteristic of the carboxylic acid and the alcohol, respectively. The two sharp peaks located at 1,700 cm^{-1} (a smaller feature of the more obvious peak at 1,650 cm^{-1}) and 1,650 cm^{-1} were likely the C=O bands for the carboxylic acid and amide, respectively. Although it was difficult to assign peaks in the fingerprint region, the sharp peak at 1,250 cm^{-1} may be the C-O for the carboxylic acid or alcohol and the peak at 1,100 cm^{-1} may be the C-N stretch of the amide.

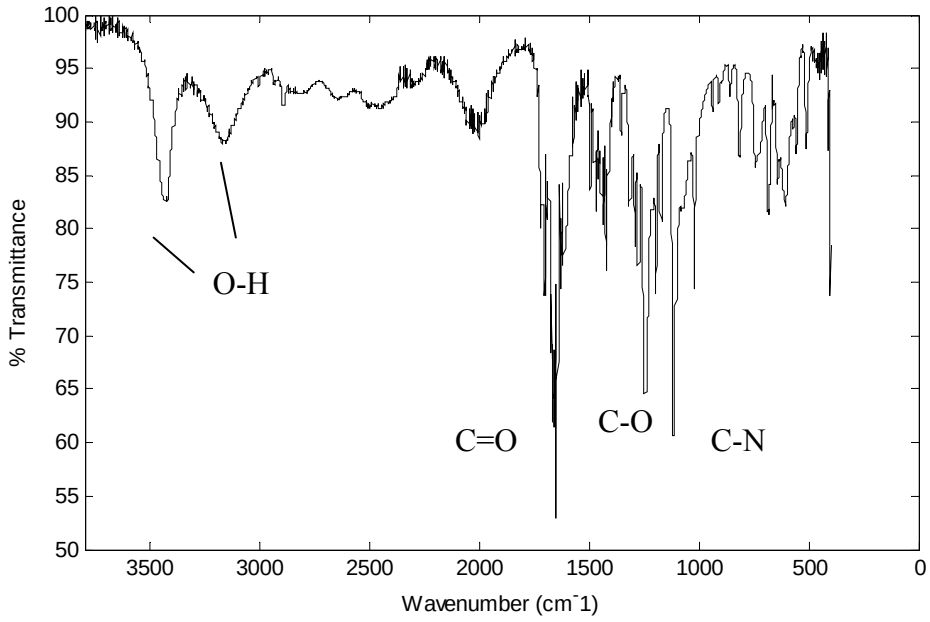

Figure 29: FTIR spectra of PYR monomer

To determine thermal information, DSC was conducted on PYR. The DSC plot of PYR is provided below in Figure 30. The melting temperature was found to be 72 °C to 74 °C. The melting temperature of pure GA is approximately 50 °C and 2-pyrrolidone is a liquid at room temperature with a melting point of 24 °C. Given the NMR and FTIR spectra of the product, as well as the elevated melting temperature of the product with respect to GA and 2-pyrrolidone, it was concluded that the desired monomer was produced and in high purity.

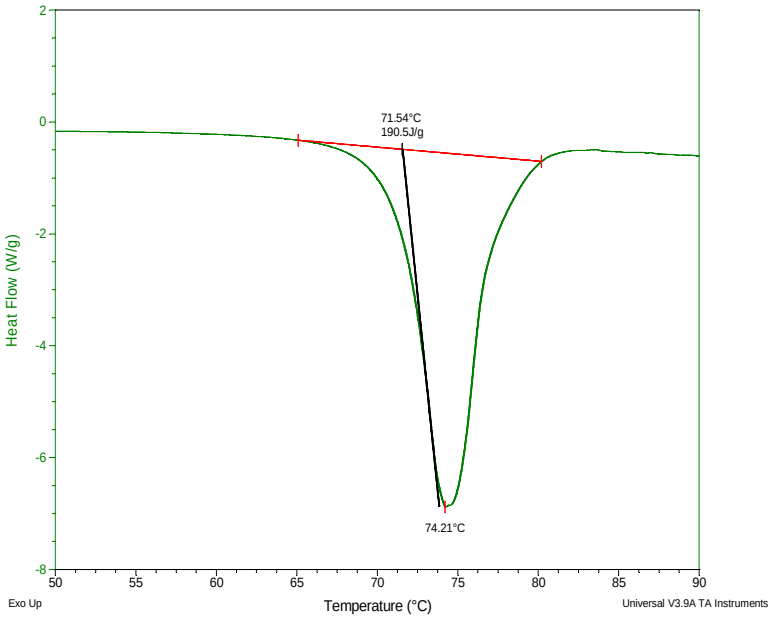

Figure 30: DSC thermogram of PYR monomer

4.3.2 The effect of varied reaction conditions and the formation of PYR

After determining that the product produced was PYR, an investigation into the alteration of experimental parameters began. First, the ratio of GA and 2-pyrrolidone was varied. It was desired to determine whether the combination of GA and 2-pyrrolidone could occur if the ratio of the two reactants were brought towards unison (for improved atom economy). It was found that the reaction proceeded effectively when the molar ratio of GA to 2-pyrrolidone was 1:0.95, producing a 95 % yield before recrystallization.

By contrast, when 2-pyrrolidone was used as the excess reagent (GA to 2-pyrrolidone, 0.95:1), PYR never precipitated out of the ether phase. Instead, only a gel-like solid remained at the bottom of the reaction flask, even after being allowed to

stand for a few days. It was found, however, that PYR could be precipitated by adding additional volumes of ether (≈ 100 mL) to the reaction flask. The resulting product was an off-white color, likely due to the presence of unreacted 2-pyrrolidone.

From this experiment, it was believed that GA actually dissolved in the 2-pyrrolidone component during reaction; plausible as 2-pyrrolidone is commonly used as a polar, aprotic solvent commercially. The solubility of PYR in 2-pyrrolidone was assessed by dissolving 100 mg of PYR in 1 mL of 2-pyrrolidone. The PYR was completely soluble at this concentration. If solvation is occurring, these experiments likely indicate that GA must be in excess to prevent the solvation of PYR in the 2-pyrrolidone component.

The effect of solvent on the reaction between GA and 2-pyrrolidone was then examined. Despite the success of the reaction in diethyl ether, other solvents were tested to create correlations between the reaction solvent and the product obtained, to better understand the reaction parameters. Solvent was believed to have an effect on the reaction because a publication by Roth et al. described conducting the reaction in refluxing acetone and obtaining PYR as a "yellowish oil", [1] rather than a white solid as when conducted in diethyl ether. Two additional solvents were tested: room temperature acetone and ethyl acetate. These solvents were chosen because solvents with lower polarities (i.e. diethyl ether) were thought to promote product precipitation.

The first solvent tested was ethyl acetate. Although PYR is soluble in ethyl acetate at higher temperatures (>60 °C) as determined during recrystallization experiments, PYR has a lower solubility at room temperature. Also, due to its moderate

polarity (polarity index of 4.4), ethyl acetate was a logical choice. The reaction was conducted under the same conditions as in diethyl ether. After reacting overnight in ethyl acetate, a thick layer of light yellow oil was observed on the bottom of the reaction vessel. The reaction mixture was allowed to stand for a few days, resulting in an off-white precipitate. The product was isolated by vacuum filtration and the yield was calculated to be 55 %. It was determined that ethyl acetate was not a suitable solvent compared to ether because the yield obtained was significantly lower and the product was optically impure.

The last solvent tested was acetone. After examining the synthesis of PYR in refluxing acetone by Roth et al., [1] a room temperature synthesis of PYR in acetone was attempted. The reaction was carried out analogously to that in diethyl ether. After reacting overnight in acetone, no solid had formed and no gel was observed at the bottom of the flask. The acetone was removed by rotary evaporation, yielding a thick, yellow oil similar to that for the reaction in ethyl acetate. Upon standing for approximately 1 h, crystals began to form in the gel. Diethyl ether was added to the flask and was stirred for 12 h. A white to tan solid precipitate was obtained in a yield of 90 %. This result was interesting because the reaction does not need to be refluxed in acetone in order to proceed. However, due to the simplicity of the reaction in diethyl ether and the high degree of purity, ether was preferred as the reaction medium.

4.3.3 A solvent free approach to the synthesis of PYR

After assessing different reaction solvents, it became apparent that solvent does impact the formation of PYR. It was then decided to determine whether or not PYR could somehow be formed by combining the two reactants without the use of a solvent. After extensive literature review, an interesting paper was found involving the combination of pyruvic acid and formamide without the use of a solvent. [11] The reaction is detailed below in Figure 31. The reaction was conducted by adding pyruvic acid and formamide at a volume ratio of 2:1, producing 2-formamido-2-hydroxypropanoic acid upon solidification.

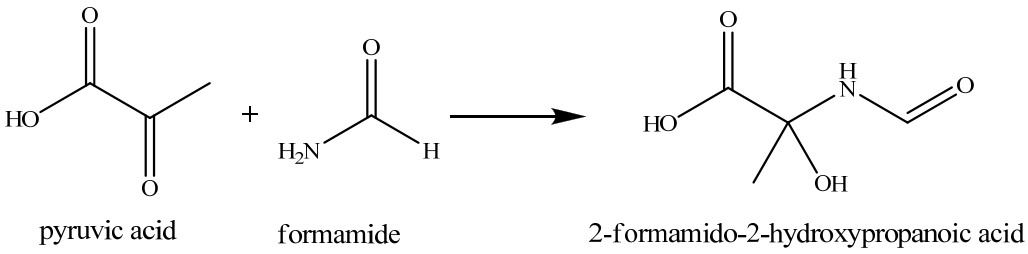

Figure 31: The formation of 2-formamido-2-hydroxypropanoic acid

Pyruvic acid is structurally similar to GA, differing only by the addition of a methyl group. Unlike GA however, pyruvic acid is a liquid at room temperature, allowing it to be both a reactant and a solvent. From this example, it was postulated that PYR could be synthesized by some similar method.

To create PYR through a solvent free method, GA was heated to approximately 60 °C under a nitrogen purge to avoid oxidation. At this temperature, GA melts, making it similar to pyruvic acid. After the GA was melted, 2-pyrrolidone was added and the reactants were mixed. The viscosity of the mixture quickly increased to

the extent that stirring was ineffective. After cooling to room temperature, the resulting product was a viscous, clear substance. To isolate and purify the product, the viscous solid was recrystallized from hot ethyl acetate. After cooling, a white solid was obtained. The product was found to be PYR, produced in a 50 % yield.

Although the product was only obtained in a 50 % yield, which is lower than the procedure using diethyl ether, the reaction may still be of value. There appears to be no report of PYR or other GA adducts being synthesized by a similar melt synthesis. One possible benefit of this procedure is a reduction in the amount of solvent used during the reaction. As there is a general movement towards green chemistry, determining synthetic methods that limit the amount of solvent needed are valuable. Additionally, if the melt procedure could be extended to other amide functionalities, solvent selection issues could be circumvented.

4.4 Synthesis of 2-Benzamido-2-Hydroxyacetic Acid (BZ)

4.4.1 The general synthesis of BZ

The monomer 2-benzamido-2-hydroxyacetic acid (BZ), commonly known as α-hydroxyhippuric acid, was produced by the reaction of GA and benzamide. The abbreviation BZ was given to this α-HA in reference to the substituent group added to GA, benzamide. The reaction is shown in Figure 32. The BZ α-HA is a naturally occurring compound and is a derivative of α-hippuric acid, a human metabolite. [12, 13] In the literature, Zoller and Ben-Ishai created BZ by reacting GA and benzamide at a molar

ratio of 1.1:1 (GA:benzamide) in refluxing acetone. [5] The reaction was conducted for 5 h and produced BZ in a yield of 72 %.

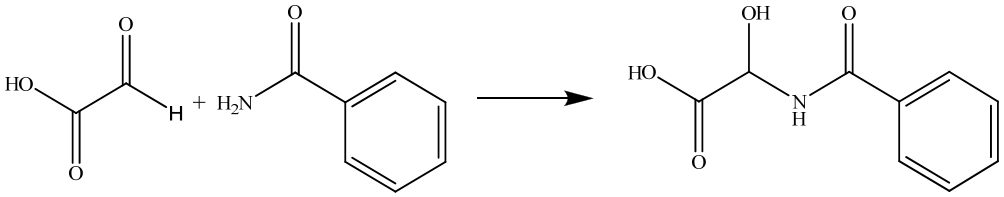

Figure 32: Synthesis of 2-benzamido-2-hydroxyacetic acid (BZ)

Diethyl ether was initially used as the reaction solvent and the molar ratios of GA and benzamide were retained from the synthesis reported by Zoller. [5] The solvent was selected based on the success of the corresponding PYR reaction. After the addition of benzamide to the GA slurry, the solution turned from clear to white. The solution then became increasingly thick and a white paste resulted after reacting overnight. The mixture was vacuum filtered and rinsed with diethyl ether. The resulting product was a white solid.

The solid precipitate was obtained in a 75 % yield. As compared with the synthesis presented in the literature, the combination of benzamide and GA in diethyl ether produces BZ in a slightly greater yield. [5] In addition to the improved yield, the reaction occurring in ether requires a less complicated experimental set-up (i.e. no heating mantle, condenser, etc.) and lower energy demands. One possible disadvantage of using ether is that the reaction time was increased compared to that in refluxing acetone. However, the advantages of the diethyl ether system may outweigh the

increased reaction time and the use of ether appears to be comparable or favorable with respect to the procedures listed in the literature.

Purification of BZ was attempted by recrystallization. Ethyl acetate, acetonitrile and isopropanol were all found to be ineffective. Isopropanol was the best of these three solvents, but produced recrystallized BZ in low yields. Ethanol was found to be an effective solvent however, and produced recrystallized BZ in a yield of 80 %. The melting point of BZ was determined by DSC to be 147 °C to 152 °C. The DSC plot of BZ is given below in Figure 33.

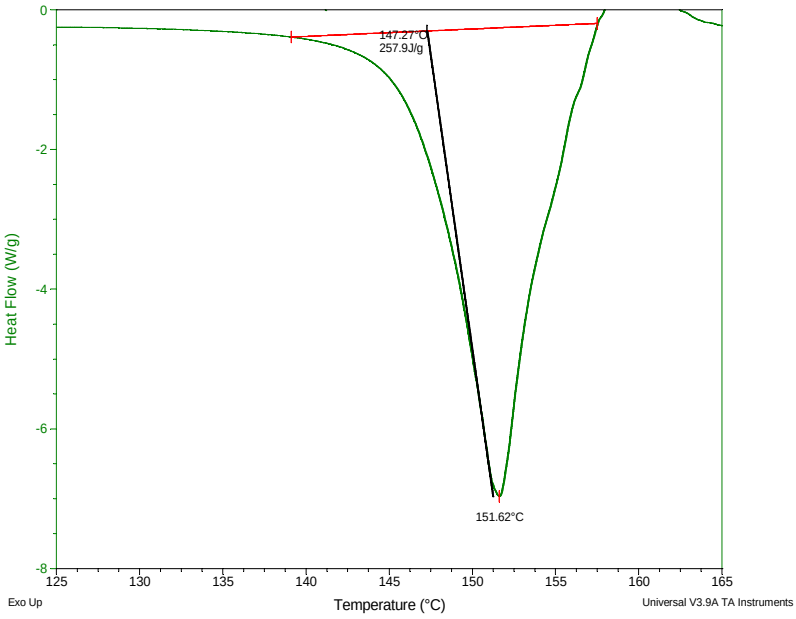

Figure 33: DSC thermogram of BZ monomer

According to the literature, the melting temperature of BZ was reported to be 157 °C to 159 °C upon resolidification after the reaction in refluxing acetone was brought from reflux to room temperature. [5] However, a melting point of approximately 200 °C

was reported after recrystallization with dioxane and chloroform. [5] According to Sigma-Aldrich, the melting temperature of BZ was listed as 211 °C. Degradation of the product occurred shortly after the thermal transition shown in Figure 33 and further thermal analysis could not be conducted (the irregularity of the line after the trough indicates degradation). The difference in melting temperatures indicated that different BZ crystal structures exist or that the BZ sample was impure following recrystallization. Water in the BZ crystal structure might also cause a melting temperature depression.

In efforts to confirm the existence of BZ, NMR and FTIR were conducted. First, NMR was conducted using *d6*-DMSO as the solvent. A plot of the ^{1}H NMR spectrum for BZ is shown in Figure 34. The peak at δ = 2.50 ppm is the residual solvent peak and the peak at δ = 3.33 ppm is water. All of the peaks match both those given in the literature [5] and the NMR spectrum of BZ provided by Sigma-Aldrich.

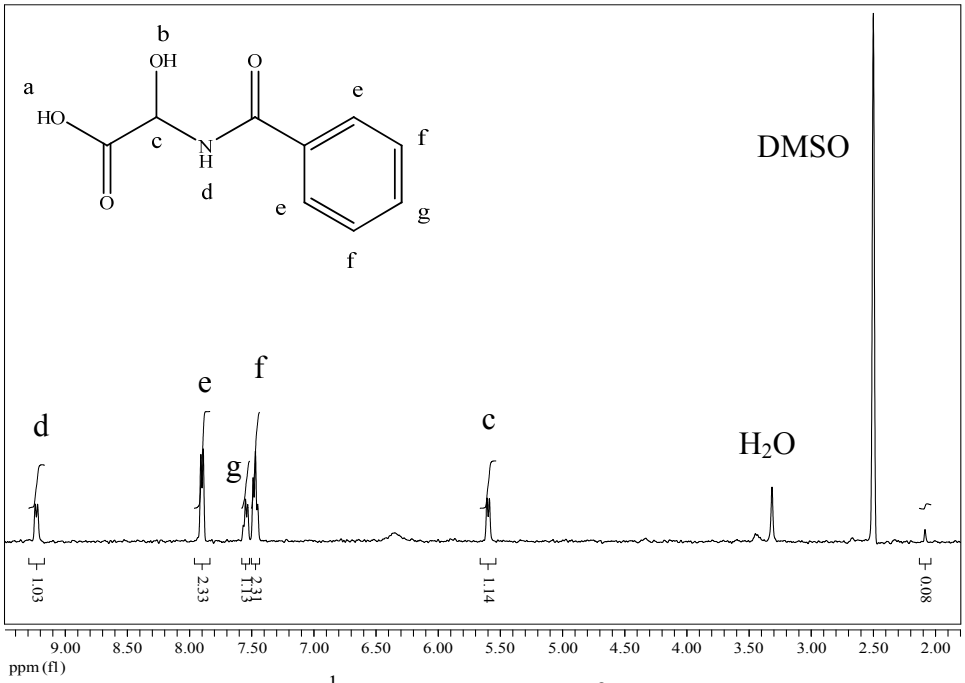

Figure 34: ^{1}H NMR spectrum of BZ monomer

The only distinction between the three spectra is that the data from Sigma-Aldrich displays a singlet at approximately 2.10 ppm, which is not listed in the literature and appears sporadically in NMR spectra obtained by the author. This peak is likely the hydrogen of the α-hydroxyl group or residual acetone from cleaning. Two peaks were observed that were thought to represent impurities. The small peak to the left of the residual water peak ($\delta = 3.45$ ppm) was thought to be residual ethanol from recrystallization. The extraneous peak at $\delta = 6.40$ ppm could not be identified.

To further validate the existence of BZ, FTIR was conducted on the monomer and is shown in Figure 35. The spectrum provided closely matches those obtained from Sigma-Aldrich as well as the description from the literature. [5] The peaks at 3,350 cm^{-1}, 3,300 cm^{-1} and 3,150 cm^{-1} were thought to be the O-H stretch of the carboxylic acid, the N-H stretch of the amide and the O-H stretch of the hydroxyl, respectively. The peaks at 3,300 cm^{-1} and 3,150 cm^{-1} were less defined than those presented by Sigma-Aldrich, but were positioned accurately. The small peak to the left of 3,000 cm^{-1} may be the =C-H stretch of the aromatic ring. The peaks at 1,750 cm^{-1}, 1,650 cm^{-1} and 1,540 cm^{-1} were likely the C=O stretch of the carboxylic acid, the C=O stretch of the amide and the C=C stretch of the aromatic ring, respectively.

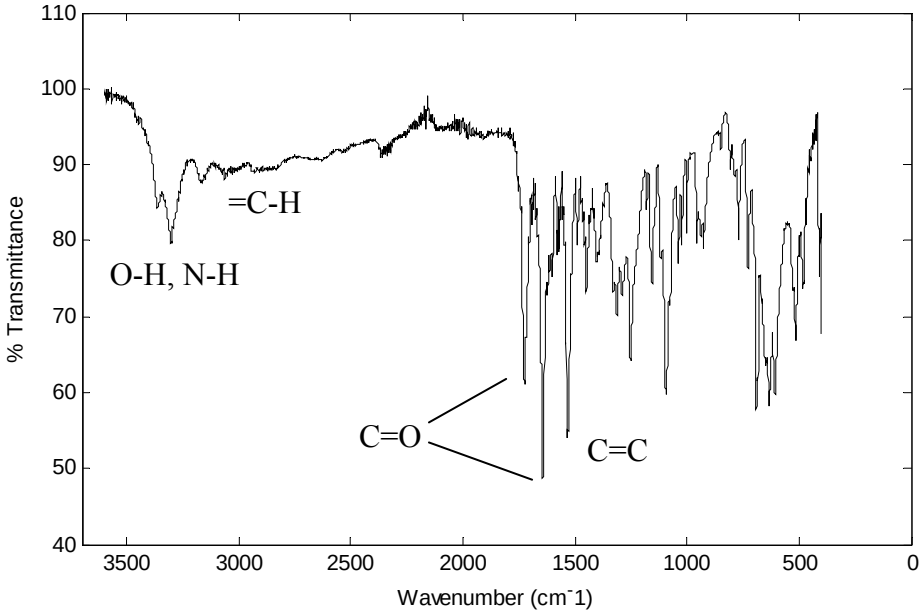

Figure 35: FTIR spectrum of BZ monomer

4.4.2 The effect of varied reaction conditions on the formation of BZ

Once BZ was isolated and characterized, experimental parameters were adjusted to optimize the system. As was done with PYR, the ratio of GA to benzamide was first manipulated to determine the effects of altered reagent excess. The GA and benzamide were reacted at a molar ratio of 1:1.05 in diethyl ether. From these reaction conditions, BZ was produced in a 42 % yield. Although the yield was lower than that under the conditions of excess GA, the BZ product was formed. The formation of the α-HA as a white solid did not occur when 2-pyrrolidone was used as the excess reagent. Thus, the formation of BZ despite the excess amide indicated that the solvent properties of the amide functionality dictated whether or not it can be applied in excess.

Two reactions were then conducted in ethyl acetate to explore the BZ synthesis and to test the limits of the excess amide. In the first experiment, a mol ratio of 1:1 with respect to GA and benzamide was used. In the second trial, the ratio of GA to benzamide was set at 1:1.2, while all other reaction conditions were maintained constant. After allowing the reactions to proceed overnight, a white solid appeared in both reaction flasks. Upon isolation by vacuum filtration, yields of 50 % and 45 % were obtained for the first and second experiment, respectively. The results were interesting because they suggest that certain α-HAs, regardless of solvent, could be made with excess amide, given that the amide does not solvate the monomer. .

4.5 Synthesis of 2-Acetamido-2-Hydroxyacetic Acid (ACE)

4.5.1 General synthesis of ACE

The monomer 2-acetamido-2-hydroxyacetic acid (ACE) was produced by the reaction of GA and acetamide. The abbreviation ACE was given to this α-HA in reference to the substituent group added to GA, acetamide. Diethyl ether was used as the reaction solvent and GA and acetamide were reacted at a mol ratio of 1.1:1. The reaction is shown in Figure 36.

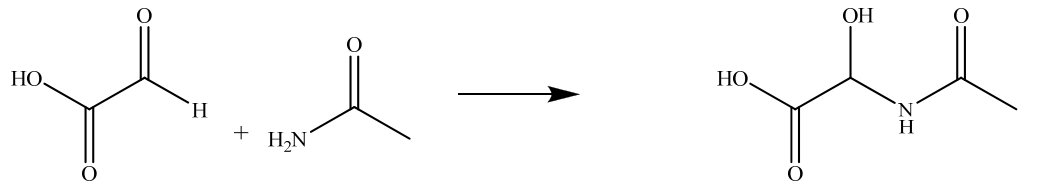

Figure 36: Synthesis of 2-acetamido-2-hydroxyacetic acid (ACE)

The ratios and solvent were selected because of the success of the other monomer systems and because of a reference in the literature by Christidis et al. [14] In the source, equimolar amounts of an aqueous 50 % glyoxylic acid solution and acetamide were combined and reacted at 50 °C for 8 h. Upon cooling, crystals began to form and ACE was recovered in a 55 % yield as a white, crystalline solid.

A few minutes after adding acetamide to the suspension of GA and diethyl ether, a clear gel-like solid formed in the bottom of the reaction flask. The solid looked similar to the product precursor observed during the formation of PYR. Unlike PYR however, the ACE product did not solidify after reacting overnight. The gel was allowed to react for another 2 d to induce solidification, but the transition to a solid never occurred. The diethyl ether was removed by rotary evaporation to yield the crude product as a thick, highly viscous substance. The oil was then allowed to dry overnight in the fumehood.

The resulting mass of the oil was found to be greater than the maximum theoretical yield, indicating that the solid was likely swollen with ether or had absorbed humidity from the air during drying. A small amount of the gel was placed under full vacuum to dry. As was the case with PYR, after only a few minutes of exposure to full vacuum, the gel began to bubble rapidly and ultimately produced a white, highly viscous solid. The formation of the viscous solid was evidence that ACE, like PYR, was capable of polymerizing if placed under a strong vacuum. To prevent the polymerization of ACE, a small sample was placed under house vacuum. After drying in vacuum for 2 d, the ACE turned from a clear gel into an opaque, semi-crystalline solid. Semi-crystalline is used to describe the crude product because white crystals were observed in a matrix of

clear to white gel. Additional time *in vacuo* did not change the product. The ACE was obtained in a yield of 90 %, however the accuracy of this measurement is uncertain because of potential solvent swelling.

A number of solvents were attempted for recrystallization, but no solvent was found to be effective. Tested recrystallization solvents included ethyl acetate, isopropanol, ethanol, chloroform and toluene. All of the solvents listed were capable of dissolving ACE at higher temperatures, but ACE did not precipitate out of these solvents to form a crystalline solid. When a product did separate from the liquid layer, it was a gel-like solid that resembled ACE prior to the addition of the recrystallization solvent (i.e. not a white solid like previous α-HAs).

Liquid-liquid extraction was investigated when recrystallization was deemed to be ineffective. The gel-solid ACE obtained after drying in house vacuum for 2 d was dissolved in water and acidified with 1 M HCl. The acidified aqueous layer was then extracted with chloroform in efforts to transfer the product into the organic phase. After drying the solvent with $MgSO_4$ and subsequent removal of the solvent by rotary evaporation, no product was obtained. As chloroform is one of the most polar, but water immiscible solvents, liquid-liquid extraction was abandoned because ACE was thought to have too great an affinity for water compared with organic solvents.

Despite the inability to purify the ACE produced, characterization of the crude product was initiated to determine the properties of the isolated product. It was theorized that the gel, while not completely a solid, was in fact ACE. This prediction was made because of the PYR reaction documented by Roth et al., [1] which produced PYR as a

yellow oil when the reaction solvent was acetone, versus the reaction conducted in ether that produced a white, solid product. It seemed plausible, therefore, that performing the reaction in ether might also change the physical state of the product compared to that produced in water.

The ACE monomer was characterized after drying under house vacuum for 2 d. The DSC plot of the gel-solid ACE is shown in Figure 37. The melting temperature determined by DSC was found to be 46 °C to 58 °C. Christidis et al. reported that ACE melted at 57 °C, [14] which is nearly identical to the peak melting temperature shown in Figure 37. The large width of the thermal transition was thought to indicate impurities.

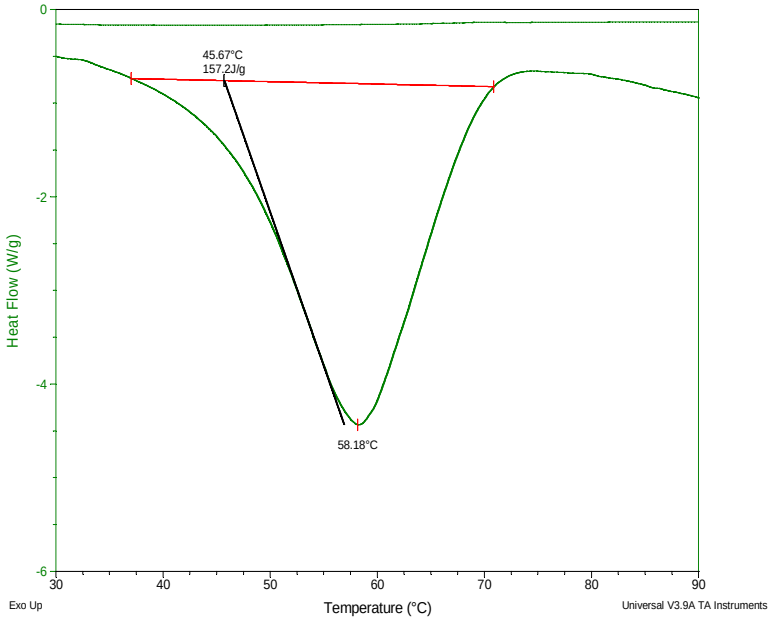

Figure 37: DSC thermogram of ACE monomer

After impurities were implicated by DSC, FTIR and NMR were conducted on the sample. The patent by Christidis et al. did not include NMR chemical shifts or IR

stretches for ACE, so no comparison could be drawn between the product produced in diethyl ether and that in the literature. [14] The FTIR spectra obtained for ACE is shown below in Figure 38.

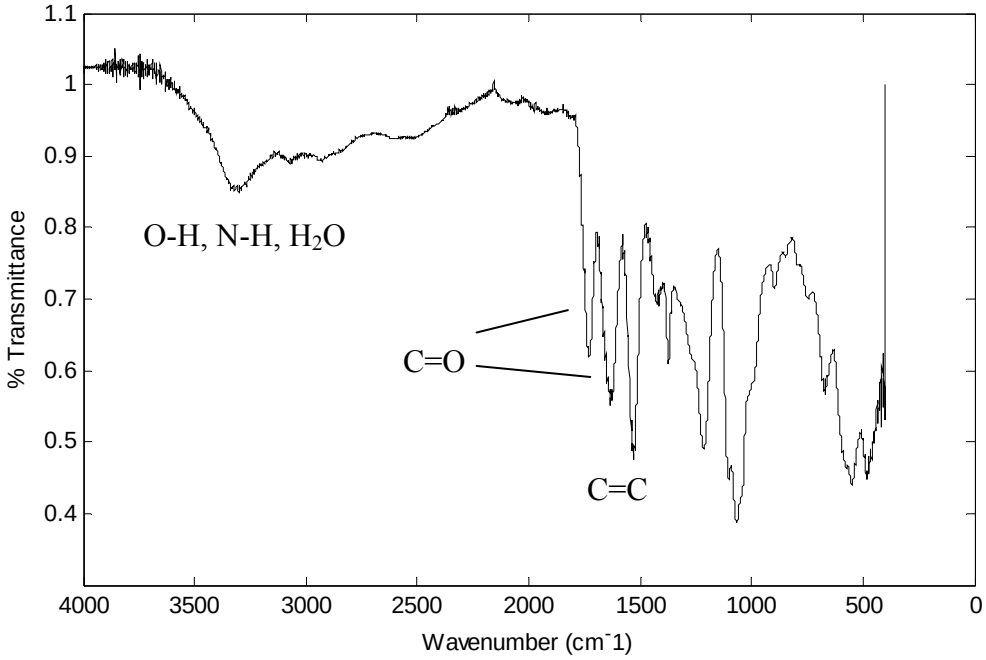

Figure 38: FTIR spectra of ACE monomer

The large and broad peak to the left of 2,000 cm^{-1} was believed to be some combination of O-H and N-H bands contributed by the acyl, hydroxyl and amido groups or an O-H stretch from water in the product. The three peaks in between 2,000 cm^{-1} and 1,500 cm^{-1} were puzzling because only two double bond stretches were expected: the C=O of the acyl group at 1,750 cm^{-1} and the C=O of the amide at 1,650 cm^{-1}. The third peak was believed to indicate the presence of an impurity possessing a pi bond because the peak resembled the aromatic C=C stretch present in BZ.

After the analysis of ACE with FTIR generated questions about the purity of the crude product, NMR was conducted on the sample. The NMR spectrum for ACE is shown below in Figure 39. As before, *d6*-DMSO was used as the solvent and the peak at $\delta = 2.50$ ppm is the residual solvent peak. The broad "hump" at $\delta \approx 3.50$ ppm is likely a residual water peak or undissolved material.

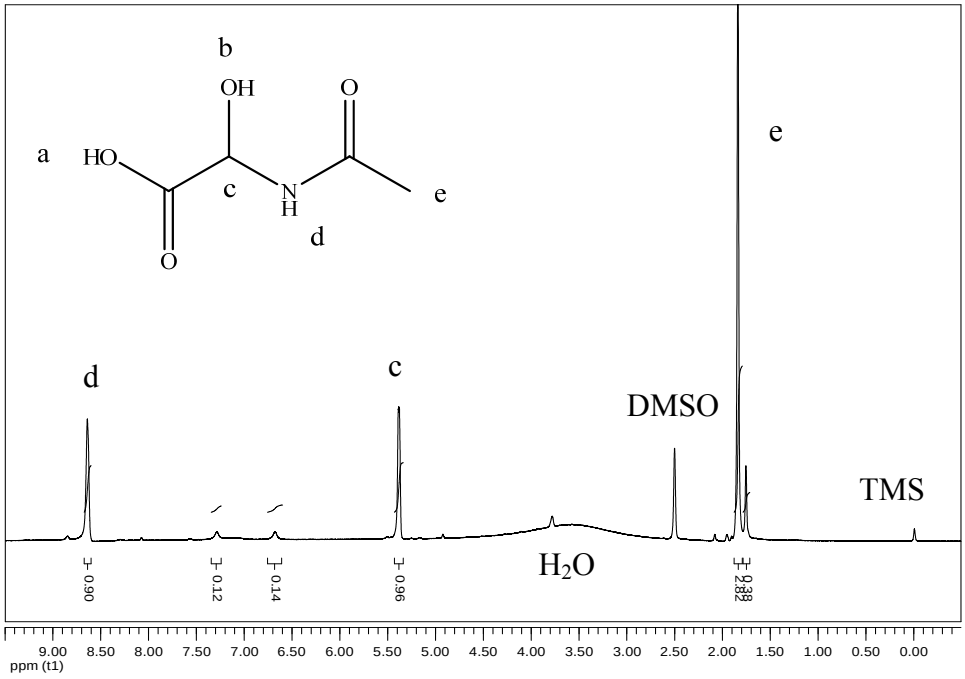

Figure 39: ^{1}H NMR spectrum of ACE monomer

A few interesting results were obtained by examining the figure above. It appeared that ACE was produced as peaks belonging to the monomer were identified and those peaks are labeled in Figure 39. However, it was believed that impurities were present in the crude product. Three peaks present in the spectrum seemed to indicate the presence of impurities: two similar peaks at $\delta = 7.29$ ppm and 6.69 ppm, and another peak at $\delta = 1.75$ ppm. Insight into the structure of these impurities was obtained from

Shive et al., who described the reaction of pyruvic acid and acetamide.[11] Due to the structural similarity between pyruvic acid and GA, it was believed that the byproducts described could be analogous to those observed for the reaction between GA and acetamide.

The possible side reactions are detailed in Figure 40. The ACE monomer is depicted at the top right, whereas the two byproducts are depicted at the bottom. The basic feature of both byproducts was the removal of the α-hydroxyl group from ACE to form an imine, 2-(acetylimino) acetic acid, or a diacetamide, 2,2-diacetamidoacetic acid. For the imine, both the E and Z geometric isomers should be possible as no stereochemical constraints were imposed during the reaction.

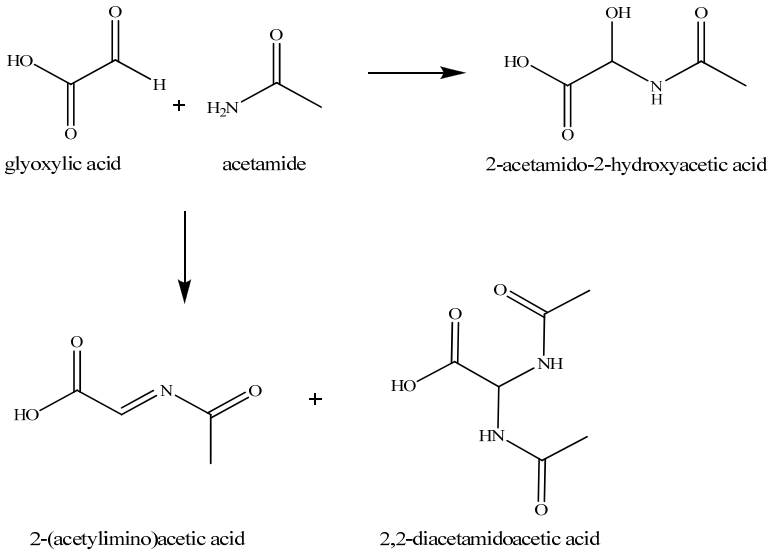

Figure 40: Possible side reactions during the synthesis of ACE

The NMR spectrum provided in Figure 39 was analyzed to determine if the extraneous peaks could be correlated to either of the proposed impurities. The integration of the two peaks at δ = 7.29 ppm and 6.69 ppm did not match the ratio of the hydrogen

atoms corresponding to 2,2-diacetamidoacetic acid. If the diacetamide was the impurity, it would be expected that the two peaks at δ = 7.29 and 6.69 ppm would be the hydrogens of the N-H bond and the α-hydrogen, respectively, and the integration would be 2:1. However, 1:1 integration was observed for the two peaks. The existence of another double bond was also supported by FTIR, which only the imine possesses. These results indicated that the two peaks represent the E and Z isomers of the imine. The peak at δ = 1.75 ppm was thought to be the corresponding -CH_3 hydrogens of the acetamide functionality attached to the imine. This analysis was further supported by the fact that the integration between the peak at δ = 1.75 ppm and either of the other two peaks at δ = 7.29 ppm or 6.69 ppm was 3:1, as would be expected for the imine.

4.5.2 The effect of varied reaction conditions on the formation of ACE

Due to the problems associated with the formation of ACE, other solvents were tested. These experiments were designed to assess whether the use of another solvent could produce ACE as a white, crystalline solid similar to that described in the literature. Ethyl acetate, dichloromethane and dry diethyl ether were all tested, but ACE was consistently obtained as clear to white oil or highly viscous gel. Dry ether was attempted because an α-HA functionalized with methylcarbamate (an analogue to acetamide) was produced by Ben-Ishai et al., using dry ether as the reaction medium. [9]

After ACE was not produced as a precipitate from any solvent, the procedure detailed in the patent by Christidis et al. was attempted. [14] The procedures established in the patent did not produce ACE as a white crystalline solid. Upon reacting for 8 h at 50 °C, the water-ACE solution turned a faint yellow color. After cooling, the product did

not precipitate from the solution despite scratching the bottom of the reaction flask and crystal seeding with ACE. Presently, no variation of the procedure detailed in the patent has produced ACE as a white precipitate.

4.6 Synthesis of 2-Acrylamido-2-Hydroxyacetic Acid (ACRY)

4.6.1 General synthesis of ACRY

Rich Natelli, a student in the Vogel research group, was largely responsible for the synthesis of ACRY. Although the work presented here concerning ACRY was completed by the author, the results obtained by Mr. Natelli prior to the inception of this thesis were examined. On account of the previous work, limited work with altered experimental variables was conducted, as significant work on this monomer was underway. Consequently, ACRY is presented here to demonstrate the variety of amido-functional groups that can be added to GA.

The monomer 2-acrylamido-2-hydroxyacetic acid (ACRY), also known as 2-acrylamidoglycolic acid, was produced by the reaction of GA and acrylamide. The abbreviation ACRY was given to this α-HA in reference to the substituent group added to GA, acrylamide. The reaction is shown in Figure 41.

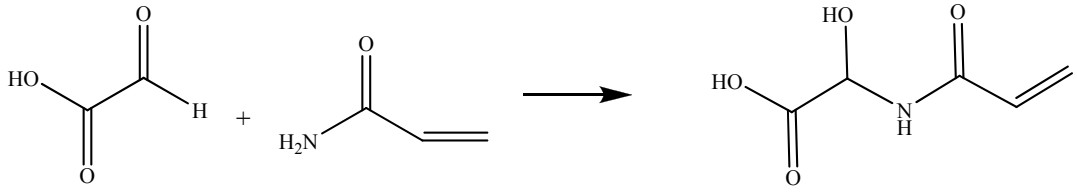

Figure 41: Synthesis of ACRY monomer

The reaction conditions for the formation of ACRY were established by modifying the procedures detailed by Christidis et al. [14] and Sidot et al. [15] In these procedures, equimolar amounts of an aqueous GA solution and acrylamide were combined. In both references, additional compounds were added to prevent the reaction of the acrylic group. The reaction mixture was then heated to approximately 45 °C, as the dissolution of acrylamide is reported to occur endothermically. [15]

The reactant ratios and solvent were chosen based on the work of Mr. Natelli and the reports in the literature. The reaction was conducted by reacting GA and acrylamide at a mol ratio of 1:1.2 in warm ethyl acetate. (*Note*: the ACRY reaction was attempted in diethyl ether, but ACRY did not precipitate) Acrylamide was added slowly to a slurry of GA and ethyl acetate. It was found that covering the reaction flask with aluminum foil suppressed photo-induced reactions of the acrylic group. Consequently, neither of the inhibitors (copper acetate and hydroquinone monomethyl ether) described in the patents were necessary.

After reacting overnight at 50 °C, ACRY was produced in a yield of 65 %, which is comparable to that in the literature. The resulting crude product was obtained as a white, crystalline solid. A few solvents were tested to recrystallize the crude product including IPA and toluene, but they were not successful. Water was found to be an acceptable recrystallization agent, but it appeared to alter ACRY. The unpurified product was used during characterization to avoid any issues associated with the ACRY recrystallized in water. The effect of water on ACRY is discussed later in this section.

First, NMR was conducted on the crude product to confirm the solid was ACRY. The NMR spectrum of ACRY is provided below in Figure 42. As before, *d6*-DMSO was used as the solvent and the peaks at δ = 2.50 ppm and 3.33 ppm are the residual solvent and water shifts, respectively. The peaks listed correspond well with the predicted monomer shifts and the product produced was believed to be ACRY. It was also noted that despite conducting NMR on an unpurified sample, no obvious impurities were seen. Once peculiar aspect of the spectrum is the observed splitting for the α-hydrogen. Rather than appearing as a singlet, the α-hydrogen is shown as a doublet. The splitting may be caused by the N-H hydrogen of the amino group.

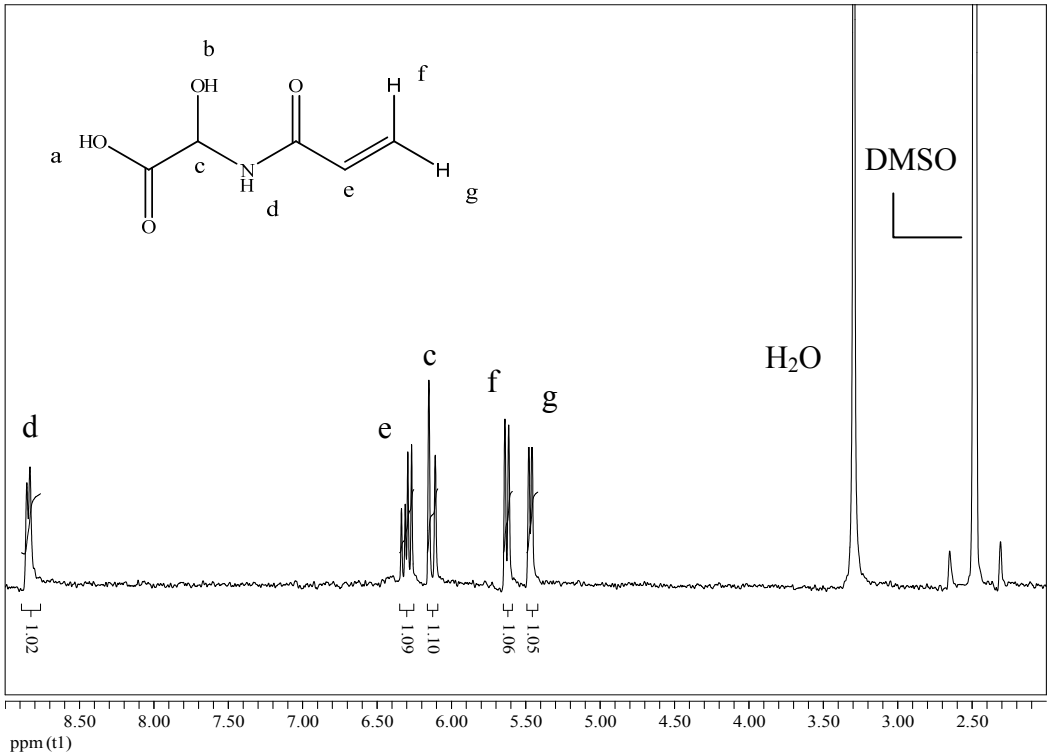

Figure 42: ^{1}H NMR spectrum of unrecrystallized ACRY monomer

FTIR was conducted to further characterize the monomer. The FTIR spectrum for ACRY is presented in Figure 43. The large peak centered at 3,250 cm^{-1} was likely the N-H stretch of the amide due to the sharpness of the peak. The peaks at 1,750 cm^{-1}, 1,600 cm^{-1} and 1,550 cm^{-1} were believed to be the C=O of the acid, the C=O of the amide and the C=C of the acrylic group, respectively.

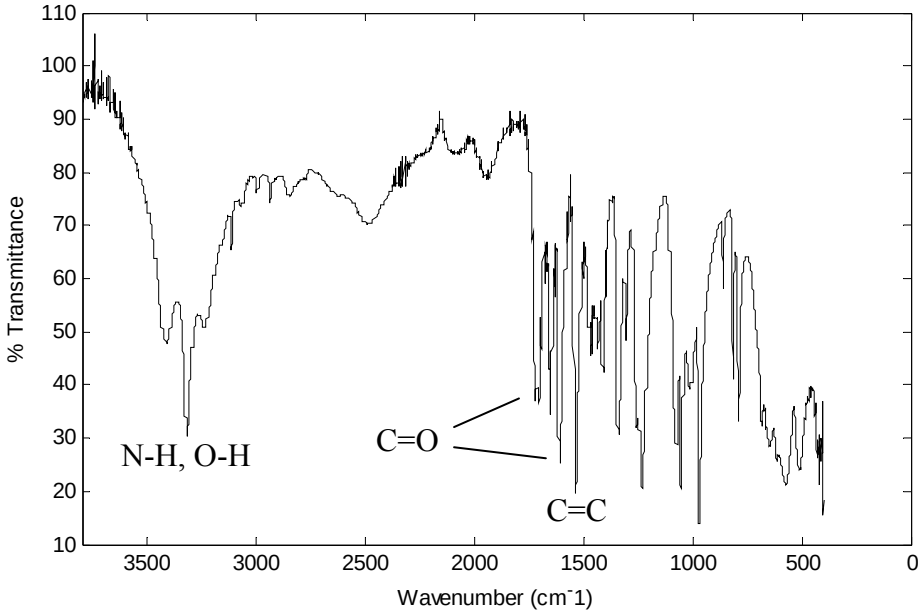

Figure 43: FTIR spectra of ACRY monomer

While ACRY was confirmed to be fairly pure by NMR, an effective recrystallization solvent was desired. As was briefly mentioned before, boiling water was found to be a suitable recrystallization solvent for ACRY. Upon cooling the ACRY-water solution to 10 °C, recrystallized ACRY was obtained as a white solid. Although water was deemed a successful recrystallization agent, water altered the thermal properties of ACRY.

From the DSC plot in Figure 44, the melting point of unrecrystallized ACRY was determined to be 122 °C to 124 °C, which is in agreement with the literature.[15] However, after recrystallizing ACRY in water, the melting point was lowered to 95 °C. It was hypothesized that water had entered into the crystal structure of ACRY and was able to alter the melting temperature. This hypothesis was confirmed after consulting Sigma-Aldrich, which supplies 2-acrylamidoglycolic acid monohydrate commercially. The melting point for this compound was reported as between 95 °C and 97 °C, which is identical to that determined for ACRY recrystallized from water. Thus, it was believed that the crude ACRY incorporated water into its crystal structure upon recrystallization from water.

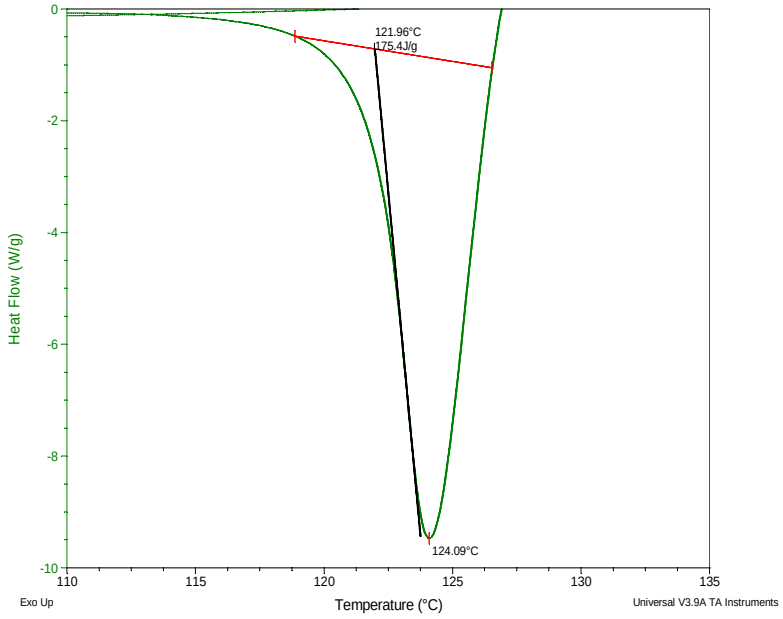

Figure 44: DSC plot of ACRY monomer

4.7 Summary of Monomer Synthesis

To aid future works, two tabular summaries were constructed. The tables were created to provide relevant physical properties obtained during experimentation. Table 2 is presented below and includes information on the best choice of reaction solvent, monomer yield and recrystallization solvent. In Table 3, physical properties of the four monomers are documented. In the solubility section of Table 3, the following abbreviations are used: i = insoluble, ss = somewhat soluble, s = soluble.

Table 2: Tabular summary of important reaction parameters for PYR, BZ, ACE and ACRY

	Reaction parameters		
Monomer	**Reaction Solvent**	**Yield (wt%)**	**Recrystallization Solvent**
PYR	Diethyl ether	99	Ethyl acetate
BZ	Diethyl ether	75	Ethanol
ACE	Diethyl ether	90	--
ACRY	Ethyl Acetate	65	Water

Table 3: Tabular summary of important physical properties for PYR, BZ, ACE and ACRY

	Physical Properties				
	Thermal	**Solubility**			
Monomer	**Melting point (°C)**	**Diethyl ether**	**IPA**	**Acetonitrile**	**Water**
PYR	74	i	s	ss	s
BZ	152	i	ss	ss	ss
ACE	58	i	s	s	s
ACRY	124	i	ss	ss	s

4.8 References

(1) Roth, E.; Ben-Ishai, D. et al. *Tetrahedron* **1995**, *51*, 801.
(2) Ben-Ishai, D.; Hirsch, S. *Tetrahedron Letters* **1983**, *24*, 955.
(3) Ben-Ishai, D.; Peled, N. et al. *Tetrahedron* **1978**, *34*, 467.
(4) Ben-Ishai, D.; Altman, J. et al. *Tetrahedron* **1977**, *33*, 1533.
(5) Zoller, U.; Ben-Ishai, D. *Tetrahedron* **1975**, *31*, 863.
(6) Leemhuis, M.; Hennink, W. et al. *European Polymer Journal* **2008**, *44*, 308.
(7) Leemhuis, M.; Hennink, W. et al. *Macromolecules* **2006**, *39*, 3500.
(8) Leemhuis, M.; Hennink, W. et al. *European Journal of Organic Chemistry* **2003**, *2003*, 3344.
(9) Ben-Ishai, D.; Bernstein, Z. et al. *Tetrahedron* **1976**, *32*, 1571.
(10) Boaz, N.; Debenham, S. US Patent 7214803, 2007.
(11) Shive, W.; Shive, G. *Journal of the American Chemical Society* **1946**, *68*, 117.
(12) Sgarabotto, P.; Abdel-Rahman, L. et al. *Polyhedron* **1999**, *18*, 2505.
(13) Ahmed, M.; Marek, J. et al. *Transition Metal Chemistry* **2004**, *29*, 675.
(14) Christidis, P.; Schouteten, V. et al. US Patent 4105690, 1978.
(15) Sidot, C.; Christidis, P. et al. US Patent 4810822, 1989.

CHAPTER FIVE:

MELT POLYCONDENSATION

5.1 Introduction to Melt Polycondensation Polymerization

After the formation of the amido-functionalized α-HAs presented in Chapter Four, a polymerization method was needed to synthesize the corresponding polymers. After observing the effects of full vacuum on some of the monomers, melt polycondensation (PC) was chosen as a starting point. This method of polyester production was thought to be advantageous because the general process is simple. In melt PC, complicated chemical methods and setups are avoided. Consequently, there is no need for toxic reagents or multi-step procedures that often accompany the synthesis of polyesters. Although the formation of PLA in the melt has historically yielded lower molecular weight chains, [1-4] the possible benefits of the polymerization were thought to be worth analysis. The remainder of this chapter serves to examine the results of experimentation with melt PC.

5.2 Melt Polycondensation of 2-(2-Pyrrolidino)-2-Hydroxyacetic Acid (PYR)

The synthesis of oligo(2-(2-pyrrolidino)-2-hydroxyacetic acid) (OPYR) occurred effectively by melt PC. The PYR monomer was an ideal candidate for polymerization because it could be produced in high yields and was recrystallized efficiently. Consequently, the greatest volume of melt PC experimentation exists for PYR compared

with the other monomers. Along with standard melt PC, the effects of catalysts on the formation of OPYR are also documented.

5.2.1 General synthesis of oligo(2-(2-pyrrolidino)-2-hydroxyacetic acid) (OPYR)

The general principle of the melt PC technique was to heat the monomer past its melting point, while under reduced pressure to remove water vapors that are released during polymerization. The accumulation of water in the reaction vessel is a detriment to polyester formation because it limits the extent of reaction and can cause chain scission (see section 2.6.1 for details and references). Recrystallized PYR was charged to a round bottom flask, which was connected to a Kugelrohr distillation apparatus (Kugelrohr). The Kugelrohr operated by heating PYR in a temperature controlled oven that could be attached to a vacuum line. Thus, the PYR could be heated to a specified temperature, while under full vacuum (≈ 102 kPa).

The flask containing recrystallized PYR was first heated to 100 °C and placed under full vacuum. The temperature was chosen in efforts to remove water from the reaction vessel. Upon heating PYR past 74 °C (the T_m of PYR), the white, crystalline solid melted into a clear, viscous substance. After approximately 10 min of melting, the substance began to bubble vigorously, a process that continued for the majority of the reaction. The released gas was thought to be water vapors because water is a side product of the condensation reaction, as shown in Figure 45. In reports of melt PC with PLA, sublimation of lactide occurs, but the formation of a 2-pyrrolidone substituted lactone was not observed.

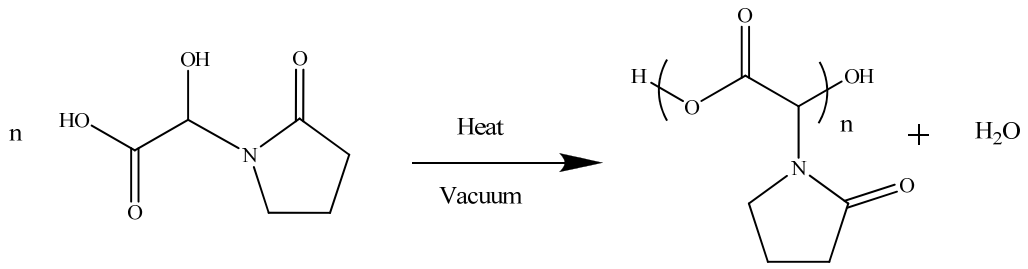

Figure 45: Polymerization of PYR monomer

The reaction vessel was removed from the Kugelrohr after bubbling ended. This occurred after approximately 18 h to 24 h of reaction time. The resulting product was a hard, clear or amber colored solid, presumably oligo(2-(2-pyrrolidino)-2-hydroxyacetic acid) (OPYR). The crude product was obtained in a yield of > 99 %. Purification of the product was attempted by precipitation. The polymer was first dissolved in a minimal amount of chloroform. Similar to the PYR monomer however, the resulting OPYR polymer was very soluble in common precipitation nonsolvents such as methanol. The OPYR could be precipitated by using diethyl ether or hexanes as the nonsolvent, but yields were typically low (40 to 20 %) and the purified polymer was a discolored, viscous substance rather than a hard solid. For convenience, the crude product was characterized by NMR and DSC, rather than the precipitated polymer.

The crude product was first analyzed by NMR to assess if the product was OPYR. The NMR spectrum for OPYR is presented in Figure 46. Although the PYR monomer was not soluble in *d*-$CHCl_3$, the crude OPYR was soluble and *d*-$CHCl_3$, which was used as the NMR solvent. The peak at $\delta = 7.26$ ppm is the residual solvent peak.

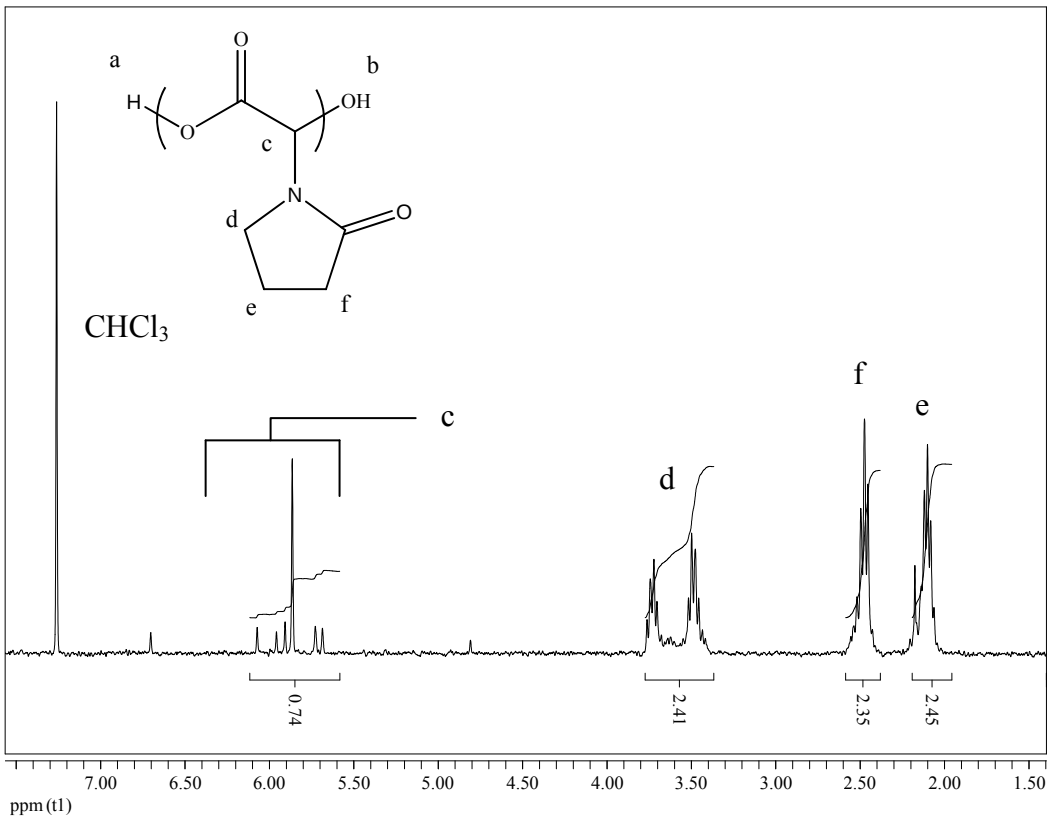

Figure 46: ^{1}H NMR of OPYR polymer

The structural features observed previously in the NMR of PYR were largely retained. However, the α-hydrogen peak was noticeably different as it consisted of multiple peaks, rather than one singlet. The appearance of numerous peaks was attributed to the formation of OPYR. Multiple α-hydrogen peaks were expected in OPYR because the α-carbon can be connected to non-equivalent functional groups, exposing the α-hydrogens to different electronic environments. For example, the α-hydrogens of the terminal repeat units (i.e. adjacent to the carboxyl and hydroxyl termini) would be chemically distinct due to the dissimilar nature of the terminal functional groups. These effects were believed to indicate the formation of

oligomer rather than polymer because the effects of end groups are only noticeable at lower molecular weights. The number of peaks also suggested that both D and L stereoisomers were present in the structure.

After characterization by NMR, DSC was conducted on the crude OPYR to determine the glass transition temperature (T_g) of the product. The DSC thermogram of OPYR is displayed in Figure 47. A thermal transition resembling a T_g at approximately 29 °C was observed. No melting temperature (T_m) was found for OPYR. A T_m was not expected because only polymers produced from enantiopure monomers posses a melting temperature due to high crystallinity from improved chain packing. The polymerization of a racemic mixture of PYR however, would result in an atactic, amorphous polymer because crystalline segments of OPYR would not form.

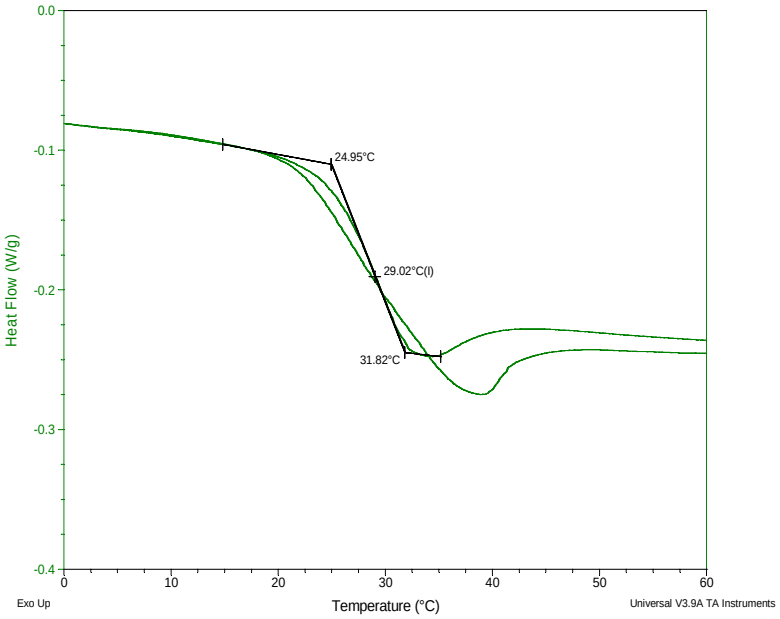

Figure 47: DSC thermogram of OPYR polymer

5.2.2 The effect of reaction time and temperature on the synthesis of OPYR

Once it was determined that the crude product was likely OPYR, GPC was used to evaluate the molecular weight of the polymer. The unpurified OPYR produced after reacting at 100 °C for 24 h was found to have a number average molecular weight (M_n) of approximately 800 g/mol. The weight average molecular weight (M_w) was found to be 830 g/mol and a polydispersity index (PDI) of 1.05 was calculated. The M_n of OPYR corresponds to a degree of polymerization (DP) between 5 and 6 repeat units. Although the molecular weights were low, OPYR was produced.

Due to the formation of oligomers, the reaction time and polymerization temperature in the melt PC procedure were varied to determine if higher molecular weight polymer could be produced. As was mentioned previously, the polymerization stopped bubbling after 18 h to 24 h and was thought to be complete. To determine the effect of reaction time on final polymer molecular weight, three samples of PYR were allowed to react for 12 h, 24 h and 36 h at 100 °C. A plot of reaction time versus molecular weight and PDI is shown in Figure 48. It was determined that 24 h was an adequate reaction time because an additional 12 h of reaction time produced a minimal increase in molecular weight, which was accompanied by an increase in PDI.

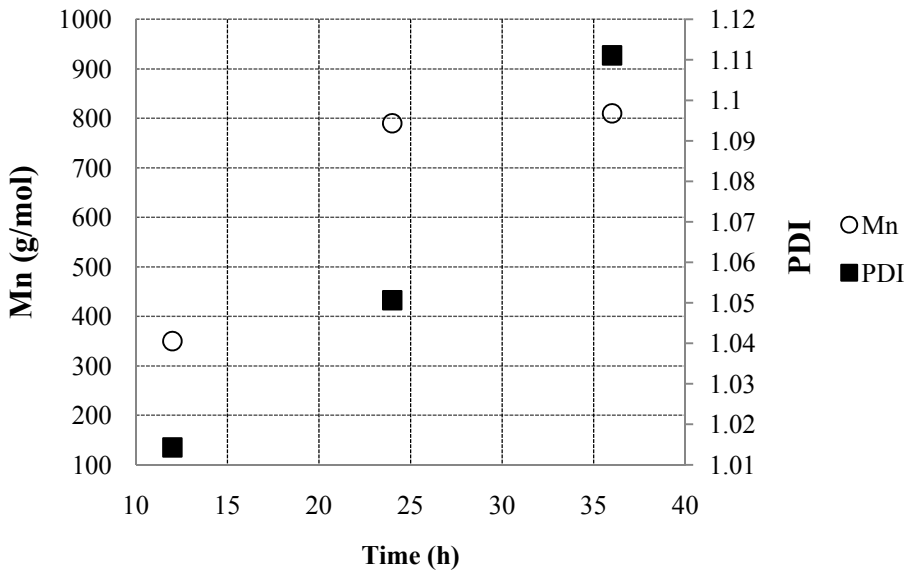

Figure 48: Plot of OPYR molecular weight versus reaction time

To test the temperature dependence of OPYR formation, PYR samples were reacted for 24 h at temperatures ranging from 85 °C to 150 °C. The limits were chosen because the monomer had to be heated past 74 °C to melt and temperatures over 150 °C were found to thermally degrade the sample. At 85 °C, the OPYR produced was a clear, highly viscous substance. As a general rule, the product became more solid-like and more amber colored with increasing temperature.

A plot of the M_n and PDI for OPYR versus temperature is shown in Figure 49. An optimum temperature range existed between approximately 95 °C and 125 °C. In this region, the highest molecular weights were achieved with the least amount of discoloration. The PDI ranged from 1.04 to 1.06, indicating that a narrow distribution of OPYR was produced regardless of reaction temperature.

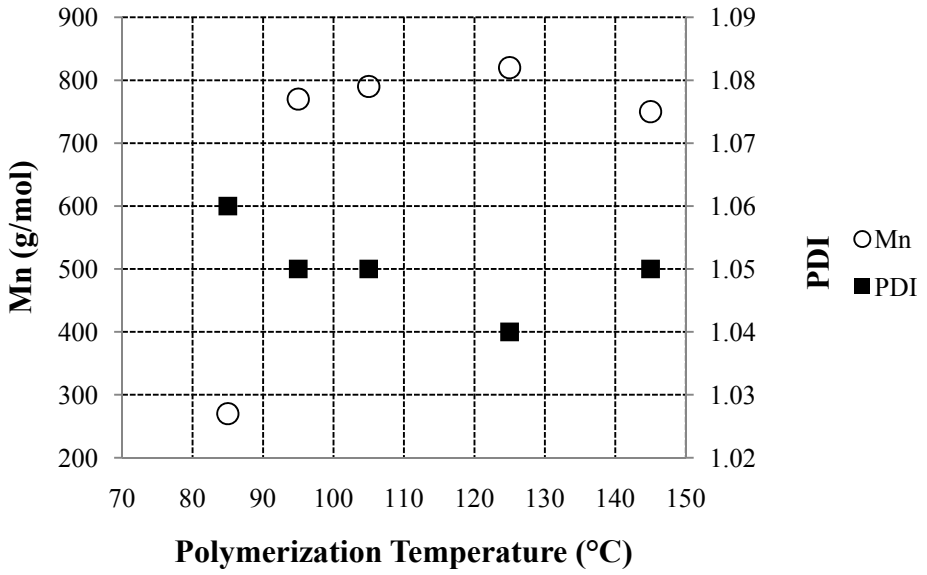

Figure 49: Plot of OPYR molecular weight and PDI versus polymerization temperature

Table 4 provides the information from Figure 49 in a tabular format. Included in Table 4 are molecular weights information, PDI values and the color of the resulting product after melt PC.

Table 4: Summary of the effects of polymerization temperature on the molecular weight of OPYR

Polymerization Temperature (°C)	Color	M_n (g/mol)	M_w (g/mol)	PDI
85	Clear	270	285	1.06
95	Pale yellow	770	810	1.05
105	Pale yellow	790	830	1.05
125	Amber	820	860	1.05
145	Amber	750	790	1.05

5.2.3 The effect of catalysts on the synthesis of OPYR

Once it was determined that OPYR could be produced via melt PC, efforts were made to increase the molecular weights of the polymer chains. One established method for increasing the molecular weight of polyesters in the melt is to add catalysts to the oligomer. Moon et al. reported being able to achieve high molecular weight PLA (>100,000 g/mol) by reacting oligomeric PLA with binary catalysts.[3, 5] The first component of the binary catalyst was a metallic oxide or chloride like TiO_2, ZnO, $SnCl_2$, etc. An organic acid was used as the second component of the binary catalyst system to prevent discoloration. Given the success of the catalytic polymerization of oligomeric PLA, the effect of catalysts on the molecular weight of PYR was studied.

Moon et al. prepared high molecular weight PLA by adding 1 wt% portions (with respect to the oligomer) of both the metallic catalyst and *p*-toluenesulfonic acid (pTSA).[3] The following metallic catalysts were selected for testing: Zn (dust, 10 microns), $ZnCl_2$, ZnO, SnO and $BiCl_3$. The catalyst experiments with OPYR were conducted by adding OPYR and 1 wt% of both the metallic catalyst and pTSA to a round bottom flask. The flask was then connected to the Kugelrohr and the reactants were heated for 24 h at 120 °C, while under full vacuum. The reaction temperature was selected because OPYR produced via melt PC at 120 °C had the highest molecular weight.

The reaction mixture was an amber solid upon completion. The crude product was characterized by DSC prior to purification to prevent degradation. An increase in the T_g over the OPYR was expected if higher molecular weight polymer had been created. A summary of the DSC results are presented below in Table 5. The row labeled “No

catalyst" represents the T_g of OPYR produced during melt PC. The thermograms for the DSC trials with OPYR and the binary catalysts are presented in Appendix A.

Table 5: Binary catalyst effect on the T_g of OPYR

Catalyst (1 % each wrt OPYR)	**T_g (°C)**
No catalyst	29
Zn dust / pTSA	36
ZnO / pTSA	46
SnO / pTSA	39
$BiCl_3$ / pTSA	43
$ZnCl_2$ / pTSA	33

A noticeable increase in the T_g was observed for all of the catalysts tested. The lowest increase was caused by $ZnCl_2$, which increased the T_g by only 4 °C. The greatest increases were caused by $BiCl_3$ and ZnO, increasing the T_g by 14 °C and 17 °C, respectively. The observed increase in T_g was thought to indicate the presence of higher molecular weight OPYR.

The catalysts used during this synthesis may be capable of damaging the GPC by lodging in the size-exclusion columns or by interfering with the detectors. Thus, the catalysts were removed before characterization by GPC. To purify the crude product of residual metals and pTSA, the solid was dissolved in chloroform and filtered through a coarse, sintered-glass frit. Both components of the binary catalyst were insoluble in chloroform and were removed during separation. Due to the purification issues reported for OPYR, the solvent was removed by rotary evaporation, but precipitation was not attempted. The samples were then dried under full vacuum to remove residual

chloroform. The resulting product was a viscous solid. The effect of the catalysts on the molecular weight OPYR is presented in Table 6.

Table 6: The effect of catalyst on the molecular weight of OPYR determined by GPC

Catalyst (1 % each wrt OPYR)	**M_n (g/mol)**	**M_w (g/mol)**	**PDI**
No catalyst	790	830	1.05
Zn dust / pTSA	780	820	1.05
ZnO / pTSA	530	580	1.08
SnO / pTSA	430	520	1.21
$BiCl_3$ / pTSA	720	730	1.03
$ZnCl_2$ / pTSA	500	770	1.54

The addition of the catalysts seemed to negatively affect the molecular weight of the OPYR and in some instances, increased the PDI substantially. Since DSC indicated the T_g of the product had increased relative to the OPYR formed in the melt, a reduction in molecular weight was surprising. It was thought that residual water in the chloroform degraded the OPYR sample. To test this hypothesis, an unpurified ZnO sample was characterized by GPC. The unpurified OPYR had a M_n and M_w equal to 780 g/mol and 800 g/mol, respectively. Although the molecular weight of the unpurified ZnO sample was higher than the purified sample (a DP $\approx$ 2), the molecular weight of the unpurified ZnO sample was nearly identical to uncatalyzed OPYR produced during melt PC. It was assumed that even if samples such as Zn dust (which had the highest molecular weight after purification) were tested before purification, the increase in observed molecular weight would be modest. It was consequently believed that an increase in molecular weight was not responsible for the increase in T_g.

A possible explanation for the T_g elevation after adding catalysts was that the catalysts had a strong interaction with the functional groups in the OPYR, causing an increase in the T_g without increasing the molecular weight. After consulting the literature, it was found that certain polyether-metal complexes experienced T_g elevation. [6] However, the increase in the T_g of OPYR did not correspond well to the polyether system. For a poly(propylene oxide)-$ZnCl_2$ complex, the T_g was elevated at a rate of approximately 1 °C per mol% of the catalyst added. [6] Although the polyether system described in the literature and the OPYR-catalyst systems were not identical, it seems unlikely that the addition of 1 wt% of the binary catalyst mixture was capable of increasing the T_g of OPYR by as much as 17 °C. To date, no conclusive explanation for the increase in T_g has been developed.

One potential discrepancy between the oligomeric PLA-catalyst system described by Moon et al. [3] and the OPYR-catalyst system examined was melting. The most successful post polymerization modifications occurred when PLA was heated above its melting temperature (≈ 180 °C) in the presence of catalysts. However, OPYR does not possess a T_m because the polymer is amorphous. Consequently, effective mixing of the catalyst throughout the sample is a potential limiting factor. To test if the non-melt state OPYR inhibited the formation of higher molecular weight, the polymerization of the PYR monomer with catalyst was tested. A number of sources in the literature cite the use of catalysts to produce PLA by direct melt PC of lactic acid. [7-9] It was believed that higher molecular weight OPYR might be produced by adding the catalyst directly to the PYR α-HA.

The catalyst experiments with PYR were conducted by adding 5 wt% of the catalyst (with respect to PYR) and recrystallized PYR to a round bottom flask. For these experiments, pTSA was not added as a co-catalyst. A catalyst ratio of 5 wt% was chosen to make the effect more pronounced. The flask was then connected to the Kugelrohr and heated for 24 h at 105 °C under full vacuum. The polymerization temperature was selected because pTSA was not added and discoloration of OPYR was therefore expected at higher temperatures. Five catalysts were investigated: Zn (dust, 10 microns), ZnO, $BiCl_3$, pTSA and Scandium (III) Triflate. Scandium (III) Triflate (ScTrf) and pTSA were selected because strong Lewis acids [10] and organic acids [11] were reported to aid in the direct melt polymerization of lactic acid. The two Zn compounds and $BiCl_3$ were selected because of the ability of these compounds to alter the T_g or the molecular weights of the OPYR samples prepared previously (Table 5 and Table 6).

After completion of the reaction, all of the samples were clear, hard solids except for the ZnO reaction, which was a white solid. The samples were analyzed by GPC without further purification. No obvious detection issues or changes in column retention were observed. The results of the experiments with catalysts and PYR are summarized in Table 7. The results for "No catalyst" are the values for the uncatalyzed melt PC of PYR at 100 °C.

Table 7: The effects of catalysts on the direct melt PC of PYR monomer

Catalyst (5 % wrt to PYR)	**M_n (g/mol)**	**M_w (g/mol)**	**PDI**
No catalyst	790	830	1.05
Zn dust	690	720	1.04
ZnO	720	740	1.03
pTSA	720	750	1.04
$BiCl_3$	690	720	1.04
ScTrf	730	770	1.05

From the results shown in Table 7, the catalysts tested did not improve the molecular weight of the OPYR produced. In fact, all of the catalysts had a negative effect on the molecular weight of the oligomer, although the difference was minimal enough that the samples were considered equal. Based on the information presented in Table 6 and Table 7, it was determined that the catalysts tested were not effective at increasing the molecular weight of either PYR or OPYR in the melt.

The results of the catalyst experiments indicate that certain system dynamics precluded the formation of higher molecular weight polymer. The most likely of these factors was the buildup of viscosity during melt PC. Increased viscosity suppresses chain mobility, which in turn prevents carboxyl and hydroxyl termini from condensing. Another likely possibility was that the equilibrium between higher molecular weight polymer and the depolymerization of those chains (by either back-biting or random chain scission) could not be controlled by the addition of catalysts. Both of these issues, as well as ineffective water removal and insufficient monomer purity have been cited in the literature as limiting factors for the formation of higher molecular weight PLA. [12] It was believed these factors limited the reaction and precluded the formation of polymer.

5.3 The Melt Polycondensation of 2-Acetamido-2-Hydroxyacetic Acid (ACE)

5.3.1 The general synthesis of oligo(2-acetamido-2-hydroxyacetic acid) (OACE)

Oligo(2-acetamido-2-hydroxy acetic acid) (OACE) was synthesized analogously to OPYR. Unrecrystallized ACE monomer was used because no purification method was developed successfully. The ACE monomer was added to a round flask, which was then connected to the Kugelrohr. The flask was heated for 24 h at 80 °C under full vacuum. The temperature was chosen based on the observation that the optimal polymerization temperature for PYR was approximately 20 °C to 25 °C above the melting temperature of the PYR monomer. Consequently, 80 °C was chosen as the original polymerization temperature because the melting temperature of ACE was 58 °C.

Before entering the flask, ACE was a clear to white semi-crystalline solid as described previously in Chapter Four. Once heating and vacuum were initiated, the ACE began to melt and then bubble vigorously. The bubbling ended after approximately 16 h to 18 h of reacting, but the reaction was allowed to proceed for 24 h. After the reaction was completed, a pale amber colored solid was observed. The polymerization of ACE into OACE is depicted in Figure 50.

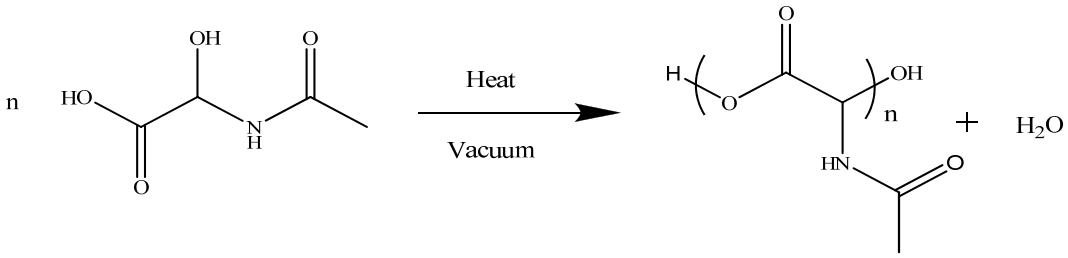

Figure 50: The polymerization of ACE monomer

Purification of the product by precipitation from chloroform was attempted, but the crude product was found to be insoluble in chloroform. The product was soluble in solvents of equal or greater polarity index to acetone (>5.1, i.e. DMSO, DMF, etc.), but no solvent-nonsolvent pair was found for precipitation. For example, the crude product was soluble in DMF, but precipitation into non-solvents like hexanes or diethyl ether did not cause precipitation. As a result, the crude product was characterized directly.

The crude product was first characterized by NMR. Since the product was found to be insoluble in chloroform, *d6*-DMSO was used. The NMR spectrum of the crude OACE product is presented in Figure 51. The peaks at δ = 2.50 ppm and 3.33 ppm were the residual solvent peak and water, respectively.

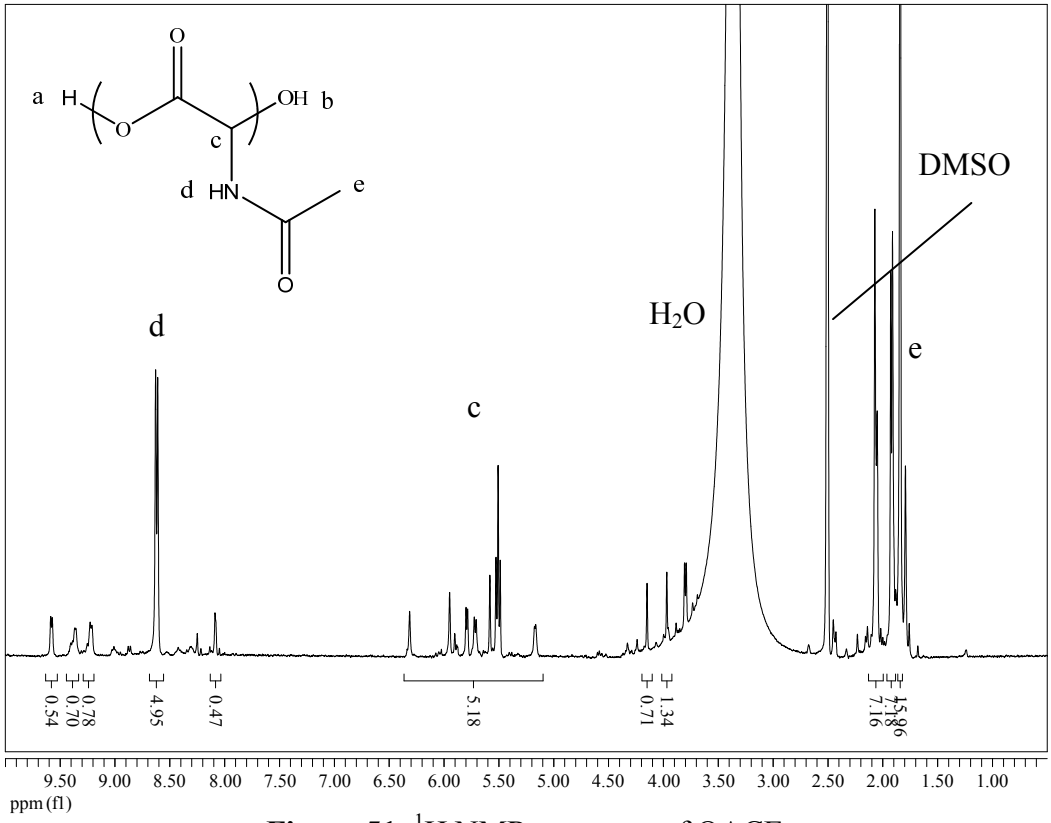

Figure 51: ^{1}H NMR spectrum of OACE

The spectrum presented in Figure 51 was somewhat similar to the NMR spectra for OPYR. The peaks centered between 5 ppm and 6 ppm were thought to be the α-hydrogens of the OACE polymer chain, caused by the D and L enantiomers of ACE or end group effects. The multitude of smaller peaks between 10 ppm and 7.5 ppm, as well as the extraneous peaks centered around 2 ppm were thought to represent impurities (artifacts from the ACE monomer or induced during polymerization) because only the α-hydrogens should show multiple peaks.

DSC was conducted on the crude product to calculate a T_g. The DSC thermogram of OACE is provided in Figure 52. From the plot, it was observed that a thermal transition resembling a T_g occurred at approximately 33 °C. No T_m was observed for the substance, which was expected due to the racemic mix of ACE enantiomers used to synthesize OACE. Based on the results of NMR and DSC, the product was characterized by GPC to determine the molecular weight of OACE.

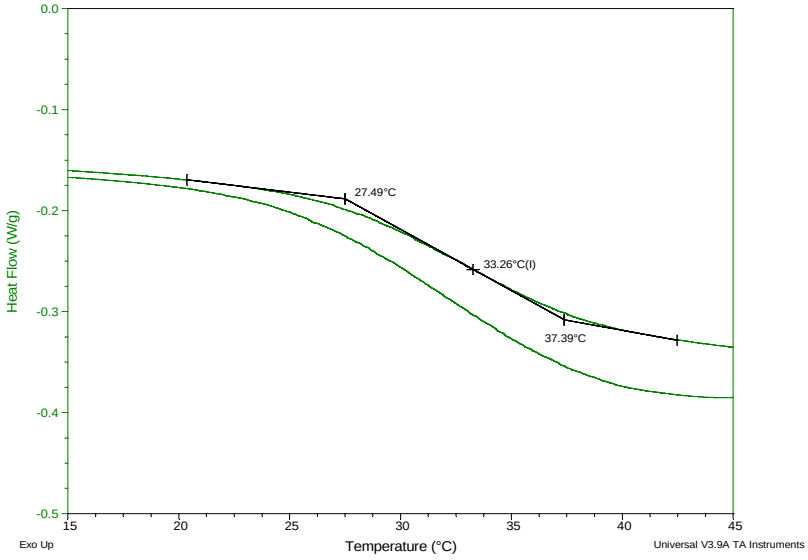

Figure 52: DSC thermogram of OACE

5.3.2 The effect of temperature on the synthesis of OACE

After examination of the crude OACE with NMR and DSC, GPC was conducted. As was the case with OPYR, it was expected that the molecular weight of OACE would exhibit temperature dependence. To test this theory, OACE was polymerized as described in the previous subsection. The melt PC reaction was allowed to proceed for 24 h at temperatures ranging from 70 °C to 100 °C. Temperatures greater than 110 °C produced thermally degraded samples. A plot of OACE molecular weight as a function of temperature is depicted in Figure 53.

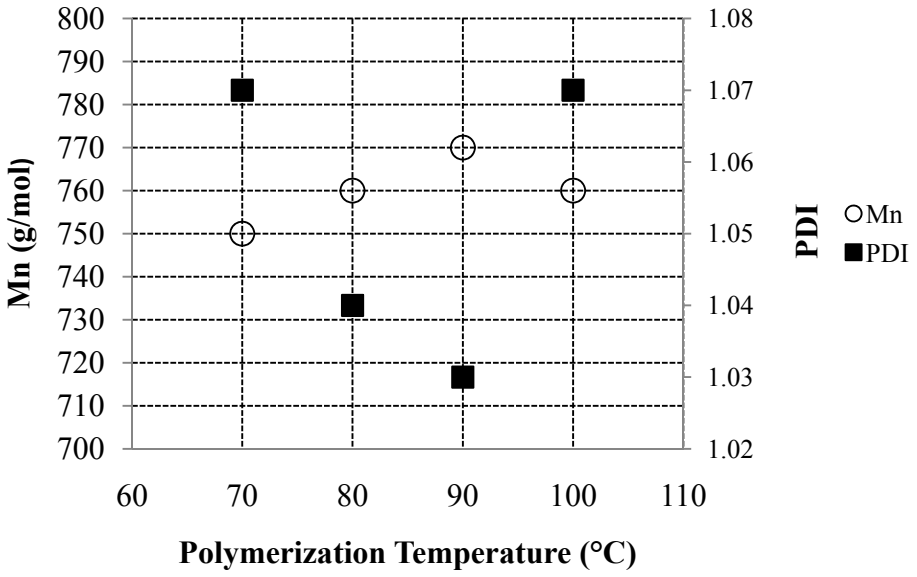

Figure 53: Plot of OACE molecular weight versus polymerization temperature

Further OACE information is included in Table 8. The table includes qualitative reaction information as well as M_n, M_w and PDI data and calculations.

Table 8: Summary of the effects of polymerization temperature on the molecular weight of OACE

Polymerization Temperature (°C)	Color	M_n (g/mol)	M_w (g/mol)	PDI
70	Clear	750	800	1.07
80	Pale Yellow	760	790	1.04
90	Pale Yellow	770	790	1.03
100	Orange	760	810	1.07

After examining the results presented in Figure 53, it was determined that an optimum melt PC temperature for OACE was approximately 90 °C. A M_n of 770 g/mol was observed at this temperature, indicating a DP between six and seven repeat units. The PDI ranged from 1.03 to 1.07. The product varied in color across the temperature range from clear at 70 °C to amber at 100 °C. Although only low molecular weight oligomers were obtained, it was interesting to note that despite being impure, the ACE was still capable of being polymerized.

5.4 The Attempted melt synthesis of oligo(2-benzamido-2-hydroxyacetic acid) (OBZ) and oligo(2-acrylamido-2-hydroxyacetic acid) (OACRY)

After OPYR and OACE were polymerized by melt PC, it was desired to produce oligo(2-benzamido-2-hydroxyacetic acid) (OBZ) and oligo(2-acrylamido-2-hydroxy-acetic acid) (OACRY) by similar means. The procedures for the melt PC of both monomers were conducted analogously to previous trials. The monomer, BZ or ACRY, was placed into a round bottom flask and attached to the Kugelrohr. The flask was then heated above the melting temperature of the monomer (155 °C for BZ and 125 °C

for ACRY) and placed under full vacuum (≈ 102 kPa). However, unlike the previous monomers, melting was not observed for either BZ or ACRY. Instead, the once white solids discolored, yielding BZ as a brown powder and ACRY as an orange, clumpy mass. Altering the temperature of the reaction conditions did not produce noticeably different products.

Efforts were made to determine the reason for the dissimilarity between BZ, ACRY and the other monomers. Thermal gravimetric analysis (TGA) was utilized to determine mass loss as a function of temperature. It was believed that TGA could indicate when and to what extent degradation was occurring. The TGA plots of BZ and ACRY are presented in Figure 54 and Figure 55, respectively.

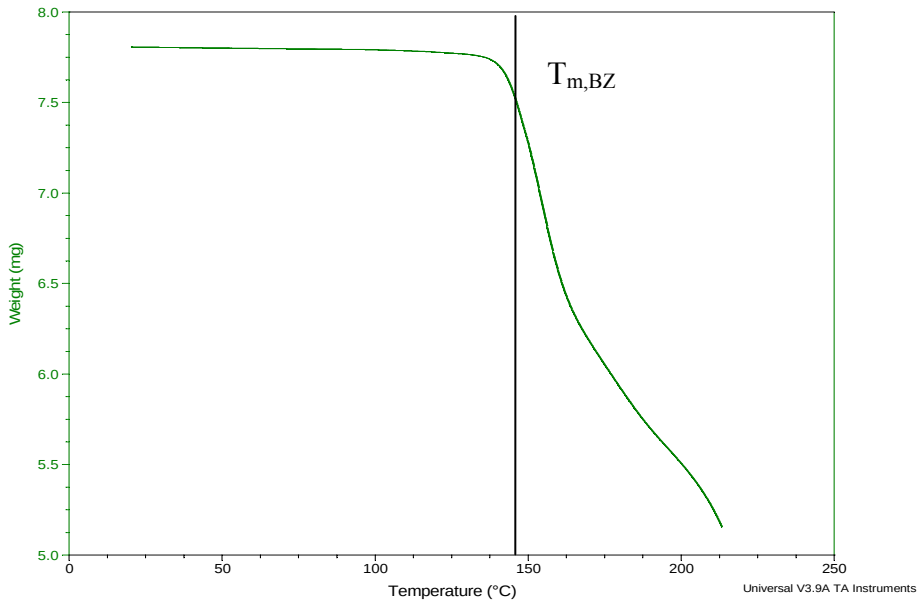

Figure 54: TGA thermogram of BZ with T_m of BZ indicated

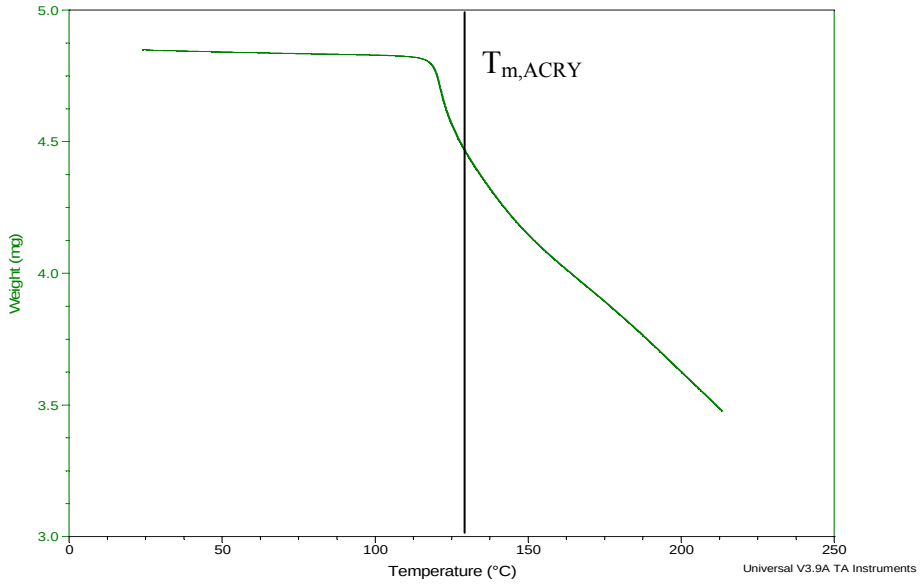

Figure 55: TGA thermogram of ACRY with T_m of ACRY indicated

For both monomers, there is a steep mass loss that occurs very near the melting points calculated for the monomers by DSC. The melting points of BZ and ACRY were determined to be 152 °C and 124 °C, respectively. These thermal transitions correlate well with the onset of mass loss determined by TGA, which occurs at approximately 142 °C for BZ and 115 °C for ACRY. This result was believed to indicate that upon reaching the melting temperature, thermal degradation of the monomers occur.

The TGA plots for PYR and ACE are shown in Figure 56 and Figure 57, respectively. There are some noticeable differences between the two sets of plots. At the onset of mass loss, both ACE and PYR gradually lose mass. The TGA of PYR also shows a change in slope at approximately 150 °C. During melt PC reactions of PYR, polymerization temperatures above 150 °C degraded, indicating that the change in slope

is likely indicative of degradation. Conversely, the TGA plots of BZ and ACRY showed a large initial rate of mass loss. Also, the mass loss associated with PYR and ACE was observed to possess a reverse S-shape, whereas the BZ and ACRY plots somewhat resembled step functions.

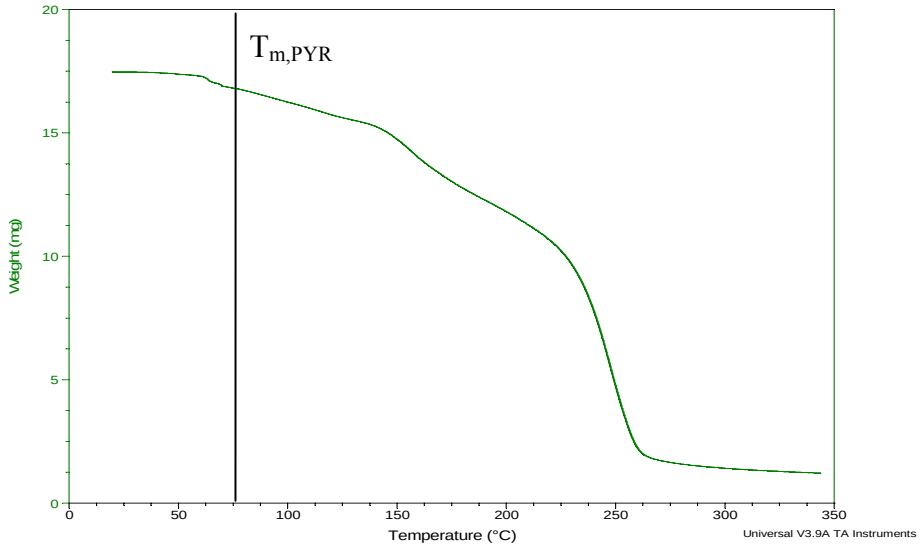

Figure 56: TGA thermogram of PYR with T_m of PYR indicated

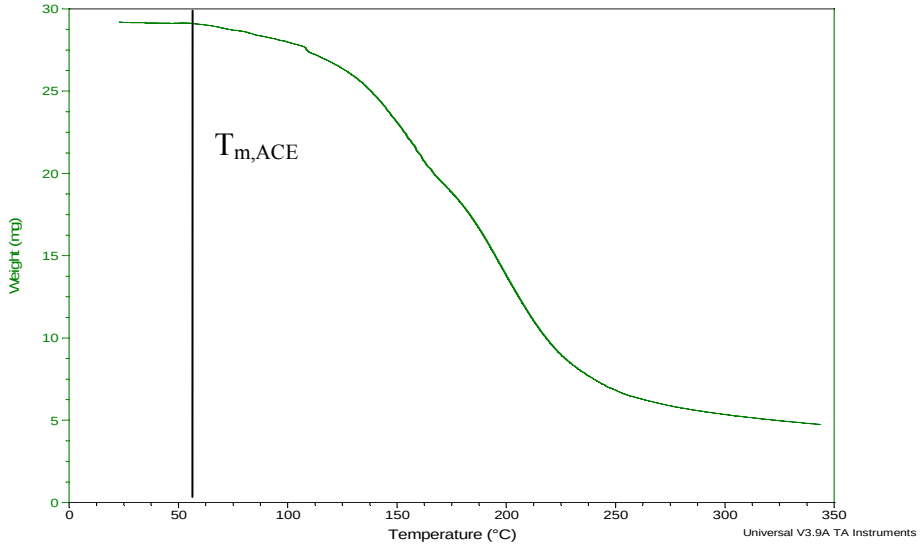

Figure 57: TGA thermogram of ACE with T_m of ACE indicated

The difference in the shape of the graphs was attributed to different degradation processes. For PYR and ACE, polymerization was observed and the gradual mass loss shown by TGA is believed to indicate dehydration occurring during polycondensation. No polymerization was observed for BZ and ACRY however, and the pseudo-step function of the TGA plots for these monomers was thought to represent a form of degradation not associated with polymerization. On account of these plots, it was believed that neither BZ or ACRY were conducive for melt PC.

5.5 Summary of Melt Polycondensation

Both PYR and ACE could be polymerized by melt PC and showed temperature dependent polymerizations. The resulting oligomers had M_n of approximately 800 g/mol, indicating a DP between five and six repeat units for OPYR and a DP of six to seven repeat units for OACE. The PDI values for both oligomers were low, typically near 1.05. Catalysts were found to be ineffective at increasing the molecular weight of OPYR, regardless of whether they were added to OPYR or PYR. Although only low molecular weight oligomer was formed, the melt PC of PYR and ACE represents the successful formation of functionalized oligo(esters) and presumably, the first reported synthesis of OPYR and OACE.

Neither BZ nor ACRY could be polymerized by melt PC. After analyzing TGA data for these monomers, it was concluded that an alternate degradation pathway was occurring instead of polycondensation. The degradation of both monomers occurred near their respective melting points. Since melt PC was incompatible with BZ and ACRY,

another polymerization method was needed. Solution polymerization was a logical choice as the necessary reactions conditions are often milder than those required during melt PC. The next chapter, Chapter Seven, examines experimentation into the solution polymerization of BZ.

5.6 References

(1) Drumright, R.; Henton, D. *Advanced Materials* **2000**, *12*, 1841.
(2) Ajioka, M.; Yamaguchi, A. et al. *Journal of Polymers and the Environment* **1995**, *3*.
(3) Moon, S.; Kimura, Y. et al. *Journal of Polymer Chemistry* **2000**, *39*, 1673.
(4) Miyoshi, R.; Sakai, T. et al. *International Polymer Processing* **1996**, *11*, 320.
(5) Moon, S.; Kimura, Y. et al. *Polymer* **2001**, *42*, 5059.
(6) James, D. B.; Brown, D. S. et al. *Polymer* **1979**, *20*, 187.
(7) Hiltunen, K.; Härkönen, M. et al. *Macromolecules* **1997**, *30*, 373.
(8) Kim, K.; Woo, S. *Macromolecular Chemistry and Physics* **2002**, *203*, 2245.
(9) Nagahata, R. et al. *Macromolecules Rapid Communications* **2007**, *28*, 437.
(10) Konishi, S.; Endo, T. et al. *Polymer Bulletin* **2010**, *64*, 435.
(11) Abiko, A.; Iwasaki, H. JP Patent 061784, 2007.
(12) Garlotta, D. *Journal of Polymers and the Environment* **2001**, *9*, 63.

CHAPTER SIX:

SOLUTION POLYMERIZATION

6.1 Introduction to Solution Polyesterification

Chapter Five determined that melt polycondensation was an unsuitable polymerization method for 2-benzamido-2-hydroxyacetic acid (BZ) and 2-acrylamido-2-hydroxyacetic acid (ACRY). It was determined that a solution polymerization was the most logical technique to test because solution polymerizations can often be conducted under mild conditions. As BZ and ACRY both degrade at elevated temperatures, a more moderate synthetic method was appropriate.

Of the solution polymerizations researched, the Steglich esterification appeared to be a good candidate for experimentation because previous research has shown that high molecular weight poly(lactic acid) (PLA) could be produced with a number average molecular weight of 86,000 g/mol.[1] An introduction to the reaction is provided in section 2.6.1 of the literature review and additional information will be provided in this chapter. Although the Steglich esterification involved some toxic chemicals, the procedure had other benefits that made it worth testing. The experimental procedure was relatively simple and the reaction was compatible with a number of different functionalities. Even chemically reactive groups were not affected during the esterification, making it appropriate for the polymerization of the amido-functionalized monomers.

6.2 Synthesis of Oligo(2-benzamido-2-hydroxyacetic acid) (OBZ) by Acid Mediated Steglich Esterification

6.2.1 Introduction to the synthesis of OBZ

The first attempts at producing oligo(2-benzamido-2-hydroxyacetic acid) (OBZ) were based on the work of Wagener et al. [2] Wagener polymerized 3-hydroxy-2-phenylpropanoic acid, an aromatic β-hydroxy acid analogue to BZ. Due to the structural similarities between BZ and the monomer polymerized in the literature, the article was used as a starting point for the synthesis of OBZ. Moore and Stupp have also reported success with variations of this procedure, producing high molecular weight polyesters from complex aromatic repeat units. [3] A simple diagram of the Steglich polyesterification of OBZ is shown below in Figure 58 to clarify the repeat structure of OBZ. Common reagents are listed and are detailed following the figure.

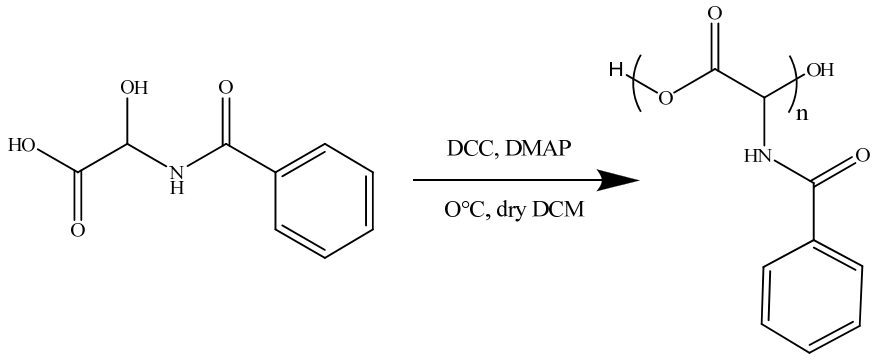

Figure 58: The formation of OBZ through the Steglich esterification

The most effective polymerization reported by Wagener et al. [2] was an acid mediated Steglich esterification using *p*-toluenesulfonic acid (pTSA) as the acid source. The procedure consisted of reacting 3-hydroxy-2-phenylpropanoic acid, dicyclohexyl-

carbodiimide (DCC), pTSA and 4-dimethylaminopyridine (DMAP) together in dry dichloromethane (DCM). Both DCC and DMAP were involved in the polyesterification, while pTSA was used to prevent side reactions.

The Steglich polycondensation of a bifunctional molecule like 3-hydroxy-2-phenylpropanoic acid is thought to occur by the mechanism depicted in Figure 59 (the compounds in the mechanism, labeled A through G, are provided in a footnote following the figure). The reaction was initiated by the carboxyl group of the monomer, which nucleophilically attacked the carbodiimide (A). This forms an O-acylurea intermediate (B) that is vulnerable to further nucleophilic attack by DMAP (E). The addition of DMAP to the O-acylurea intermediate forces the release of a dialkylurea (F) and the formation of an activated acylpyridinium cation (G). The acylpyridinium cation is highly reactive because the DMAP substituent is a superior leaving group. Due to the reactivity of G, the molecule is vulnerable to nucleophilic attack by a hydroxyl group from another monomer or a hydroxyl terminus of an existing polymer chain.

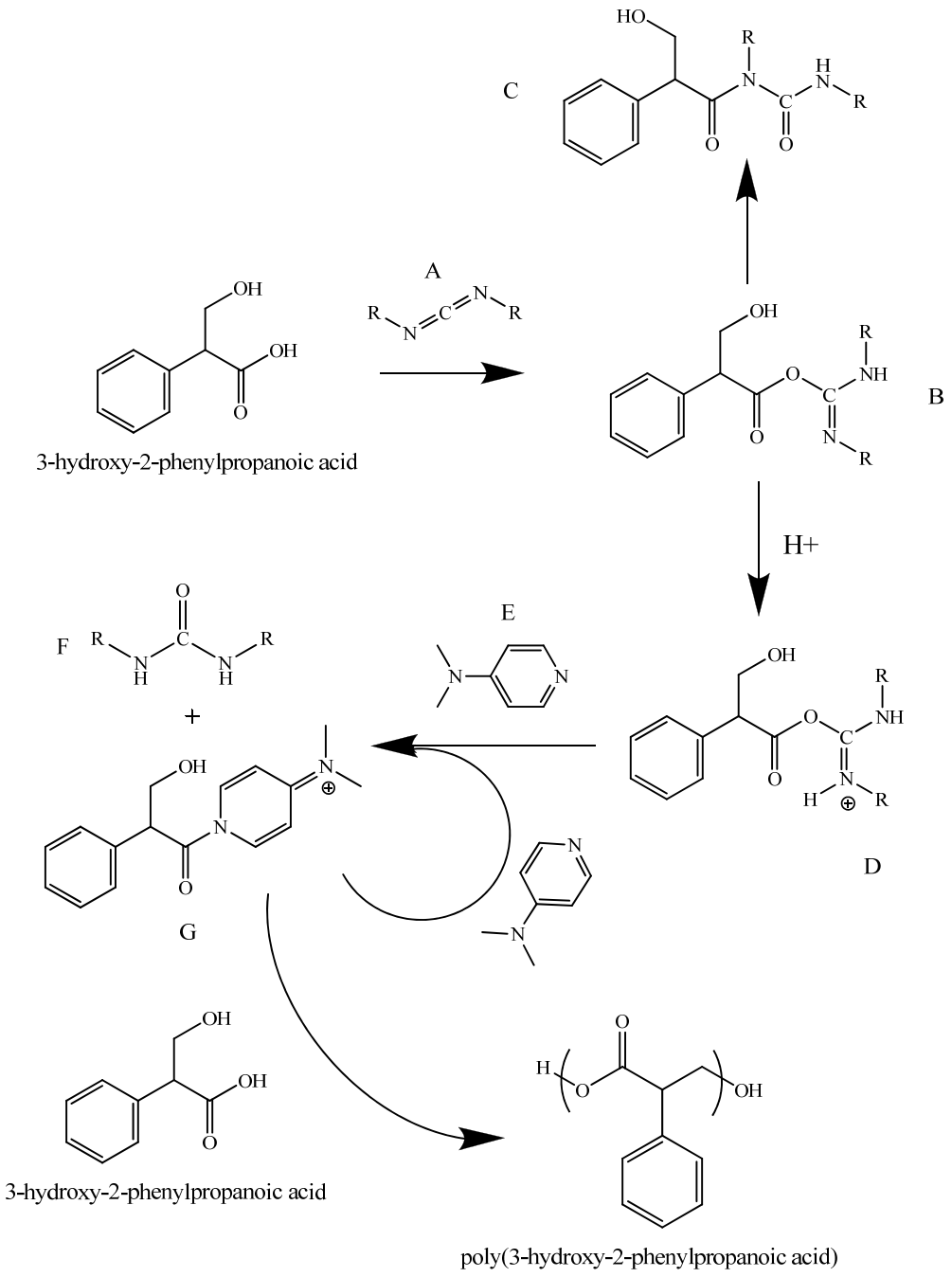

Figure 59: Proposed Steglich esterification mechanism for 3-hydroxy-2-phenylpropanoic acid*

*A: Carbodiimide (R = cyclohexyl or isopropyl); B: O-Acylurea intermediate; C: N-Acylurea byproduct; D: Protonated O-acylurea intermediate; E: 4-Dimethylaminopyridine (DMAP); F: Dialkylurea; G: Acylpyridinium cation

A variety of factors contributing to the success of the Steglich esterification were found in the literature. The solvent and the concentration of the monomer in the solvent appeared to be the most critical factors. [4, 5] A direct correlation between the extent of reaction and the donor number of the solvent has been shown. Solvents with lower donor numbers like DCM were proven to be more effective for polyester synthesis compared to solvents with higher donor numbers like DMF. [3, 5] The decreased reactivity is likely caused by stabilization of the acylpyridinium cation (G in Figure 59) in the higher donor number solvent, reducing the conversion. Qian and Mathiowitz also showed that the hydrogen-bond acidity versus basicity of a solvent influenced the polymerization of poly(anhydrides) in the presence of dehydrating agents. [6] Solvents exhibiting low hydrogen bond acidity (THF) produced lower molecular weight polymers and higher polydispersities compared to solvents with higher acidity (DCM). [6]

The concentration of the monomer was found to be important because higher concentrations of the alcohol group reduced the formation of the N-acylurea (C). [5] Higher alcohol concentrations decreased the formation of the N-acylurea because the probability of condensation with the O-acylurea intermediate (B) was increased, reducing the amount of N-acylurea that could be formed. Lastly, it was noted that the carboxyl group reacted preferentially with the carbodiimide, leaving the hydroxyl unreacted and therefore, available for condensation. [7]

6.2.2 The general synthesis of OBZ by acid mediated Steglich esterification

The first attempted polyesterification of BZ was conducted by adding BZ, DMAP and pTSA at ratios of 1:0.6:0.6 mol equivalents to a round bottom flask. The flask was sealed and flame dried under a nitrogen purge to remove water and dry DCM was syringed into the flask. Care was taken to avoid contacting the reactants with the flame. To lower the initial temperature of the reaction, the flask was rinsed with cold water and placed in a freezer for 1 h at which time, a solution of cold DCC and DCM was added. The ratio of DCC to BZ was 1:1 mol equivalents

After approximately 15 min of reaction, a faint yellow color was observed. Upon reacting overnight, the solution turned completely orange. The color change was not anticipated as OBZ was expected to be white, consistent with most polyesters. The formation of a colored product was thought to indicate a side reaction. The Steglich polyesterification of BZ is provided in Figure 60 to clarify the reaction as it applies to BZ. The main side reaction reported during Steglich esterification is the formation of an N-acylurea. For BZ, the N-acylurea is shown as letter C in Figure 60. The production of the N-acylurea byproduct is undesirable because it would suppress the production of polymer by acting as a non-reactive endgroup. The addition of the organic acid pTSA was thought to inhibit the formation of the N-acylurea by protonating the imide of the O-acylurea intermediate (B in Figure 60). The protonation of the imide functional group in the O-acylurea intermediate is thought to prevent the imide from attacking the adjacent acyl group, thus preventing the formation of the N-acylurea.

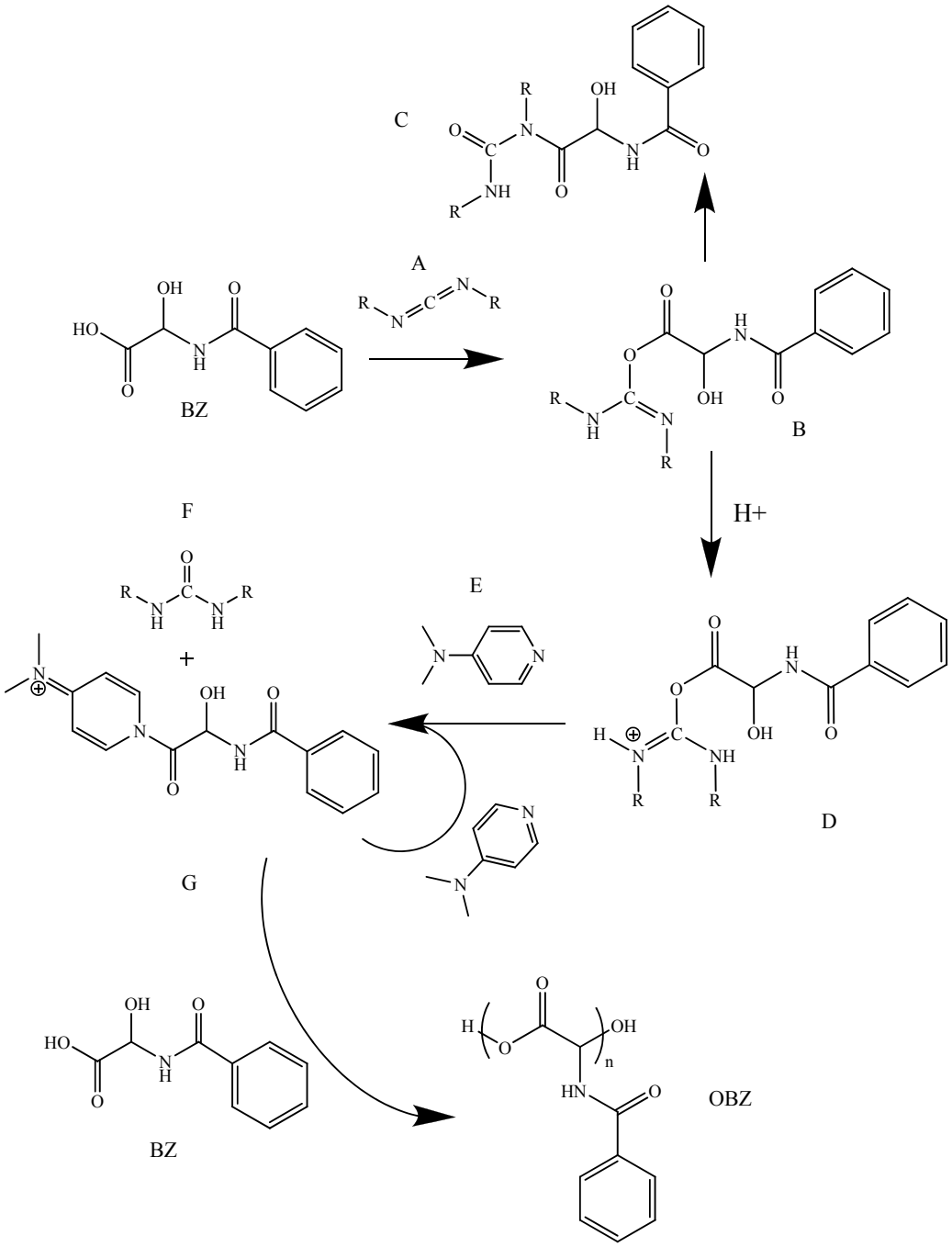

Figure 60: Proposed Steglich esterification mechanism for BZ [*]

[*] A: Carbodiimide (R = cyclohexyl or isopropyl); B: O-Acylurea intermediate; C: N-Acylurea byproduct; D: Protonated O-acylurea intermediate; E: 4-Dimethylaminopyridine (DMAP); F: Dialkylurea; G: Acylpyridinium cation

To characterize and purify the crude product, the orange mixture was vacuum filtered to remove insoluble material. Dicyclohexylurea (DCU), labeled F in Figure 60, is produced during the reaction and is insoluble in DCM. After separation of DCU, excess solvent was removed by rotary evaporation to yield an orange solid product. The crude product was not purified further before characterization to avoid product degradation.

The crude product was first analyzed by NMR to identify the products formed during the reaction. The NMR spectrum of the reaction mixture is shown in Figure 61. The spectrum was obtained using *d6*-DMSO as the solvent and the peaks at $\delta = 2.50$ ppm and 3.33 ppm are residual solvent and water peaks, respectively. Although the existence of the N-acylurea could not be proven definitively, a reasonable identification of the peaks was concluded.

The chemical shift of the α-hydrogen of the N-acylurea (labeled "e" in the figure) was determined by matching the integration of "e" with the other aromatic hydrogens ($\delta = 8.00$ ppm to 7.00 ppm) and comparing the observed shift to the α-hydrogen of the BZ α-HA. The existence of the N-acylurea was validated by peak "f" because its integration matches the peak at $\delta = 9.20$ ppm, thought to be the N-H hydrogen of the amido linkage in the N-acylurea. Given that the hydrogens are in similar electronic environments and they exist stoichiometrically in the molecule, the ratio of their peak integrations should be 1:1. If the N-acylurea did not form, peak "f" should not be observed. The third peak, labeled "g", was the N-H hydrogen of DCU because no other peaks were believed to occur in this region and the integration did not match the proposed N-acylurea peaks, indicating it was a feature from another compound. The

cyclohexyl groups could not be completely resolved to further confirm this theory. Peaks for pTSA were not observed because pTSA is insoluble in DCM and was removed during filtration.

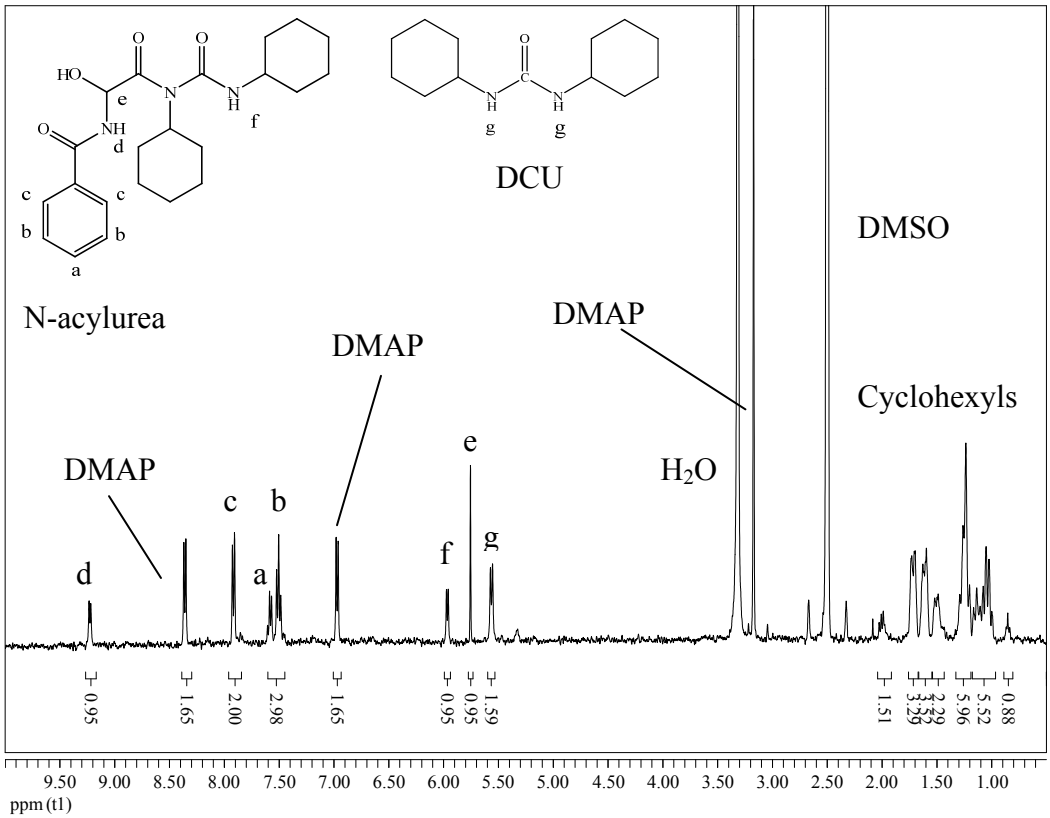

Figure 61: ^{1}H NMR spectra of OBZ via acid mediated Steglich esterification

Analysis or the crude product with GPC established that OBZ was formed. Although the crude product was not completely soluble in THF (the GPC eluent), the extract was found to contain a substance with a number average molecular weight (M_n) and a weight average molecular weight (M_w) of 800 and 850 g/mol, respectively, corresponding to a polydispersity index (PDI) of 1.06. The GPC peak was believed to be OBZ, equivalent to a degree of polymerization (DP) of approximately four repeat units.

Another peak was also observed by GPC with a M_n and M_w of 225 g/mol and 235 g/mol, respectively (PDI = 1.04). This peak was thought to be residual dicyclohexylurea (F) as the molecular weight of the compound was 224 g/mol, supporting the results obtained by NMR.

The crude product was then tested by DSC to determine the glass transition temperature (T_g). The DSC plot of the crude product is shown below in Figure 62. Although the thermal transition was slight, a T_g was found. The T_g of the product was determined to be approximately 11 °C. Due to the bulky aromatic side groups, the T_g of the OBZ polymer would be expected to be higher relative to the other oligomers (i.e. OPYR, etc.). However, such a low T_g supported the fact that only low molecular weight oligomers were created.

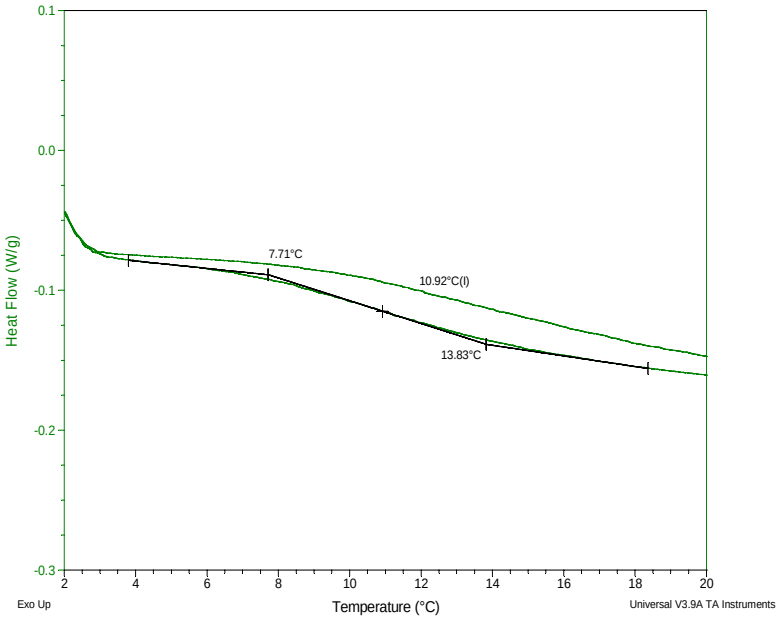

Figure 62: DSC plot of crude OBZ from acid mediated Steglich esterification

6.2.3 The effect of reactant ratios on the formation of OBZ by acid mediated Steglich esterification

Although OBZ was synthesized, the formation of the N-acylurea accompanied the desired product. The ratios of the reagents in the Steglich esterification were varied to try and eliminate the formation of the N-acylurea, as well as to produce higher molecular weight polymer. The results of these trials are presented below in Table 9.

Table 9: The effect of reactant ratios on the formation of OBZ during Steglich esterification

Trial	DMAP (mol eq.)	DCC (mol eq.)	pTSA (mol eq.)	Reaction color	Mn (g/mol)	Mw (g/mol)	PDI
1	0.7	1.0	0.7	Orange	800	850	1.06
2	0.7	0.7	0.7	Yellow	360	370	1.02
3	0.3	0.3	0.3	Orange	230	260	1.13
4	0.7	0.7	0.1	Off-white	780	790	1.01
5	1.0	0.7	0.7	Light Yellow	780	800	1.03
6	0.7	0.7	0.0	White	760	780	1.03
7	0.1	0.8	0.0	Yellow	410	450	1.10
8	0.7	1.0	0.0	Yellow	240	270	1.13

The experiments indicated that a ratio of DMAP to DCC of 1:1 was most successful (trials 4 and 6), producing a white product with relatively high molecular weights. Trials where the ratio of DMAP to DCC was lower than 1:1 (trials 1, 7 and 8) generally resulted in the formation of the N-acylurea (orange byproduct) and lower molecular weight oligomers. The formation of a non-white product under excess DCC helped to substantiate the assumption that a color change was the result of the N-acylurea impurity (trial 7).

The addition of pTSA did not help to increase the molecular weight of the oligomers or suppress the formation of the N-acylurea. After comparing trials 2, 4 and 6, it was observed that decreasing the amount of pTSA decreased the amount of N-acylurea (increasingly white product). Analyzing these trials further, it was interesting to note that when DCC, DMAP and pTSA were added in equimolar amounts (trial 2), the lowest molecular weight was achieved. However, the addition of excess DMAP was capable of diminishing the negative effects of pTSA. When DMAP was added in excess (trial 5), a light yellow color was observed and the molecular weight was higher.

It was noted that pTSA, despite the success of Wagener et al., [2] was a detriment to the formation of OBZ. The acid did not seem to prevent the formation of side reactions, but instead, seemed to induce other byproducts. The ratio of DMAP to DCC was also found to be important for the successful formation of OBZ. Due to these observations and the exclusive production of oligomers, the literature was consulted to modify the esterification to produce polymeric OBZ.

6.3 Synthesis of OBZ by Scandium (III) Triflate Catalyzed Steglich Esterification

6.3.1 General synthesis of OBZ by catalyzed Steglich esterification

Given that only low molecular weight OBZ was formed in the previous experiments and the acid mediated Steglich esterification was determined to be ineffective, it was desired to test other variations of the reaction. A plausible reaction was found in the literature that replaced the carbodiimide DCC with Diisopropylcarbodiimide (DiPC) and was catalyzed by Scandium (III) Triflate (ScTrf).

The addition of ScTrf, a strong Lewis acid, was shown to increase the reactivity of the acylpyridinium cation formed during the Steglich esterification. [8] The addition of ScTrf was originally intended for the esterification of tertiary alcohols, which are notorious for being unreactive. The effect of the ScTrf is depicted in Figure 63. The ScTrf increases the rate of the reaction by coordinating the two acyl carbonyls connected to the DMAP complex, making the carbonyls more electrophilic and more susceptible to nucleophilic attack by another BZ hydroxyl group. [8]

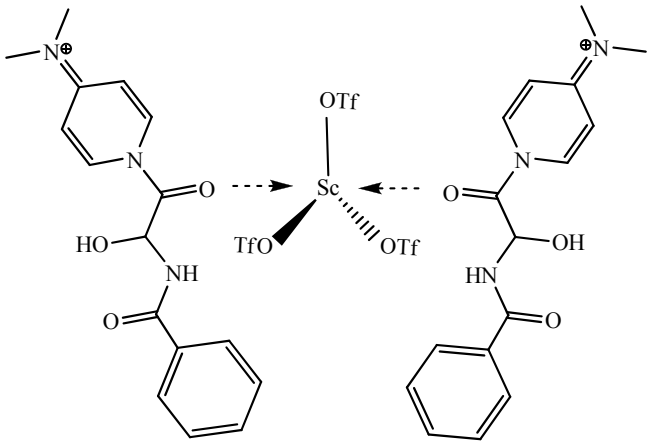

Figure 63: The theoretical effect of ScTrf on the acylpyridinium cation

The procedure employing ScTrf (both the reaction and purification) was developed largely from that of Zhao et al. [8] The reaction was conducted in dry DCM with DMAP, DiPC and ScTrf at a ratio of 3:3.1:0.6. The slurry was cooled in a freezer for 1 h and then reacted in an ice bath for 30 min before being brought to room temperature where it reacted for an additional 2 h. No color change was observed during the reaction. The mixture was by purified by vacuum filtered to remove insoluble material and the filter cake was rinsed with DCM. The filtered solvent was then

extracted with four consecutive aqueous washes. The organic layer was dried and the solvent was removed by rotary evaporation, leaving a white residue in a yield of approximately 40 %.

After purification, the product was characterized by NMR to determine the structure of the product. The NMR spectrum for OBZ generated from the ScTrf catalyzed reaction is shown in Figure 64. The solvent used was *d6*-DMSO and the residual solvent and water peaks are δ = 2.50 ppm and 3.33 ppm, respectively. The DiPU abbreviation stands for diisopropylurea, the DiPC analogue of DCU.

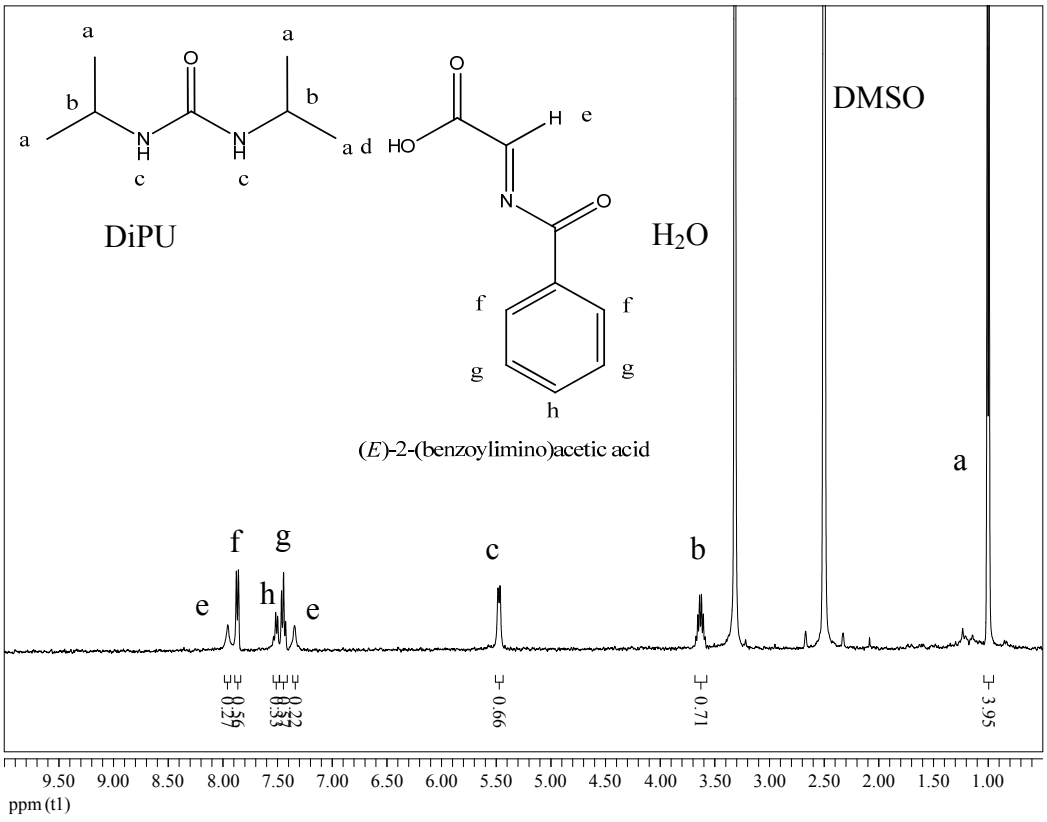

Figure 64: ^{1}H NMR spectrum of OBZ produced by ScTrf catalyzed Steglich esterification

The results of characterization with NMR did not indicate that OBZ was formed. Instead, the formation of an imine appeared to occur. Both geometric isomers of the proposed imine are shown in Figure 65. The formation of an imine was proposed because of the two peaks that appeared at $\delta = 7.95$ ppm and 7.35 ppm. The peaks were separated by 0.60 ppm, similar to the impurities in 2-acetamido-2-hydroxyacetic acid (ACE), which were thought to be the =C-H hydrogens of the E and Z isomers of an imine. The generation of an imine was further supported by the fact that no α-hydrogen, hydroxyl hydrogen or amido hydrogens were observed. A brief literature review revealed that carbodiimide coupling agents have been used to dehydrate similar molecules like α-substituted-β-hydroxyphenolpropanoates in the presence of $CuCl_2$. [9]

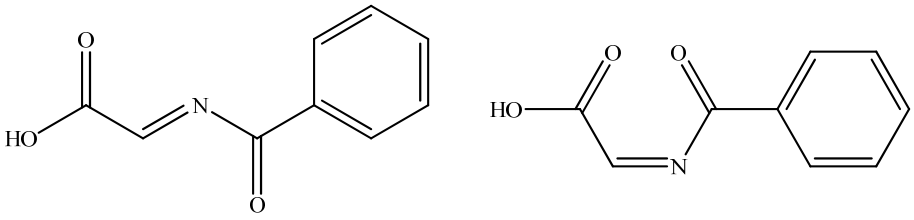

Figure 65: Possible imine byproducts during BZ esterification

Contrary to the pTSA acid mediated procedure, the formation of the N-acylurea was not readily observed. The absence of the N-acylurea was determined because the integration between the labeled DiPU peaks agreed, but the integration of the aromatics with respect to these peaks did not. If the NMR peaks at $\delta = 5.50$ ppm and 1.00 ppm were from the N-acylurea, the ratio of peak integrations should be 1:12, but a ratio of 1:6 is observed, indicating the peaks are representative of DiPU.

Although the NMR did not indicate the existence of polymer, the purified product was analyzed by GPC. A small amount of oligomeric substance was observed. The M_n and M_w were found to be 780 and 810 g/mol, respectively. The results of NMR and GPC seemed to indicate that although a side reaction occurred, OBZ was synthesized due to the formation of a product with elevated molecular weight. The M_n corresponds to a DP = 4 repeat units for OBZ. The existence of the imine in the product could provide an explanation for the exclusive formation of low molecular weight oligomers. If the hydroxyl terminal of the polyester chain was dehydrated, the imine could be formed. The lack of any N-H hydrogen in Figure 64 (typically observed at $\delta = 9.20$ ppm) also indicated that even the amido group of the carboxylic terminus may be deprotonated. The formation of both imine groups would suppress the formation of polymer by elimination of the reactive end groups. The structure of the imine capped OBZ molecule is depicted in Figure 66.

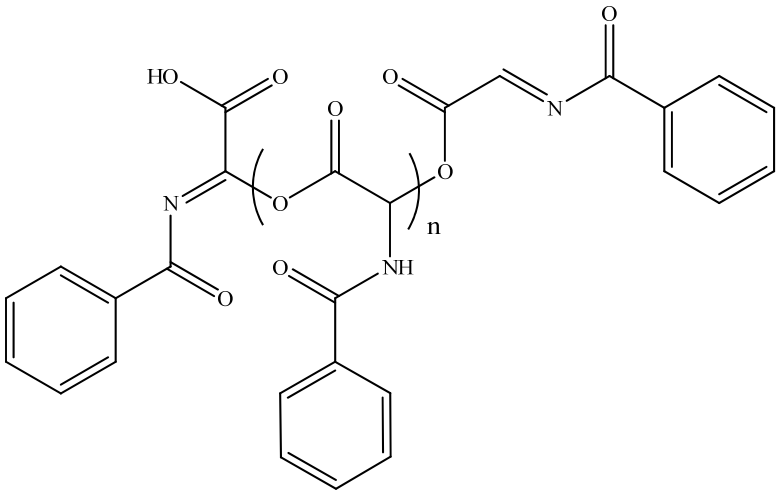

Figure 66: Proposed imine termination of OBZ by hydroxyl terminus dehydration and carboxyl terminus amido-deprotonation

Another possible mechanism for high molecular weight suppression might be the formation of cyclic oligomers. Since the highest DP obtained for OBZ was four repeat units, it was theorized that intramolecular condensation of the terminal hydroxyl group and the carboxyl terminus of OBZ could occur, producing a cyclic polymer. The formation of a cyclic polymer would explain why neither the hydroxyl or carboxyl hydrogens were observed by NMR and would provide a termination mechanism for the polycondensation. The proposed structure of the cyclic tetramer is depicted in Figure 67.

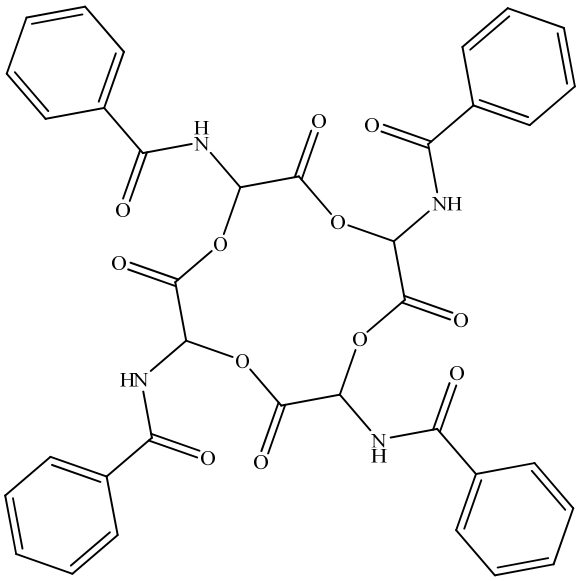

Figure 67: A cyclic tetramer of BZ

6.4 Reaction Screening for Future Work with Steglich Esterifications

After a number of complications were experienced during the attempted Steglich polyesterification of BZ, a brief screening process was conducted to determine the effect of individual reagents on the reaction. Screens were conducted by creating a stock solution of BZ in THF at a concentration of 20 mg BZ per 1 mL of dry THF. Dry THF

was selected as the screening solvent because BZ is more soluble in THF than in DCM. A small, nonquantitative amount of the tested reagents were added to approximately 1 mL of the stock solution. The results of the trials are detailed in Table 10. The abbreviation PPT is used for precipitant.

Table 10: Steglich polyesterification reagent screening

Reagent (added to BZ / THF solution)	Result
DMAP / ScTrf	Cloudy solution, white PPT
DMAP	Opaque solution, no PPT
ScTrf	Clear solution, no PPT
DiPC	Yellow solution, no PPT
DCC	Faint yellow solution, white PPT
N-methylmorpholine (NMM)	Faint yellow solution, no PPT
Imidazole	Clear solution, no PPT
Triethylamine	Faint yellow solution, no PPT
4-(4,6-dimethoxy-1,3,5-triazin-2-yl)-4-methylmorpholinium (DMTMM)	Clear solution, white PPT
DMTMM / DMAP	Clear solution, white PPT

N-methylmorpholine, DMAP, imidazole and triethylamine were added to test the effect of different organic bases on the reaction. Other than the DMAP screen, the organic bases generally produced a clear to faint yellow solution with no precipitate. The

observation of a cloudy solution when DMAP and ScTrf were added was likely the result of poor ScTrf solubility in THF.

The two carbodiimides, DiPC and DCC, resulted in the formation of colored solutions, which indicated the formation of the N-acylurea. Of the two, DCC seemed to produce less N-acylurea than previous experiments would have predicted. The compound 4-(4,6-dimethoxy-1,3,5-triazin-2-yl)-4-methylmorpholinium (DMTMM) was tested because it is an effective esterification agent for carboxylic acids and alcohols. [10] The precipitate observed was likely unreacted DMTMM as the compound is somewhat insoluble in THF. Esterifications involving DMTMM are often catalyzed by a base. Consequently, DMAP was added with DMTMM in a separate trial. No noticeable difference was observed by adding DMAP in tandem with DMTMM.

From observations of the screens, a few selected trials were characterized by GPC to test for the formation of polymer. The screens of the following reagents were tested: DMAP, DMAP/ScTrf, DCC and DMTMM. The DMAP trial was selected for characterization because the solution turned opaque and the viscosity appeared to be greater than other trials, potentially indicating the formation of higher molecular weight polymers. Due to the observations of the DMAP trial, DMAP/ScTrf was tested because ScTrf is known to increase the reactivity of the DMAP complex. The DCC trial was tested to determine if the addition of either DMAP, pTSA or ScTrf limited the Steglich esterification unexpectedly. The DMTMM trial was tested to evaluate if DMTMM was a possibility for future experimentation. The results of GPC characterization of the four screens is presented in Table 11.

Table 11: GPC characterization of selected BZ screens

Reagent	M_n (g/mol)	M_w (g/mol)	PDI
DMAP	760	780	1.03
DMAP / ScTrf	780	800	1.03
DCC	400	410	1.03
DMTMM	260	280	1.08

The screen involving DMAP demonstrated that OBZ could be formed without the use of a carbodiimide. Although the molecular weight was low, corresponding to a DP ≈ 4, oligomers were formed. The OBZ synthesized equals the highest molecular weight OBZ obtained throughout the solution polymerization trials. Since an equivalent molecular weight of OBZ was obtained using DMAP without a carbodiimide, the effectiveness of the carbodiimide as a coupling agent is uncertain. The addition of ScTrf to DMAP did not increase the molecular weight of the OBZ, despite its reported ability to increase the reactivity of the DMAP-monomer complex. Neither DCC nor DMTMM were found to be effective at forming oligomers. The results of the DCC trial indicated that either the N-acylurea or BZ dimers were formed, as both compounds have molecular weights near 400 g/mol. The screen with DMTMM did not form even dimers of BZ. This result may indicate that DMTMM is not an effective condensing agent for BZ or that THF is not an effective solvent.

6.5 Summary of Solution Polymerization

Solution polymerization conducted by Steglich esterification was found to produce only low molecular weight OBZ. No polymer chains of greater than four repeat

units were observed. The formation of the N-acylurea byproduct was thought to occur when the molar ratios of DMAP and the carbodiimide deviated from 1:1 and was optically identified by product discoloration. It was also observed that neither the acid mediated nor the ScTrf catalyzed Steglich esterifications produced high molecular weight polymer. The acid mediated procedure involving pTSA seemed to negatively affect the polymerization and the ScTrf catalyzed produced a product likely containing an imine, although the acidic workup may have caused the iminization.

6.6 References

(1) Bucholtz, B. US Patent 5302694, 1994.
(2) Wagener, K.; O'Gara, J. et al. *Journal of Macromolecular Science* **1994**, *A31*, 775.
(3) Moore, J.; Stupp, S. *Macromolecules* **1990**, *23*, 65.
(4) Belcheva, N.; Tsvetanov, C. et al. *European Polymer Journal* **1991**, *27*, 479.
(5) Belcheva, N.; Lazarova, S. et al. *Makromoleculare Chemie* **1990**, *191*, 213.
(6) Mathiowitz, E.; Qian, H. *Macromolecules* **2007**, *40*, 7748.
(7) Akutsu, F.; Sunahara, M. et al. *Polymer Journal* **1998**, *30*, 421.
(8) Zhao, H.; Greenwald, R. et al. *Journal of Organic Chemistry*. **1998**, *63*, 7559.
(9) Sai, H.; Ohmizu, H. *Tetrahedron Letters* **1999**, *40*, 5019.
(10) Kunishima, M.; Tani, S. et al. *Tetrahedron* **1999**, *55*, 5327.

CHAPTER SEVEN:

CONCLUSIONS

7.1 Introduction to Conclusions

The Seventh Chapter serves to summarize key observations made throughout this thesis. All of the information presented here pertains to the production of functionalized polyesters from amdio-functionalized α-hydroxy acids. The results were broken down into three separate chapters, chapters Four, Five and Six, to illustrate the three phases of polyester research. Firstly, amido-functionalized α-hydroxy acids were synthesized. Secondly, oligo(esters) were prepared by melt polycondensation. Lastly, solution polymerization was attempted via Steglich polyesterification. Important conclusions are provided on each of the research phases in the following sections.

7.2 Synthesis of Amido-Functionalized α-Hydroxy Acids

The primary goal of experimentation with the amido-functionalized α-hydroxy acids was to further understand the reaction in efforts to apply that knowledge to the synthesis of future α-hydroxy acids (α-HAs). As the α-HAs are bifunctional (with a carboxyl and hydroxyl group), they could be polymerized by polycondensation, leaving the amido-functionality as a pendant group. The monomer synthesis is simple compared with other techniques in the literature. Glyoxylic acid monohydrate (GA) and a primary or secondary amide are condensed to form the corresponding amido-functionalized α-HA by combining the two reactants in a suitable solvent.

Diethyl ether proved to be the most widely effective reaction medium and the most effective recrystallization agents were found to be moderately polar solvents. It was realized during monomer synthesis that the ratio of GA to the amide was important for the successful formation of the desired α-HA. Excess GA commonly produced the α-HA in the highest yield. It was hypothesized that water in the GA crystal structure (19 wt%) was accounted for by conducting the reaction in excess GA. If GA was added in excess, the reaction was actually conducted with near equimolar quantities of the reactants by accounting for inherent water in GA. This analysis would suggest the synthesis of future α-HAs begin with a 1.2:1 mol ratio of GA to amide and use diethyl ether as the solvent.

7.3 Melt Polycondensation of Amido-Functionalized α-HAs

Melt polycondensation (PC) involved heating the monomer past its melting temperature, while exposing the monomer to vacuum. For both 2-(2-pyrrolidino)-2-hydroxyacetic acid (PYR) and 2-acetamido-2-hydroxyacetic acid (ACE), melt PC produced oligomers, averaging approximately six repeat units. Low polydispersity indexes (PDI) were calculated for both oligomers, commonly less than 1.07. The polymerizations of both oligomers were temperature dependent. An optimum melt PC range was observed at approximately 25 °C above the melting temperature of the respective monomer. Lower temperatures produced lower molecular weights and higher temperatures caused discoloration and thermal degradation. The effect of catalysts was found to be negative or negligible on the molecular weight of oligomer produced from

PYR melt PCs. Conversely, an increase in glass transition temperature was observed by addition of the catalysts.

Although PYR and ACE were polymerizable by melt PC, both 2-benzamido-2-hydroxyacetic acid (BZ) and 2-acrylamido-2-hydroxyacetic acid (ACRY) were not. Rather than polymerizing, the monomers thermally degraded under analogous reaction conditions to those used for PYR and ACE. Thermal gravimetric analysis (TGA) was conducted on BZ and ACRY. For these monomers a large, step-like mass loss was observed prior to the melting point. Comparing the TGA thermograms of PYR and ACE with those of BZ and ACRY indicated that thermal degradation did occur, precluding melt PC as a possible polymerization technique.

7.4 Solution Polymerization of Amido-Functionalized α-Hydroxy Acids

Solution polymerization was conducted by Steglich esterification. This technique was attempted to polymerize BZ because the monomer could not be polymerized during melt PC. Two types of Steglich polyesterification were attempted: acid mediated and Lewis acid catalyzed. A number of important variables were identified during experimentation including monomer concentration, reactant ratios and solvent polarity. When one of the aforementioned ratios was out of balance, an orange or yellow byproduct was typically observed.

Neither of the Steglich polyesterification procedures (organic acid mediated or Lewis acid catalyzed) were found to be very successful because only low molecular weight oligomers were created. The oligomers were produced with a low polydispersity

index (<1.07), but the longest chains contained only four repeat units. A possible esterification termination mechanism was postulated as an imino group was thought to have formed. Another possible termination mechanism could be the formation of a cyclic-tetramer, but the actual formation of this molecule is inconclusive.

CHAPTER EIGHT:

FUTURE WORK

As the work detailed in this thesis was aimed at synthesizing novel, amido-functionalized biodegradable polyesters, future work should focus on the development of new functionalized monomers and methods to improve the polymerization of these monomers. These two primary goals would facilitate the creation of a library of functionalized polymers and would expand future research into biopolymer chemistry.

The synthetic method described for the production of amido-functionalized α-hydroxy acids is a highly versatile reaction. Consequently, new amides and carbamates should be explored as substituent groups to test the limits of the reaction. Techniques to prepare carbamates or amides should be investigated in the event that the desired substituent cannot be purchased. For example, some introductory work has been conducted into the preparation of an oligo(ethylene glycol) carbamate as a possible functional group. Beta-lactum antibiotics (Penicillin, amoxicillin, etc.) possess secondary amide functional groups and could potentially be condensed with glyoxylic acid to form the repeat unit of a biodegradable polyester bearing antibiotic pendant groups.

An additional goal of future monomer work should be to produce chiral monomers. As the polymerization of the amido-functionalized polyesters improves, the advent of an isotactic polymer may be desired. Unless stereochemical control is exerted on the reaction, a racemic mixture of enantiomers will form during monomer synthesis. One solution to this problem may be to use of chiral sugars or other chiral auxiliaries to

inhibit the formation of both enantiomers, thereby improving the enantiopurity of the α-hydroxy acid synthesized.

Copolymers of the synthesized oligo(α-hydroxy acids) and PLA or other biodegradable polyesters should be investigated. Due to the unique properties of the α-hydroxy acids synthesized, the addition of these molecules to common polyesters may produce novel polymers with tailored physical properties. Such properties might include degradation rate, hydrophilicity, mechanical properties and biocompatibility. Degradation and toxicity tests would necessary after the successful formation of the copolymers to assess their viability as biomaterials.

Possibly the most important future work would be the development of improved polymerization methods. Improved polymerization techniques are essential to the advancement of this research. Presently, melt polycondensation produced low molecular weight oligomers and was incompatible with half of the monomers. Solution polymerization by Steglich polyesterification was also found to be incompatible with the synthesis of high molecular weight polyesters. In order for the amido-functionalized α-hydroxy acids to reach their full potential as functionalized monomers, a more effective and robust method of polymerization must be developed. Possible methods may include other solution polymerizations, O-carboxyanhidride ROPs or ROPs utilizing cyclic α-HA dimers.

APPENDIX A:

DSC THERMOGRAMS OF OPYR AND BINARY CATALYSTS (UNPURIFIED)

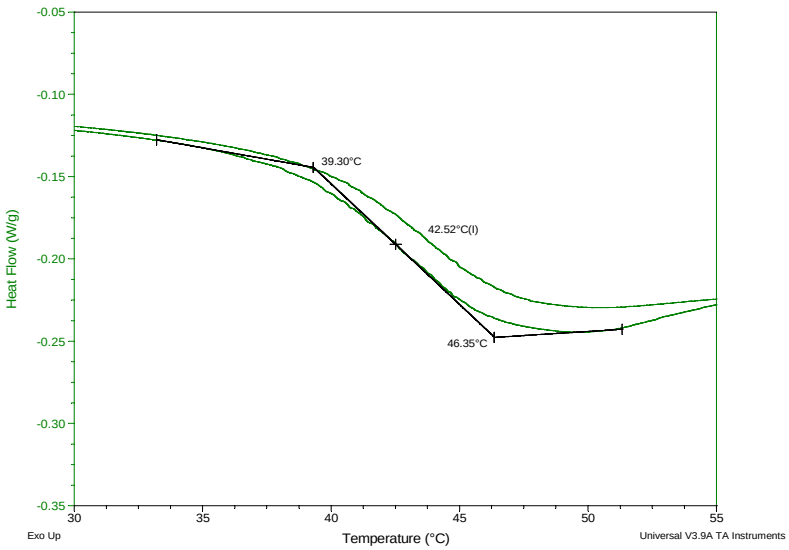

Figure 68: DSC thermogram of OPYR with 1 wt% $BiCl_3$ and 1 wt% *p*-toluenesulfonic acid

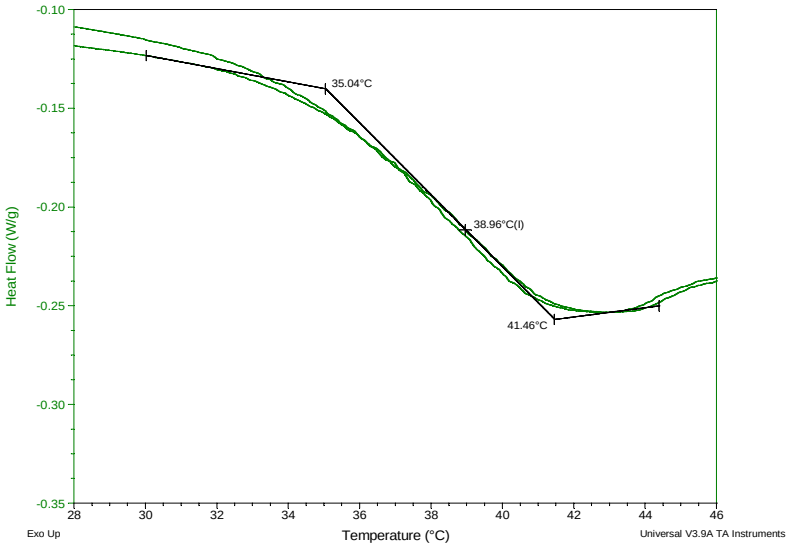

Figure 69: DSC thermogram of OPYR with 1 wt% SnO and 1 wt% *p*-toluenesulfonic acid

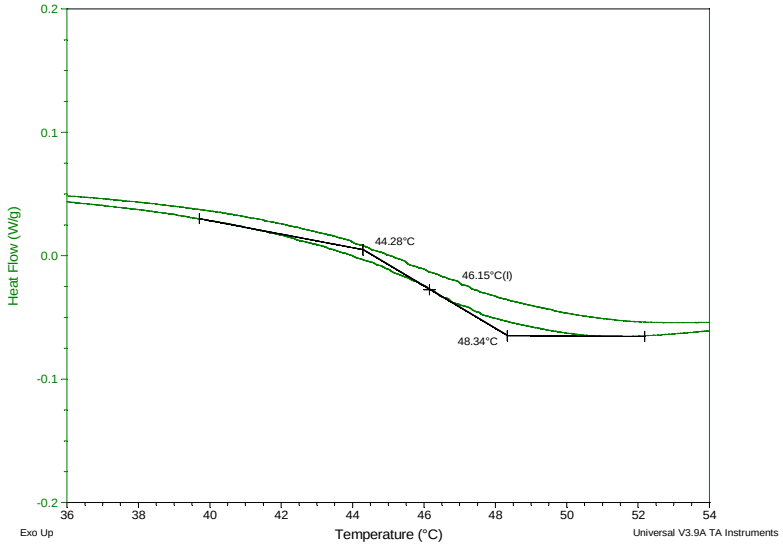

Figure 70: DSC thermogram of OPYR with 1 wt% ZnO and 1 wt% *p*-toluenesulfonic acid

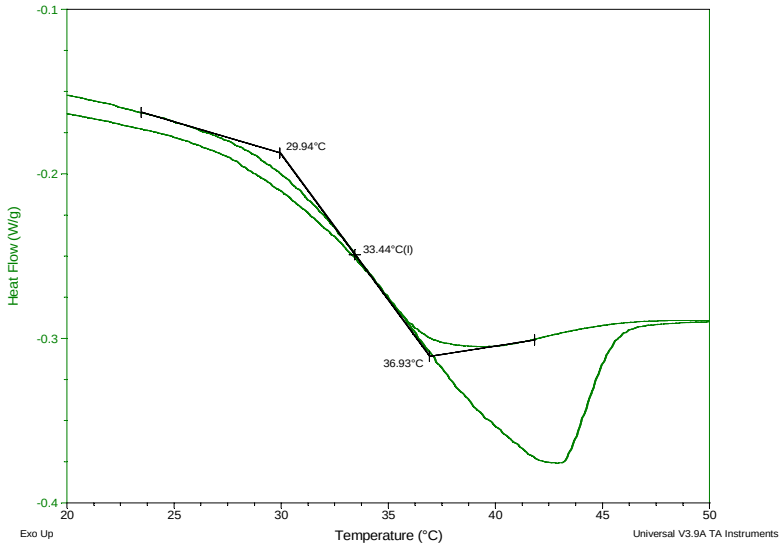

Figure 71: DSC thermogram of OPYR with 1 wt% $ZnCl_2$ and 1 wt% *p*-toluenesulfonic acid

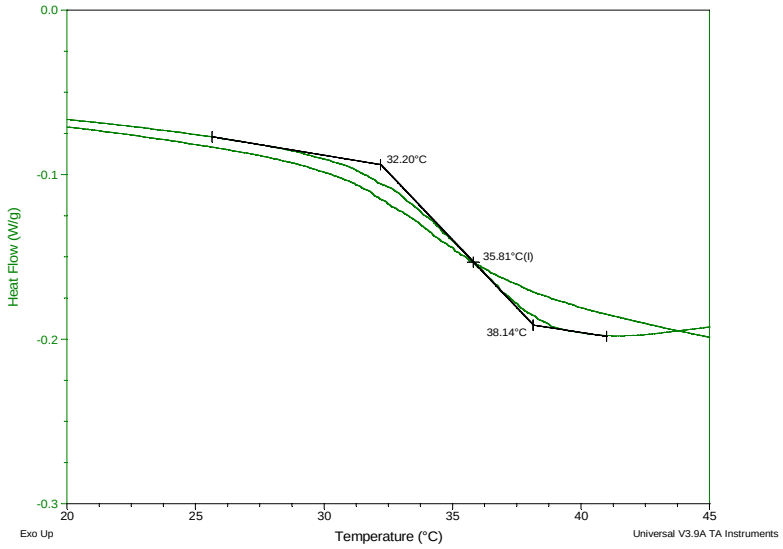

Figure 72: DSC thermogram of OPYR with 1 wt% Zn dust and 1 wt% *p*-toluenesulfonic acid

APPENDIX B:

CHARACTERISTIC GPC ELUTION PROFILES

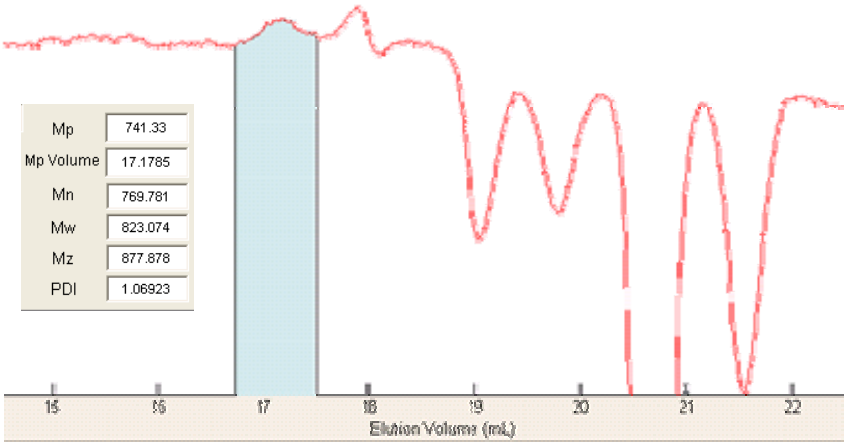

Figure 73: Characteristic GPC elution profile for melt PC synthesized OPYR (24 h, 105 °C)

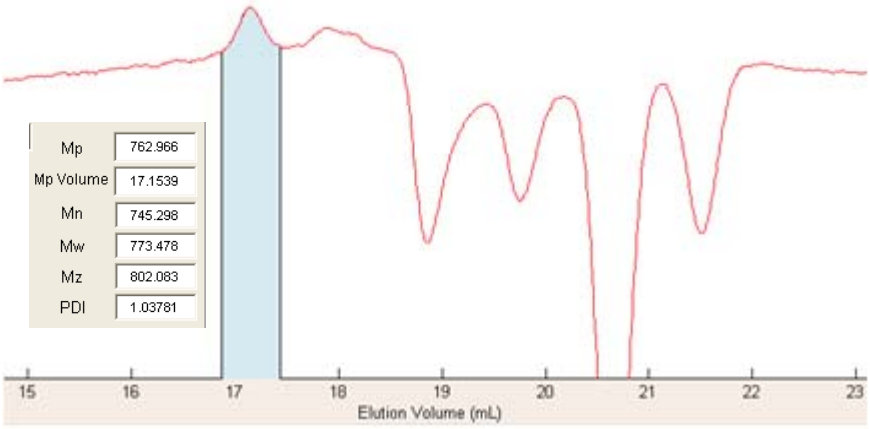

Figure 74: Characteristic GPC elution profile for melt PC synthesized OACE (24 h, 85 °C)

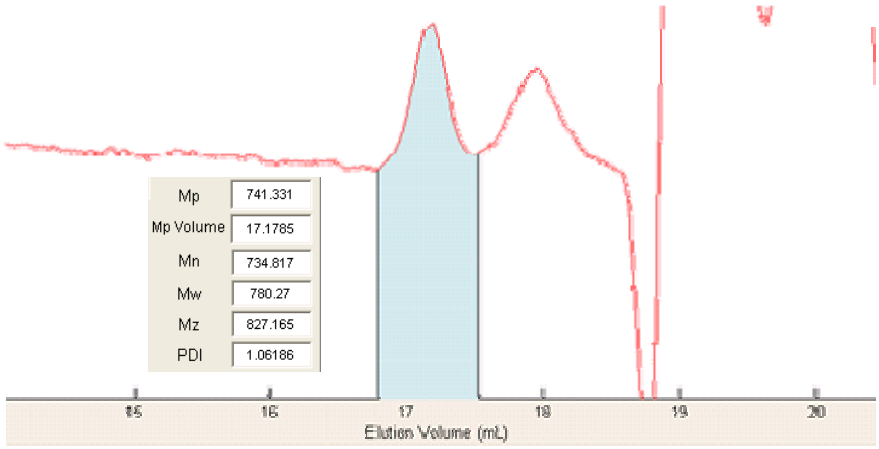

Figure 75: Characteristic GPC elution profile for ScTrf catalyzed melt PC of OPYR (24 h, 105 °C)

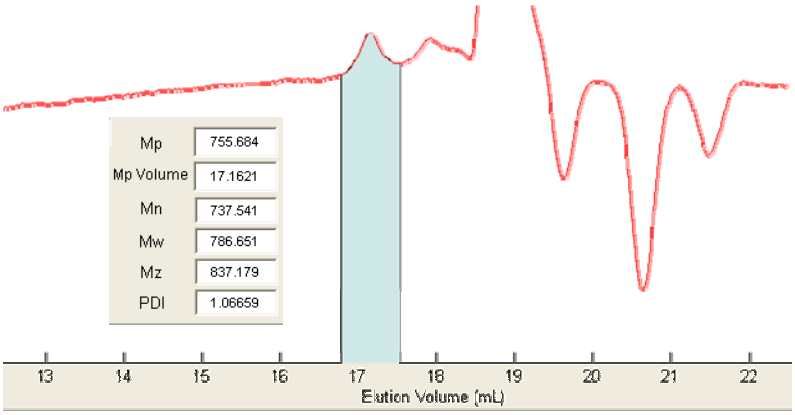

Figure 76: Characteristic GPC elution profile for Steglich polyesterification of OBZ (DCC, DMAP)